Chapter 1

Introduction

Tectonic and Stratigraphic Framework

1.1 General Setting

In this book, we describe the greater Gulf of Mexico (GoM) basin as extending from the coastal plain in the southern USA to the coastal plain of southern Mexico, the Chiapas and Tabasco region, and east across the Yucatán Platform to Cuba, the Florida Straits, and the Florida onshore area (Figure 1.1). The Gulf basin has a central abyssal plain that generally lies at 13 km depth (Bryant *et al.* 1991). The eastern Gulf floor is dominated by the morphology of the Late Quaternary Mississippi Fan.

The continental slope of the northern Gulf margin displays a bathymetrically complex morphology that terminates abruptly in the Sigsbee Escarpment to the west and merges into the Mississippi Fan to the east (Steffens *et al.* 2003). The hallmark of the central Gulf continental slope is the presence of numerous closed to partially closed, equi-dimensional, **slope**

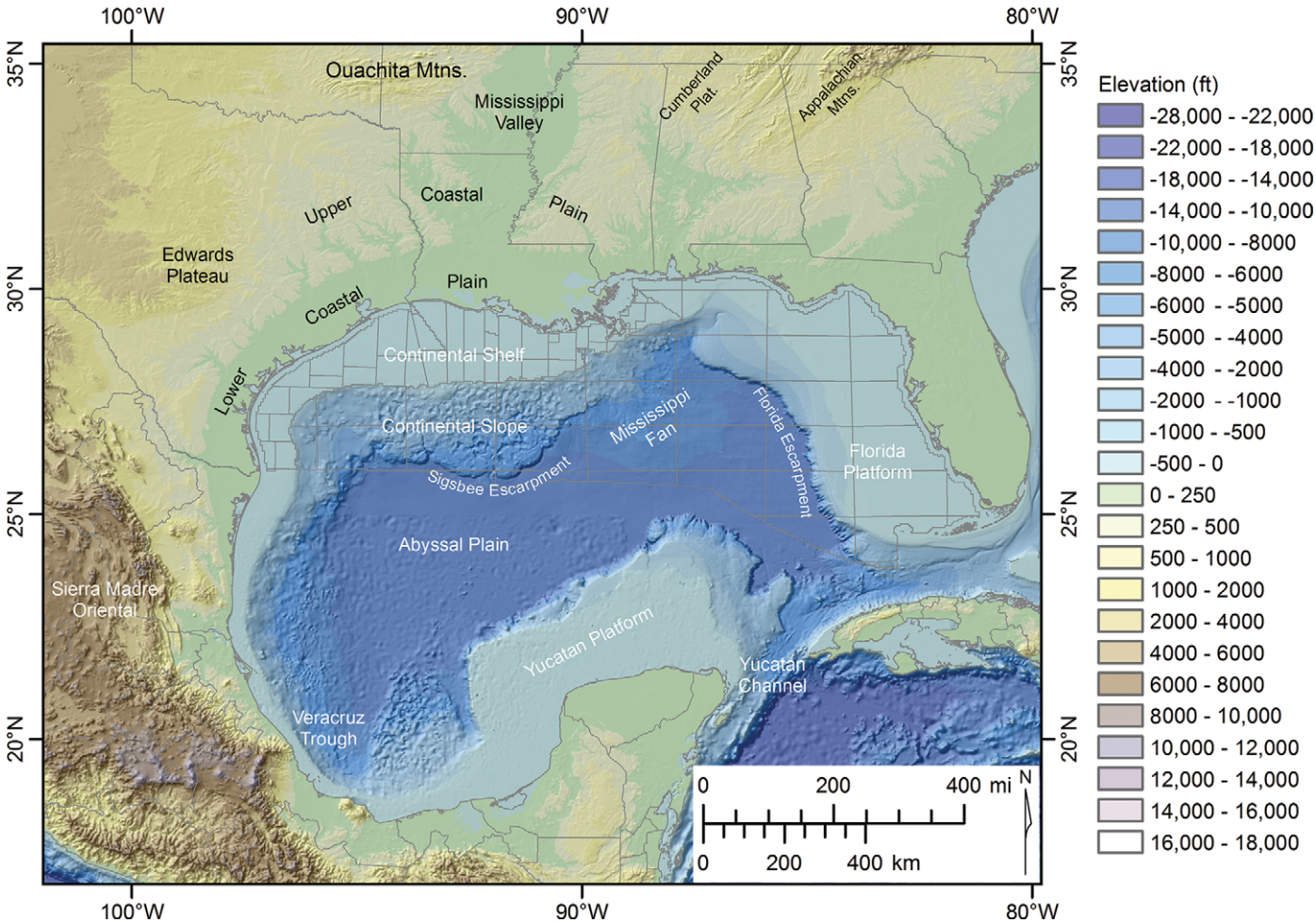

Figure 1.1 Location map for greater GoM basin, including important geographic and bathymetric features.

https://doi.org/10.1017/9781108292795.003 Published online by Cambridge University Press

minibasins. In contrast, the Florida Platform forms a broad ramp and terrace that terminates at depth into the nearly vertical Florida Escarpment. The western Gulf margin displays intermediate width, and it too is quite bathymetrically complex. Here, numerous contour-parallel ridges and swales dominate the mid- to lower-slope morphology. The modern **shelf margin**, as reflected by a well-defined increase in basinward gradient, generally lies at a depth of 100–120 m. Landward, the northwestern, northern, and eastern GoM is bounded by broad, low-gradient shelves that range from 100 to 300 km in width (Figure 1.1). Today, and throughout its history, the Florida and Yucatán Platforms, which bound the basin on the east and south, persist as sites of carbonate deposition.

On shore, the northern and northwestern Gulf margins display a broad coastal plain (Figure 1.1). The lower coastal plain, a flat, low-relief surface, is underlain by Neogene and Quaternary strata. The upper coastal plain displays modest relief of less than about 100 m (328 ft) created by Quaternary incision into older Neogene, Paleogene, and Upper Cretaceous strata by numerous large and small rivers. The basin is bounded by a variety of Cenozoic, Mesozoic, and remnant Paleozoic uplands, including the Sierra Madre Oriental of Mexico, the Trans-Pecos mountains of west Texas, the Lower Cretaceous limestone-capped Edwards Plateau, Ouachita Mountains of southern Arkansas, and the Cumberland Plateau and southern Appalachian Mountains of northern Mississippi and Alabama. The northeast Gulf basin merges into the southern Atlantic coastal plain across northern Florida; however, the structural basin boundary is generally placed near the current west coast of the Florida peninsula.

Mexico's onshore topography strongly reflects the Sierra Madre Oriental in the north and the Chiapas deformational belts in the south of the country. The eastern onshore portion of Mexico is marked by short but steep gradient rivers that carry modern sediments toward a wave-dominated shoreline, a narrow shelf, and steep slope that terminates abruptly at the abyssal plain. Offshore, bathymetric maps show the sea floor complexity resulting from recent tectonic events: (1) the elongate, generally north–south oriented structures called the Mexican Ridges; and (2) the recent salt inflation and compression evidenced in the rugose hydrography of the Campeche and Yucatán salt provinces.

Across the Bay of Campeche lies the Yucatán carbonate platform, with equally steep margins that circumscribe the platform and its border with the adjacent Caribbean basin. The Yucatán channel separates Yucatán from Cuba, a tectonically complex mélange of various microplates that merged over 100 million years. Cuba lies across the Florida Straits from the South Florida basin, a short distance, but a world away in terms of its geological evolution.

1.2 Structural Framework

In order to understand the depositional evolution of the GoM, it is necessary to consider the structural framework that underpins and influences the sedimentary loading history of this immense natural repository. This extends to the deep crystalline crust and even mantle that can, in some cases, be detected by modern seismic reflection and refraction data. The accumulated sediment mass, including both siliciclastics and carbonates, also drove **gravity tectonics**, particularly where **evaporites** like salt respond in a ductile fashion at burial depths attainable by modern wells.

1.2.1 Deep Crustal Types

For many years, the form and lithology of the deep structure in the GoM was a matter of conjecture and inferences based upon rare penetrations of **basement** rock or sometimes-equivocal gravity and magnetic data. Recently, seismic refraction studies have greatly illuminated the form of the mantle and overlying crystalline and sedimentary crust (Van Avendonk *et al.* 2013, 2015; Christeson *et al.* 2014; Eddy *et al.* 2014). In addition, new plate tectonic models have altered previous suppositions on timing of basin opening and emplacement of **oceanic crust** (Norton *et al.* 2016). Alternative models, particularly for the pre-spreading rift phase, show convergence toward a consensus solution.

In general, these studies agree that the Gulf basin is largely surrounded by normal continental crust of the North American plate. Most of the structural basin is underlain by **transitional crust** that consists of **continental crust** that was stretched and attenuated by Middle to Late Jurassic rifting (Hudec *et al.* 2013a). Two types of transitional crust are differentiated (Figure 1.2). The basin margin is underlain by a broad zone of thick transitional crust, which displays modest thinning and typically lies at depths between 2 and 12 km subsea (Sawyer *et al.* 1991). The area of thick transitional crust

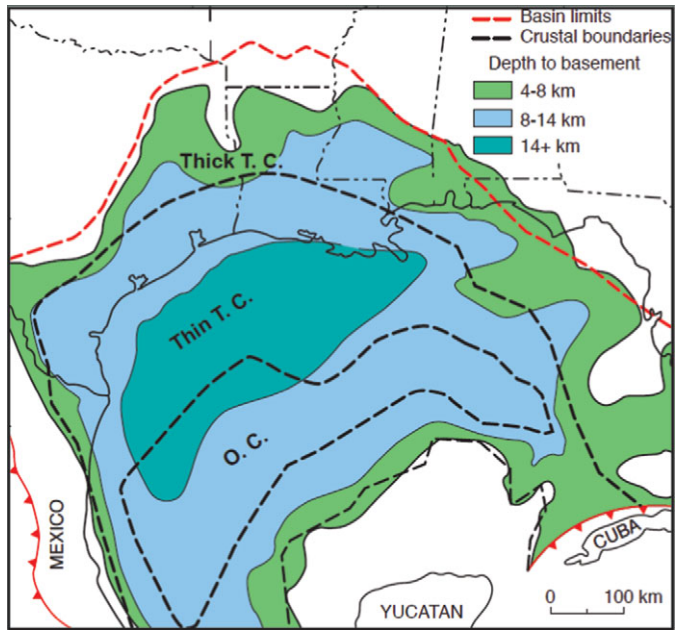

Figure 1.2 GoM crustal types. Modified from Galloway (2008).

https://doi.org/10.1017/9781108292795.003 Published online by Cambridge University Press

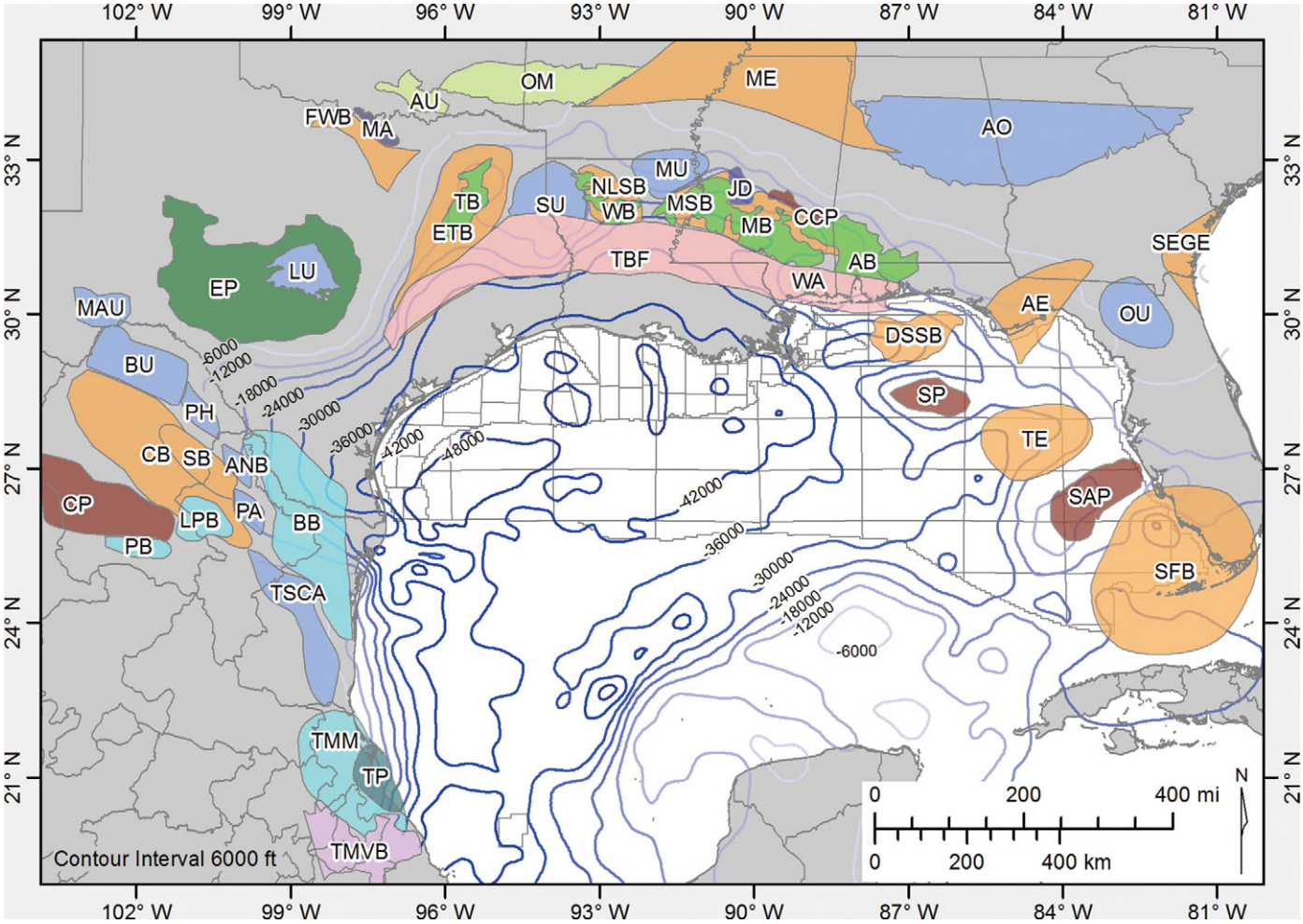

Figure 1.3 Key tectonostratigraphic features, northern GoM. Basement depths based on seismic structural mapping. Abbreviations: AB, Alabama basin; AE, Apalachicola Embayment; ANB, Anahuac Block, BB, Burgos basin; AO, Appalachian Orogen (Cretaceous limit); AU, Arbuckle Uplift; BU, Burro Uplift; CCP, Clarke County Platform; CP, Coahuila Platform; DSSB, DeSoto salt basin; EP, Edwards Platform; ETB, East Texas basin; FWB, Fort Worth basin; JD, Jackson Dome; LPB, La Popa basin; LU, Llano Uplift; MA, Muenster Arch; MAU, Marathon Uplift; MB, Mississippi Basin; ME, Mississippi Embayment; MSB, Mississippi salt basin; MU, Monroe Uplift; NLSB, North Louisiana salt basin; OM, Ouachita Mountains; OU, Ocala Uplift; PB, Parras basin; PH, Peyotes High; SAP, Sarasota Platform; SEGE, Southeast Georgia Embayment; SFB, South Florida basin; SP, Southern Platform; SU, Sabine Uplift; TB, Tyler basin; TE, Tampa Embayment; TMM, Tampico–Misantla–Magiscatzin; TP, Tuxpan Platform; TSCA, Tamaulipas/San Carlos Arch; WA, Wiggins Arch; WB, Winnfield basin. Terminology from various public sources, including Ewing and Lopez (1991).

consists of blocks of near-normal thickness continental crust separated by areas of stretched crust that has subsided more deeply. The result is a chain of named arches and intervening embayments and salt basins around the northern periphery of the Gulf basin (Figure 1.3).

Much of the present inner coastal plain, shelf, and continental slope is underlain by relatively homogeneous thin transitional crust, which is generally less than half of the 35 km thickness typical of continental crust and is buried to depths of 10–16 km below sea level. Reconstructions of deep seismic traverses (Peel *et al.* 1995; Radovich *et al.* 2007, 2011; Hudec *et al.* 2013b) indicate that basement may lie below 20 km in the central **depocenter** beneath the south Louisiana coastal plain and adjacent continental shelf. The deep, central Gulf floor is underlain by an arcuate belt of basaltic oceanic crust that was intruded during Late Jurassic through Early Cretaceous sea floor spreading (Hudec *et al.* 2013a; Norton *et al.* 2016). Surprisingly, the central Gulf crust generally lacks the magnetic signature typical of oceanic crust (Figure 1.4), which compounds interpretation difficulties, but recent gravity mapping (Sandwell *et al.* 2014) confirm earlier models of the location of the updip or landward limit of oceanic crust (LOC).

1.2.2 Seismic Refraction Studies of Deep Crust

The majority of data obtained for petroleum exploration is **seismic reflection data**, which allows both imaging through common depth point solutions and measurement of compressional seismic velocities to depths approaching 40,000 ft (12.2 km), depending on the energy source and cable. **Seismic refraction** data involves measurement of the compressional seismic velocities at much greater depths, approaching 40 km (25 miles). These velocities are a function of density in the deep earth and allow one to differentiate between mantle,

https://doi.org/10.1017/9781108292795.003 Published online by Cambridge University Press

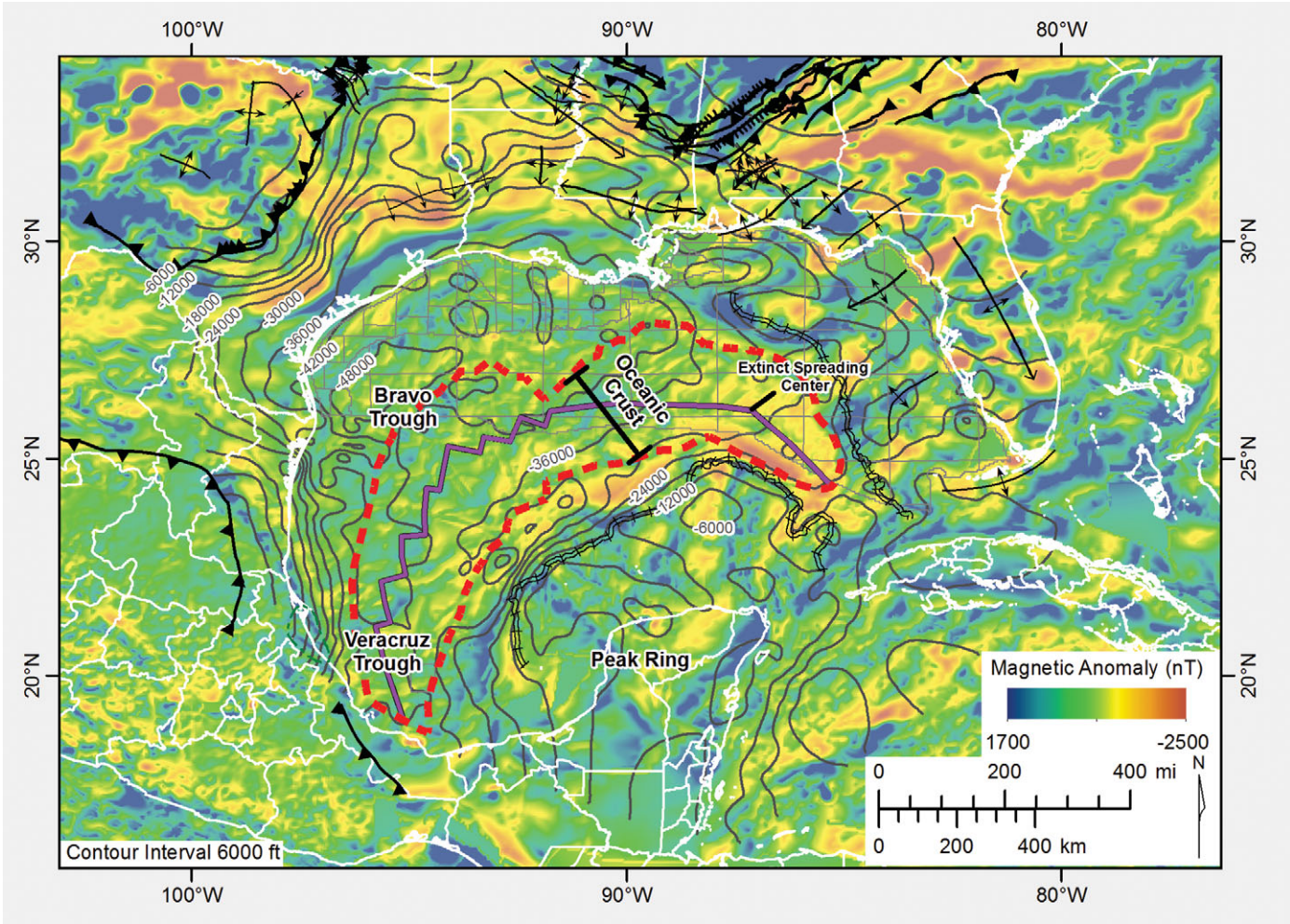

Figure 1.4 Mapped top of seismically defined basement with overlay of EMAG2 magnetic anomaly (Sandwell *et al.* 2014). Key tectonic features are discussed in the text. The limit of oceanic crust (red dashed line) is based on Hudec *et al.* (2013a, 2013b).

crystalline crust, and sedimentary crust, even where buried below thick intervals of salt and sedimentary rocks (Figure 1.5). In the northern GoM, a series of long (>500 km) seismic refraction lines were collected using bottom sensors (Figure 1.5). A line across the eastern GoM revealed the top of the mantle to shallow from about 34 km (21 miles) below the thick transitional crust below the Florida Platform to depths as shallow as 15 km (9 miles) in the area where oceanic crust is known to be present (Christeson *et al.* 2014; Figure 1.5). Above the mantle here lies a crystalline crust interval with unusually low velocities (in comparison to other areas), suggesting moderately attenuated continental crust. The sedimentary interval has compressional velocities in the range of 5.0 km/s (carbonate-dominated platform) to 3.0 km/s, where Miocene and younger strata are known to be present from well penetrations. The seismic refraction data also allow locating the boundaries of the LOC, here at a distance of 350–400 km from the start of the line just offshore of Florida. An intriguing observation is higher-than-expected seismic velocities at the LOC, suggestive of massive basalt emplacement associated with sea floor spreading (Christeson *et al.* 2014).

In the western GoM, seismic refraction data (Gumbo Line 1) revealed an unusual interval between high compressional velocity mantle and penetrated sedimentary crust (Van Avendonk *et al.* 2013). Below base of salt lies an unknown interval with considerable lateral crustal heterogeneity, thought to be rifted (attenuated) sedimentary crust with igneous intrusions. This interval ranges from 10–12 km at the top to as deep as 28 km depth above mantle rock. The lateral velocities variations that suggest igneous intrusions are documented in the shallow **pre-salt** interval of onshore areas, to be discussed in Section 2.2. The LOC is located inboard of the present-day Sigsbee Escarpment, though there is some uncertainty, given the thick salt canopy here (Van Avendonk *et al.* 2013). The presence of a pre-salt (Late Triassic[?] to Middle Jurassic[?]) interval in the deep northern GoM is consistent with observations from seismic reflection data in a pre-salt province

https://doi.org/10.1017/9781108292795.003 Published online by Cambridge University Press

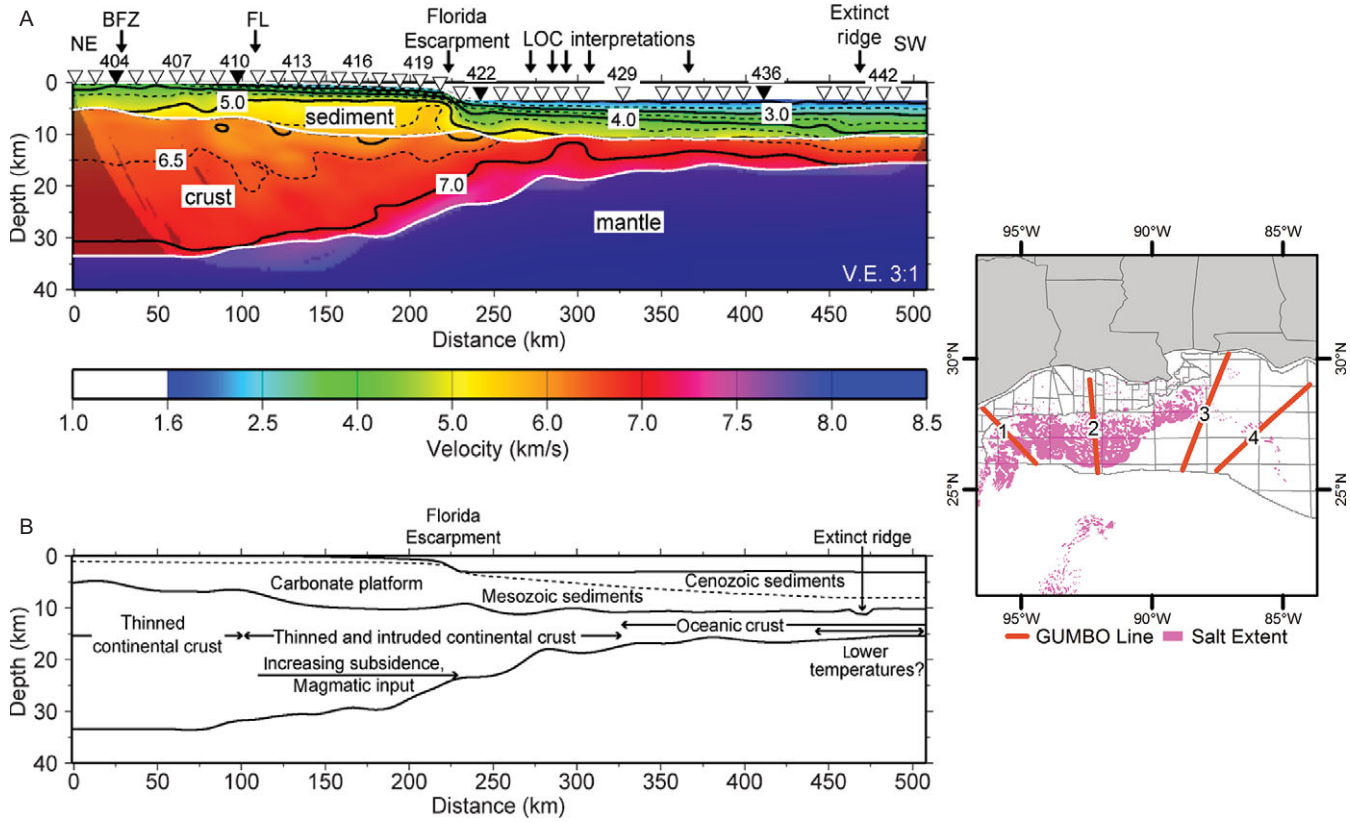

Figure 1.5 Seismic refraction data and interpretation, Gumbo Line 4, eastern GoM. Modified from Christeson *et al.* (2014).

offshore of Yucatán Province (Williams-Rojas *et al.* 2012; Miranda Peralta *et al.* 2014; Saunders *et al.* 2016).

1.2.3 Seismic Reflection Studies of Deep Crust

Seismic reflection surveys shot for oil and gas exploration provide some corroboration of seismic refraction interpretations, particularly for the eastern GoM where the salt canopy is absent. Here the general position of a Jurassic–Early Cretaceous **spreading center** in the eastern GoM has been suggested for many years, yet the precise location was not precisely known until Snedden *et al.* (2014) used several seismic criteria to define its location (Figure 1.6). Lin *et al.* (2019) subsequently refined its structure and evolution using newer vintage seismic reflection and gravity data. The extinct spreading center here displays morphological characteristics associated with slow-spreading mid-ocean ridges (rates of 1–4 cm/year; Perfit and Chadwick 1998): (1) large and wide axial valleys, 5–20 km wide; (2) deep axial valleys, often over 2 km deep; (3) normal faults that dip toward axial valleys; and (4) discontinuous, isolated basement highs, with elevations over 1 km above regional oceanic basement depth. Using seismic refraction data, Christeson *et al.* (2014) calculated a full spreading rate of 2.2 cm/year on a profile (Figure 1.5) in the same area. This estimate falls squarely in the slow spreading rate range globally and specifically for the comparable Mid-Atlantic Ridge system (McDonald 1982). Slow-spreading ridges express wide variety in tectonic and volcanic character, reflecting relatively unfocused magmatism (Sempere *et al.* 1993).

Structural-balanced restorations of the eastern Gulf further confirm the LOC location and timing of sea floor spreading (Curry *et al.* 2018). Upper Jurassic (Smackover and Norphlet) strata downlap onto oceanic crust, suggesting oceanic crust formation contemporaneous with deposition (Figure 1.6; see also Section 3.3.4). Latest Upper Jurassic (Haynesville-equivalent) and Cotton Valley intervals extend across all oceanic crust, constraining the end of sea floor spreading at about 155 Ma. These units are also contemporaneous with post-Smackover rafting in the eastern Gulf, suggesting a genetic relationship, as will be explored in Section 3.3.4.

1.2.4 Magnetic Data

Early attempts at mapping the extinct spreading center and LOC (Figure 1.4) were challenged by the generally indistinct character on magnetic data collected from the northern Gulf (e.g., Imbert and Phillippe 2005). This can be partly attributed to the low paleolatitude of the Gulf during the Jurassic, resulting in shallow magnetization vectors that subdued magnetic intensity at the surface but also the poor resolution of older surveys. Newer aeromagnetic data acquired for hydrocarbon exploration in Mexico have better constrained the location of oceanic crust, particularly when integrated with

https://doi.org/10.1017/9781108292795.003 Published online by Cambridge University Press

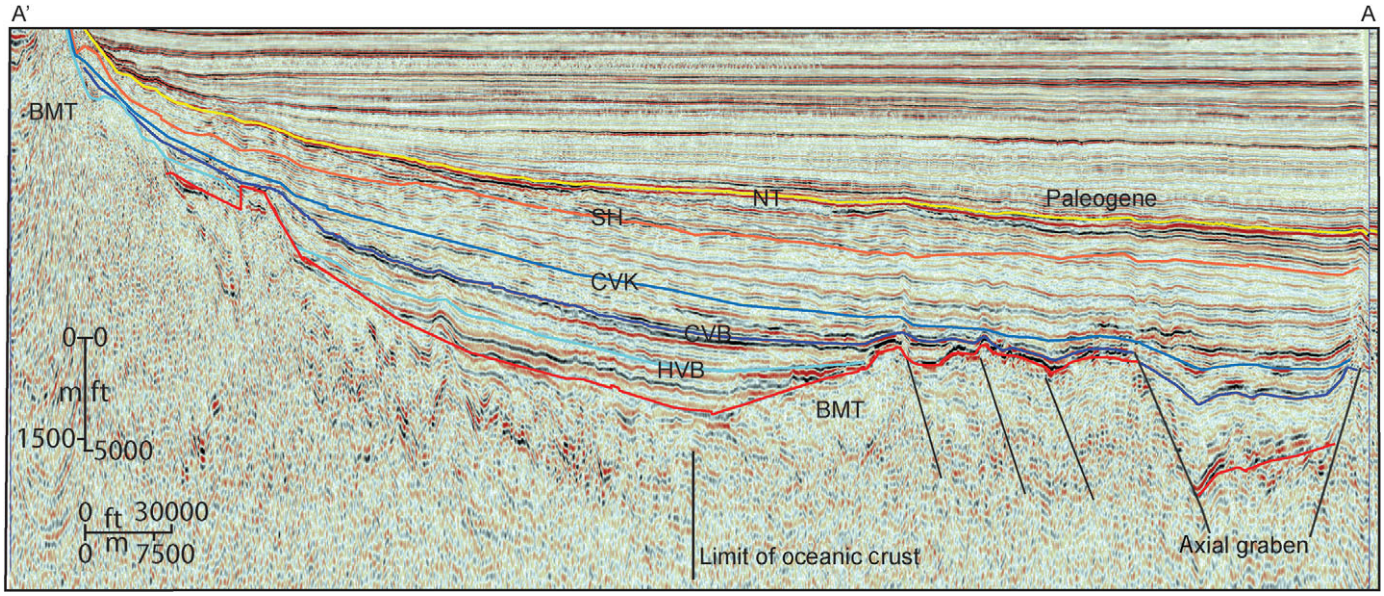

Figure 1.6 Seismic line interpretation in eastern GoM, extending from the Florida Platform across the inferred axial graben of the extinct spreading center showing lapout of HVB, CVB, and CVK supersequences onto oceanic crust. Other correlated horizons are SH, NT, and Paleogene (Wilcox) supersequences. Modified from Snedden *et al.* (2014). Seismic line courtesy of Spectrum. Abbreviations HVB, Haynesville–Buckner; CVB, Cotton Valley–Bossier; CVK, Cotton Valley–Knowles; SH, Sligo–Hosston; NT, Navarro–Taylor; BMT, basement.

comparable vintage northern Gulf data (Pindell *et al.* 2016). One prominent magnetic anomaly located in the central GoM has a distinctive pattern of orthogonally cross-cutting linear features superimposed upon an elongate margin parallel magnetic anomaly, thought to indicate the location of the youngest oceanic crust and thus the position of the extinct spreading center (Pindell *et al.* 2016). The calculated full spreading rates of 1–3.6 cm/year for the entire GoM are comparable to the slow spreading rates (2.2 cm/year) estimated for the eastern GoM (Christeson *et al.* 2014). Another trend, called the Campeche magnetic anomaly, is located downslope of the Yucatán **Platform margin** and constrains the Yucatán (Mayan) block position at the start of pre-salt deposition here, as discussed in Chapter 3.

1.2.5 Gravity Data

Sandwell gravity maps (Sandwell *et al.* 2014) also provide further documentation of the present-day crustal types and their position. Continental crust is generally indicated by gravity highs (e.g., Yucatán block) and oceanic crust by gravity lows, but local variations can occur as a function of igneous intrusions, salt, and depth variations along prominent escarpments.

1.3 Gravity Tectonics

Above the crystalline basement in the greater GoM basin, a thick sedimentary interval exists, deposited largely in the Mesozoic and Cenozoic. Beginning in the Jurassic, robust depositional systems delivered sediment into the basin, the siliciclastic systems fed by rivers draining a variety of source terranes in the northern Rockies, southern Rockies, Appalachians, Quachita Mountains (USA), and Sierra Madres and other areas of Mexico. Siliciclastic systems are particularly prominent in the Cenozoic, but Mesozoic systems of the Jurassic and Cretaceous were, at times, equally impressive in terms of accumulated thickness and caliber of sediment grade. Cenozoic deposition, which extended past the rigid Mesozoic carbonate margins, induced significant basinward translation due to gravitational loading. Shelf margin sediment loading and faulting created accommodation space and, where the Louann Salt was encountered, major salt evacuation. The resulting sedimentary accumulations were unusually thick (often >25,000 ft) but barely kept pace in the northern GoM with sediment influx from numerous continental-scale rivers. Loading onto salt also created complex salt mobilization and salt–sediment interaction that set up a wide diversity of trap types, heat flow variations, pathways for hydrocarbon migration, **depositional architectures**, and seal rock distributions.

As will be discussed in Section 9.4, improvements in imaging and illumination of the **subsalt** structure has vastly enhanced our understanding of the early basin history in the slope and **abyssal plain**. Regional to basinal scale seismic analysis has led to recognition of both extensional and contractional tectonics (and even raft tectonics) throughout the Mesozoic and Cenozoic. The extensive seismic and well control means that the structures here are well-imaged and thus studied (Worrall and Snelson 1989; Nelson 1991; Jackson *et al.* 1994; Diegel *et al.* 1995; Peel *et al.* 1995; Watkins *et al.* 1996a; Rowan *et al.* 2000, 2016; Radovich *et al.* 2007).

It is therefore worthwhile to describe some of the important structural styles that have been identified to date. It is also useful to view these tectonic features in the context of structural domains (Section 1.4) and 10 basin-scale cross-sections (Section 1.5).

https://doi.org/10.1017/9781108292795.003 Published online by Cambridge University Press

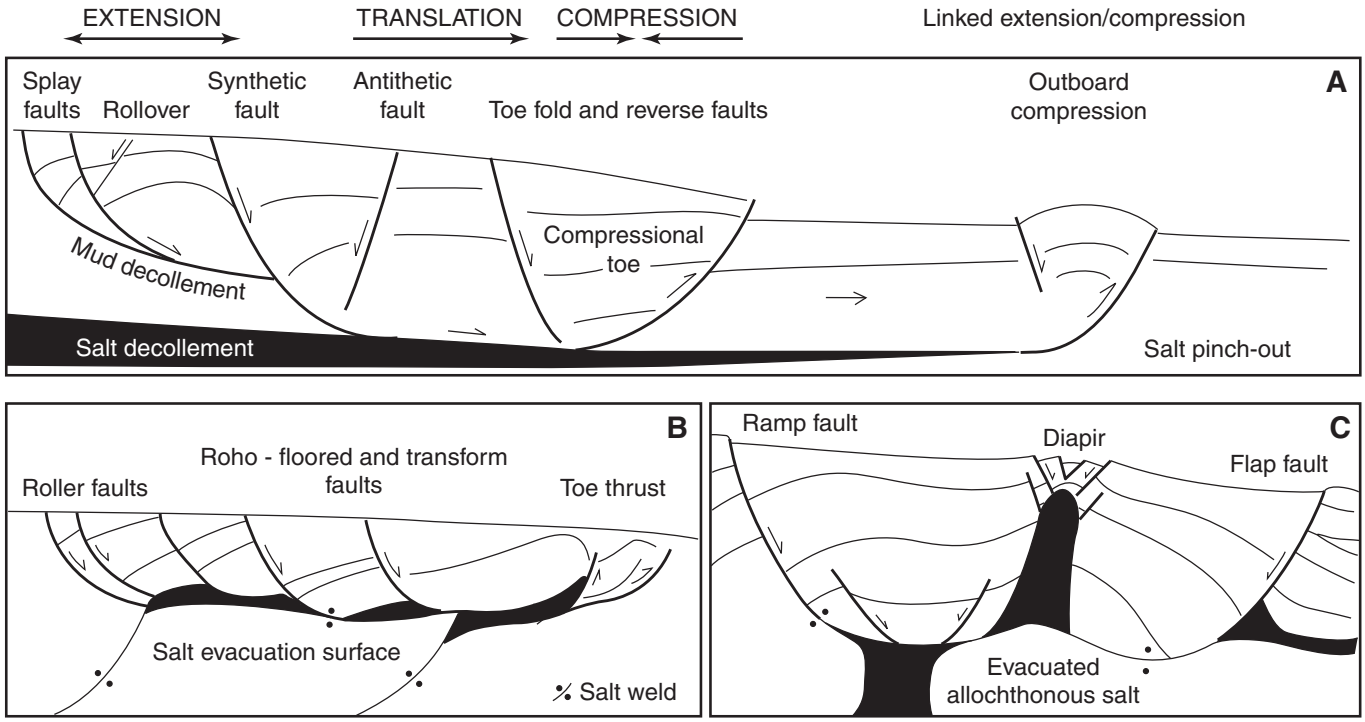

Figure 1.7 GoM gravity tectonics. (A) Linked extension and compression. (B) Roho salt detachment. (C) Salt withdrawal minibasin. From Galloway (2008).

Several pre-conditions set up the complex and diverse assemblages of GoM basin gravity tectonic structures. The combination of a thick, basin-floor Louann Salt substrate, rapid sediment loading, and offlap of a high-relief, continental margin sediment prism has resulted in mass transfer of salt and overpressured mud upward and basinward throughout Gulf history.

1.3.1 Growth Fault Families and Related Structures

Growth faults tend to nucleate and grow during active deposition at the **continental margin** (Winker 1982; Watkins *et al.* 1996b; Jackson and Hudec 2017). Here, extension results from basinward gravitational gliding or translation of the sediment wedge along a **detachment** zone, typically found within salt or overpressured deep marine mud (Rowan *et al.* 2004). Extension creates a family of features, including primary synthetic growth faults, splay faults, antithetic faults, and rollover anticlines (Figure 1.7A). In many parts of the GoM, updip extension is more or less balanced by a similar degree of contraction in downdip areas, as discussed in the following sections.

1.3.2 Basin-Floor Contractional Fold Belts

Basinward gravity spreading or gliding along a detachment zone, and resultant updip extension, requires compensatory compression at the toe of the displaced sediment body (Weimer and Buffler 1992; Hall *et al.* 1993; Fiduk *et al.* 1999; Trudgill *et al.* 1999). Contractional features include anticlinal toe folds and reverse faults (Figure 1.7A). They commonly form at the base of the slope, but can also extend onto the basin plain where a stepped discontinuity or termination of the decollement layer occurs. The deepwater fold belts (Atwater, Mississippi, etc.) are thought to represent adjustments to significant updip extension (Radovich *et al.* 2007). In other areas, extension may be balanced by squeezing salt bodies or salt weld development (Jackson and Hudec 2017; see Section 1.3.6).

1.3.3 Allochthonous Salt Bodies, Including Salt Canopies and Salt Sheets

Loading of the Louann Salt has resulted in regional extrusion of salt basinward and upward (Diegel *et al.* 1995; Fletcher *et al.* 1995; Peel *et al.* 1995). **Allochthonous salt** canopies typically develop beneath the continental slope, where salt rises as a series of coalescing diapirs or as injected tongues. Salt may also be extruded to the surface, forming salt sheets, or nappes, which move basinward, much like salt glaciers (Jackson and Hudec 2017).

1.3.4 Roho Fault Families

Lateral salt extension by gravity spreading creates a linked assemblage of extensional faults and compensating, downslope compressional toe faults, anticlines, and salt injections in the overlying sedimentary cover (Rowan 1995; Schuster 1995). In some cases, the top of allochthonous salt can acts as a decollement surface for faults (Figure 1.7B), as does autochthonous salt previously described. These are called **roho systems** and often occur in stratigraphically distinct fault groups or **fault families**.

https://doi.org/10.1017/9781108292795.003 Published online by Cambridge University Press

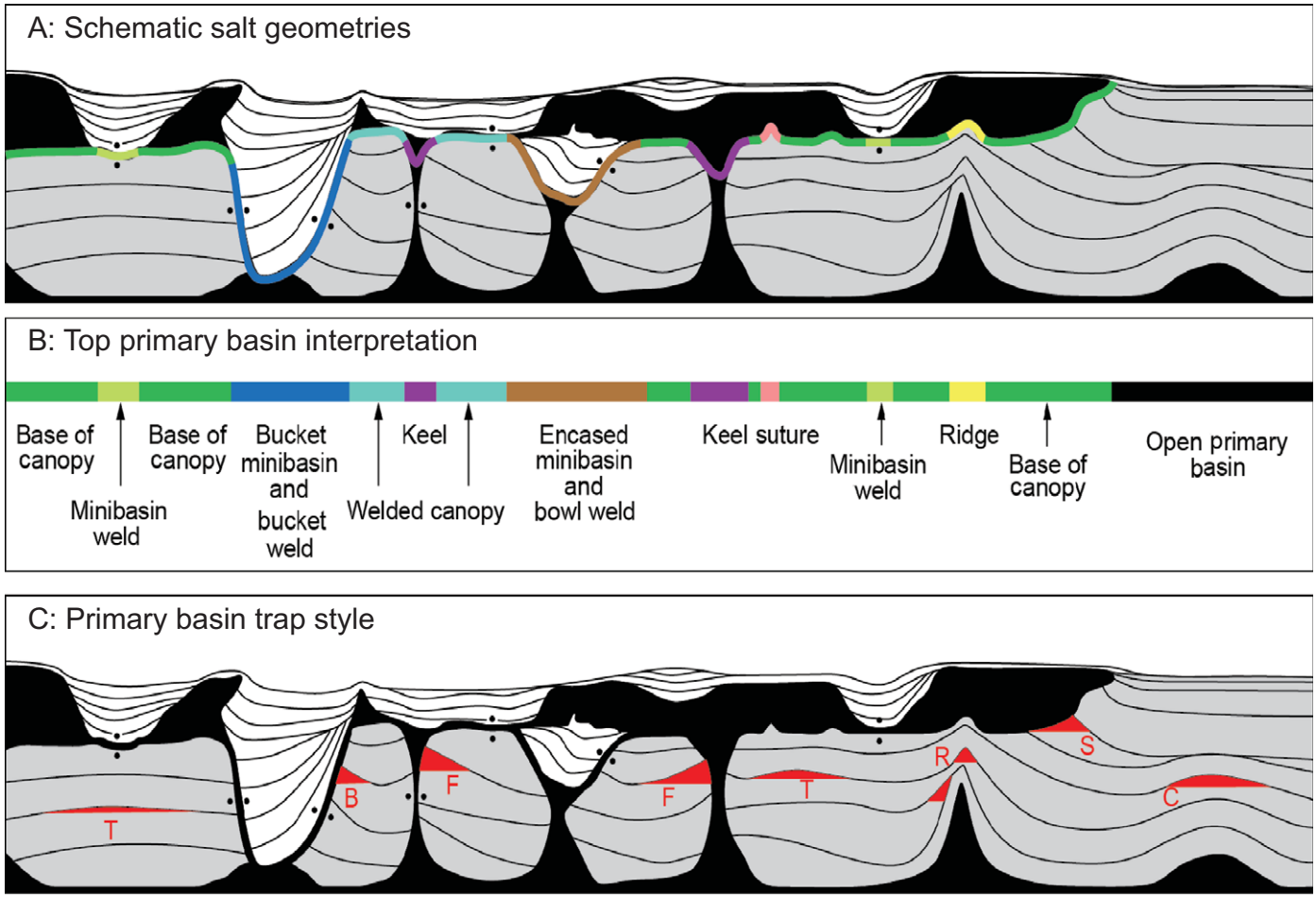

Figure 1.8 Schematic cross-sections of the bucket weld province. (A) Schematic salt geometries based on seismic interpretation. (B) Primary top basin interpretation. (C) Primary basin trap style. Letters indicate different trap styles in subsalt domain. Modified from Pilcher *et al.* (2014).

1.3.5 Salt Diapirs and Their Related Withdrawal Synclines and Minibasins

In the Gulf margin basins and embayments, salt **diapirs** rise directly from the autochthonous Louann "mother" salt (Seni and Jackson 1983; Fletcher *et al.* 1995; Rowan 1995; Rowan and Weimer 1998). Basinward, depositional loading of salt canopies and sheets beneath shelf and slope areas also causes renewed salt stock evacuation, creating high-relief salt diapirs and intervening depressions (Figure 1.7C). Progressive **salt evacuation** creates shifting, localized sites of extreme subsidence and sediment accumulation. Resulting features include withdrawal synclines created by local evacuation of salt from diapir flanks, bathymetric depressions, called minibasins, that form local depocenters, turtle structures, and local fault families, including down-to-basin ramp faults, counter-regional flap faults, and crestal faults above salt bodies.

1.3.6 Salt Welds

Salt welds are surfaces or zones that join strata originally separated by either autochthonous or allochthonous salt (Hudec and Jackson 2011). These are present where nearly complete expulsion of salt from stock feeders, dikes, salt tongues, or salt canopies has occurred (Jackson and Cramez 1989; Jackson *et al.* 1994; Figure 1.7B,C). Because the welds form some time after the deposition of adjacent strata, these juxtapose discordant stratigraphic intervals, sometimes with significant angularity of converging reflections (Hudec and Jackson 2011). Primary, secondary, and tertiary welds can be identified on the basis of the type of salt body that was welded (Jackson and Hudec 2017). Welds can also serve as detachment surfaces for younger listric faults.

Younger (secondary) sedimentary minibasins may be welded against older (primary) minibasins, resulting in drastically different ages, lithologies, and subsurface pressures (Pilcher *et al.* 2011; Figure 1.8). These are particularly prominent in a portion of the central GoM, the so-called "**bucket weld**" province. These bucket welds can act as lateral boundaries to hydrocarbon traps.

Salt welds can also act as regional decollement surfaces even when obvious linkage to downdip contraction is lacking. Regional decollements at welds are also known to be significant horizontal pressure barriers, with a significant increase in

https://doi.org/10.1017/9781108292795.003 Published online by Cambridge University Press

pressure in sub-weld intervals and attendant increase in risk, uncertainty, and well costs (see Section 9.20.1 on the Wilcox deep shelf play). Reverse faults can occur along welds (thrust welds), as observed in Campeche.

1.3.7 Rollovers and Expulsion Rollovers

Thickening and bending of strata toward a listric normal fault is commonly observed in the GoM Cenozoic and Mesozoic intervals. If expulsion of salt occurs to cause stratal thickening and rotation, with or without a fault, this structure is referred to as an **expulsion rollover** (Ge *et al.* 1997; Jackson and Hudec 2017). Large expulsion rollover structures have been identified in the Mississippi Canyon protraction block and represent some of the largest undrilled prospects in the basin (Harding *et al.* 2016). The orientation of these expulsion rollovers may indicate the general direction of sediment transport and loading (McDonnell *et al.* 2008), though these features are several orders of magnitude larger than depositional clinoforms and should not be used to indicate the location of paleo-shelf margins.

1.3.8 Carapaces and Rafts

When moving salt carries roof material that is not firmly attached to surrounding strata, stratigraphic discontinuities can occur. Transported roof material can be tens of kilometers in lateral extent and sometimes as thick as the salt body (Jackson and Hudec 2017). The term carapace is used here in a restrictive sense to describe detached blocks above salt that have moved vertically relative to the surrounding strata, either actively by diapir rise or passively as younger sediments are deposited around the salt-supported blocks (Figure 1.9). Early drilling at or around the allochthonous salt canopy encountered blocks which tended to be older, thinner, and/or more stratigraphically condensed than the adjacent non-carapace interval (Hart *et al.* 2004). Carapaces are often structurally much higher than the regional level of coeval strata. For example, the Norton well (GB 754 #1) penetrated a carapace block where Top Cretaceous was encountered at 7180 ft (2189 m), much shallower than the regional depths of Cretaceous, closer to 30,000 ft (9.1 km; Cunningham *et al.* 2016). Initially, stratigraphic discontinuities within carapaces caused considerable confusion, including the misinterpreted Middle Cretaceous unconformity (MCU), which later analyses proved was actually the Cretaceous–Paleogene boundary (K–Pg; Dohmen 2002).

Carapaces do accumulate sediment above a diapir documenting that diapir's history, but also record information on older strata that is relevant to regional or basin reconstructions. Carapaces containing organically enriched intervals within both the Tithonian and Ceno-Turonian intervals provide critical evidence in characterization of these source rocks (Cunningham *et al.* 2016).

Rafts are more complicated salt tectonic features that are defined in two different ways. First, we recognize rafts as

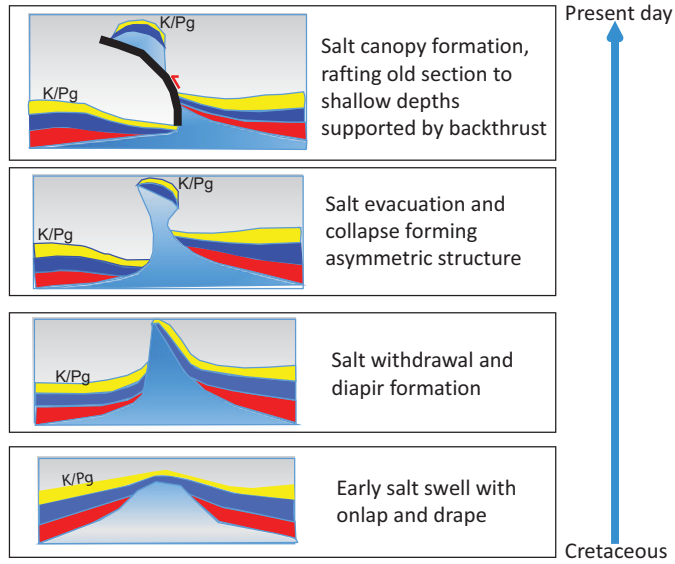

Figure 1.9 Development of a salt-related carapace structure. Modified from M. Rowan (pers. comm.).

stratigraphic blocks formed as part of raft tectonic processes. Raft tectonics is a form of thin-skinned extension, with unusually large degrees of extension such that the footwall and hanging wall are often not in contact, unlike growth faults (Jackson and Hudec 2017). Raft gaps are filled in by synkinematic (syn-extensional) strata. Raft tectonics is well-documented in the Albian interval of Angola and the Oxfordian interval of the DeSoto Canyon protraction block (Pilcher *et al.* 2014).

A second use of the term raft applies to stratigraphic blocks that have been moved considerable distances downslope by allochthonous salt. For example, it is established from 3D seismic analysis that the salt canopy in the deepwater northern GoM has transported over 20 raft blocks across the Alaminos Canyon, Keathley Canyon, Walker Ridge, and Green Canyon protraction blocks, with distances ranging from less than 3 km to more than 80 km from their original positions (Fiduk *et al.* 2014). Over 3100 km^2 of rafted strata was identified, largely accumulating near the terminus of the salt canopy.

Primary or secondary minibasins (terminology of Pilcher *et al.* 2011) can become encased in salt as allochthonous salt flows over the minibasin subsiding onto a deeper salt level (Hudec and Jackson 2011). In some cases, salt evacuation continues, and the minibasin is instead surrounded by welds (Rowan and Inman 2011).

Thus, it is very important to consider the tectonic history of vertical and lateral salt transport when analyzing stratigraphic information from carapaces, rafts, and encased minibasins. Stratigraphic discontinuities are common, and in areas of poor seismic imaging are only revealed by drilling and biostratigraphic analysis. Some wells have penetrated salt-overturned intervals, where biostratigraphic datums are encountered in reverse order, resulting in major drilling "surprises" (Box 1.1).

https://doi.org/10.1017/9781108292795.003 Published online by Cambridge University Press

Box 1.1 Stratigraphic Surprises Caused by Salt Tectonics

Seismic correlations in the deepwater GoM are often challenging due to the complexity of salt tectonics, limits on illumination below the thick and continuous allochthonous salt canopy, and imaging constraints around parautochthonous salt. In some areas, seismic imaging has failed to reveal the true stratal geometries, resulting in unanticipated structural interpretation problems encountered while drilling (Olson *et al.* 2015).

A prime example is a well drilled in the Green Canyon protraction block 639 (GC 639 #1), drilled in 2009 (Figure 1.10). After drilling through a normal Pleistocene to Pliocene stratal interval, and then a thick allochthonous salt body, the well began to encounter Cretaceous strata in reverse stratigraphic order. The quality of biostratigraphic tops was reasonably good, with most referred to as "definite" (DEF). Plotting the absolute ages of the various biohorizons indicates some variation but an overall downward younging of the interval (Figure 1.10A). This must have caused some concern, particularly if the trend was unanticipated. The well reached total depth (TD) near the top of the overturned Cretaceous. It is likely that the Mesozoic interval penetrated by GC 639 #001 was overturned by salt (Figure 1.10B).

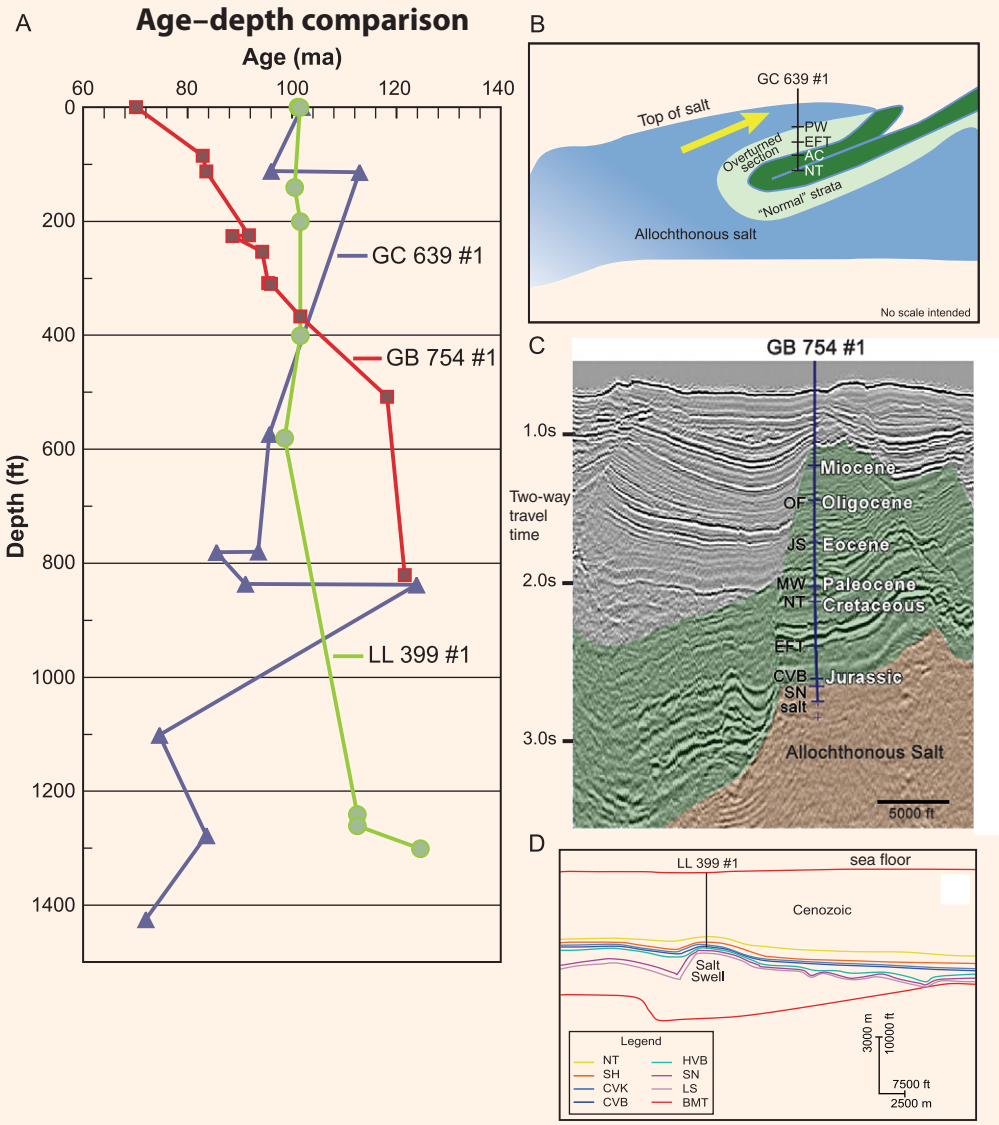

Figure 1.10 (A) Age–depth comparison of three deepwater GoM wells with depths (in feet) normalized to shallowest Mesozoic horizon penetrated in each well. Diversity of Mesozoic well penetrations in the deep GoM basin are illustrated by (B). (B) Well GC 639 #1 shown on a schematic structural configuration drawn from the original 2D seismic line. (C) Well GB 754 #1 (modified from Hart *et al.* 2004) is shown with stratigraphic horizons used in this book shown to the left of the well bore. (D) Well LL 399 #1 on a schematic structural configuration drawn from the original 2D seismic line. Sediment accumulation rates and structural geology related to the wells are discussed in the text.

https://doi.org/10.1017/9781108292795.003 Published online by Cambridge University Press

Box 1.1 (*cont.*)

The GC 639 #1 well contrasts with the normal stratigraphic order encountered by two other wells penetrating the same stratigraphic interval elsewhere in the basin (Figure 1.10). GB 754 #1 (Norton **Prospect**) drilled through a stratigraphically condensed interval above a shallow salt structure or carapace feature (Figure 1.10C). LL 399 #1 (Cheyenne Prospect) tested a deep (parautochthonous) salt structure (Figure 1.10D).

GB 754 #1 has a relatively continuous, but low-sloping trend in comparison with most of the LL 399 #1 interval penetrated (the exception being the bottom 30.48 m [100 ft] just above the salt). The estimated sediment accumulation rates (<16 ft/my [4.8 m/my]) of GB 754 #1 are far lower than those of LL 399 #1 (>55 ft/my [16.7 m/my]), consistent with the former well having penetrated a condensed interval on a salt–carapace structure (Figure 1.10C). LL 399 #1 well penetrated a lower relief salt structure, with high sediment accumulation rates above the salt-influenced zone and lower rates just above the salt (Figure 1.10D). Seismic data confirm these structural differences. Taking overturning of the Mesozoic interval by salt into account, calculated sediment accumulation rates of >47 ft/my (14.3 m/my) for GC 639 #1 is more comparable with that of LL 399 #1 than with GB 754 #1, consistent with the idea that the interval penetrated in GC 639 #1 was originally within a subsiding, deepwater, primary basin until salt emplacement overturned the Mesozoic interval, rather than a modified carapace structure or other structural oddity.

Numerous other wells have encountered either reverse stratigraphic intervals, thin and condensed intervals on carapaces, or intervals that are spatially out of place due to salt rafting (Hart *et al.* 2004; Fiduk *et al.* 2014). Biostratigraphic analyses are a key tool for understanding such stratigraphic surprises, particularly where imaging and illumination are hampered by salt thickness and complexity.

1.4 Structural Domains

Original basin-scale cross-sections of the greater GoM largely used well logs to define structural provinces of the basin (e.g., Morton *et al.* 1988; Morton and Ayers 1992). This was due to the lack of long, regional 2D seismic lines or poor imaging around salt or various complex structures. Nonetheless, broad structural domains were defined and have, for the most part, been confirmed by new seismic interpretations. The exceptions are subsalt structural provinces, for obvious reasons, and areas with limited well control.

1.4.1 Basement Structural Province

The periphery of the greater GoM basin, underpinned by thick transitions to the continental crust, is segmented by a series of prominent basement structures (Figure 1.3; Ewing and Lopez 1991). Their influence on overlying stratigraphy has long been known as early exploration efforts targeted these, based on gravity, magnetics, or early single- or multi-fold seismic reflection. Established structures include a halo of embayments (epicratonic basins that open to the central Gulf) and closed basins and intervening arches and uplifts (Figure 1.3; Ewing 1991). The basins and embayments typically contain a significant thickness of Louann Salt and thicker sequences of Jurassic and Lower Cretaceous strata relative to the adjacent arches and uplifts. Salt-floored basins, including the East Texas basin, North Louisiana salt basin, Mississippi salt basin, and Apalachicola Embayment (also known as the DeSoto Canyon salt basin) contain well-described families of salt domes and related structures (e.g., Seni and Jackson 1983).

Basement highs, arches, and anticlines like the Wiggins Arch, Sabine Uplift, Llano Uplift, Middle Ground Arch, etc., are known to have been reactivated multiple times during multiple Mesozoic and Cenozoic tectonic events (Ewing 1991). Several of these marginal highs, including the San Marcos Arch, Sabine Arch, and Monroe Uplift display short pulses of uplift of as much as a few hundred meters, creating angular unconformities in Middle Cretaceous and Lower Eocene strata (Laubach and Jackson 1990). These pulses generally correlate to stages of Laramide thrusting, in turn related to changing rates of Pacific margin plate convergence and changing intracratonic compressional stress. Extensive crustal heating across northern Mexico and the southwestern USA (Gray *et al.* 2001) uplifted and tilted Mesozoic and Early Cenozoic strata of the western Gulf. The boundary between thick and thin transitional crust is reflected by a subsidence hinge that became the focus for development and stabilization of the Cretaceous continental shelf margin, most clearly marked by an extensive reef system.

Most of these structures formed in the Mesozoic, but their influence on depositional trends persisted into the Cenozoic. The basement highs sometimes acted as drainage divides between major paleo-river systems. For example, mapping of the Tuscaloosa paleo-river system indicated that fluvial channels avoided the structural highs of the Wiggins Arch and surrounding positive features, terminating at the coeval lowstand shelf margin where the Ceno-Turonian interval is greatly expanded (Woolf 2012; Snedden *et al.* 2016b).

The Middle Ground Arch (Southern Platform), which is entirely offshore, is thought to have influenced radial rafting of the Smackover–Norphlet interval (Pilcher *et al.* 2014), as will be discussed in Section 3.3.4.

1.4.2 Gravity Tectonic Domains

Downdip of the basement structures is a mosaic of genetically related gravity tectonic features that can be grouped into two distinct structural domains, above and below the allochthonous salt canopy (Peel *et al.* 1995; Hudec *et al.* 2013b; Figures 1.11 and 1.12). The configuration of basement rock below the canopy controlled the original Louann Salt distribution and its immediate post-depositional downdip migration onto contemporaneous or newly formed oceanic crust. The near-end of Cretaceous canopy architecture in turn influenced Cenozoic depositional patterns and faulting, detachment, and further basinward translation of salt and sediments.

https://doi.org/10.1017/9781108292795.003 Published online by Cambridge University Press

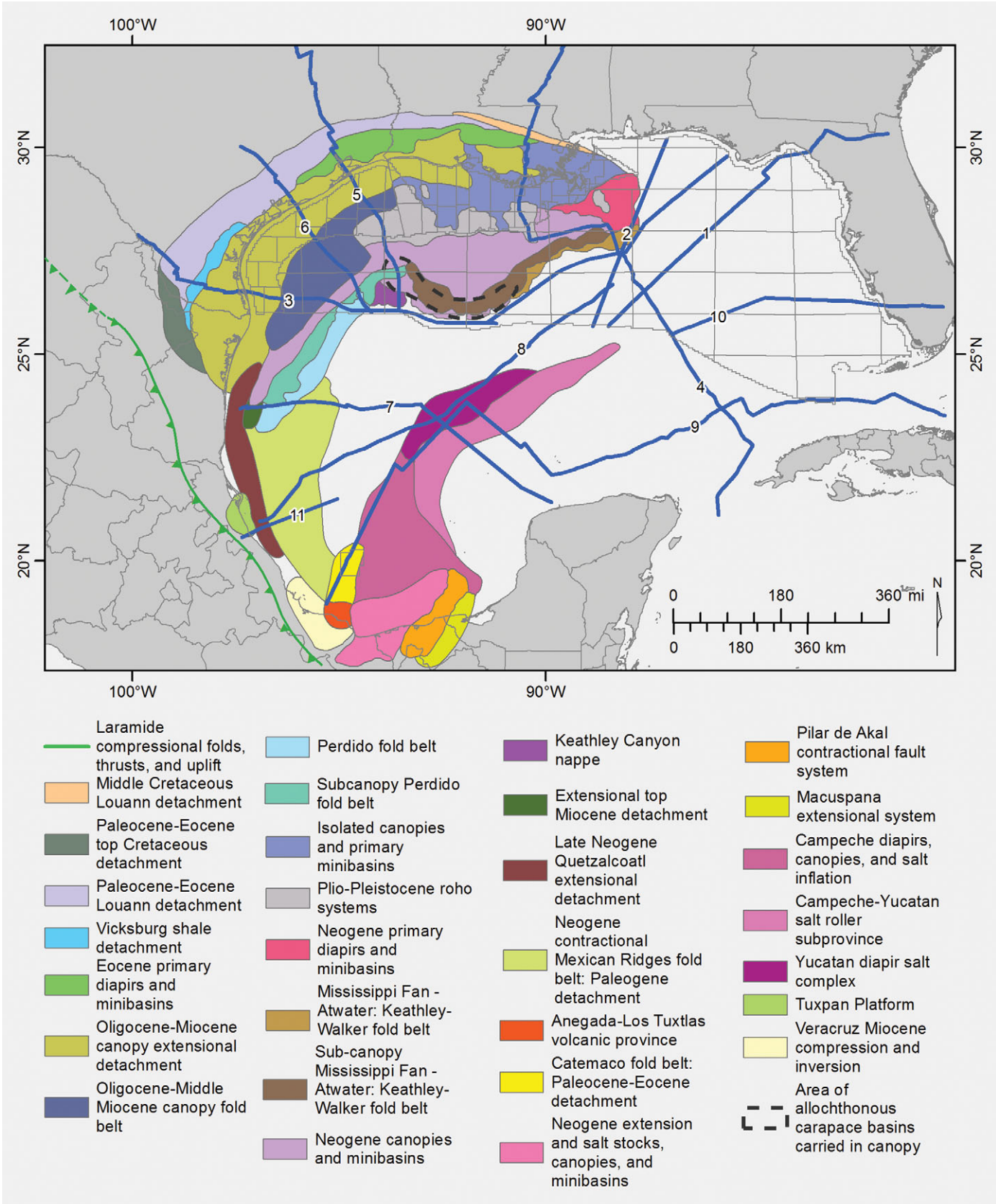

Figure 1.11 Tectonostratigraphic provinces with cross-section locations (blue lines) for Figures 1.13–1.22.

https://doi.org/10.1017/9781108292795.003 Published online by Cambridge University Press

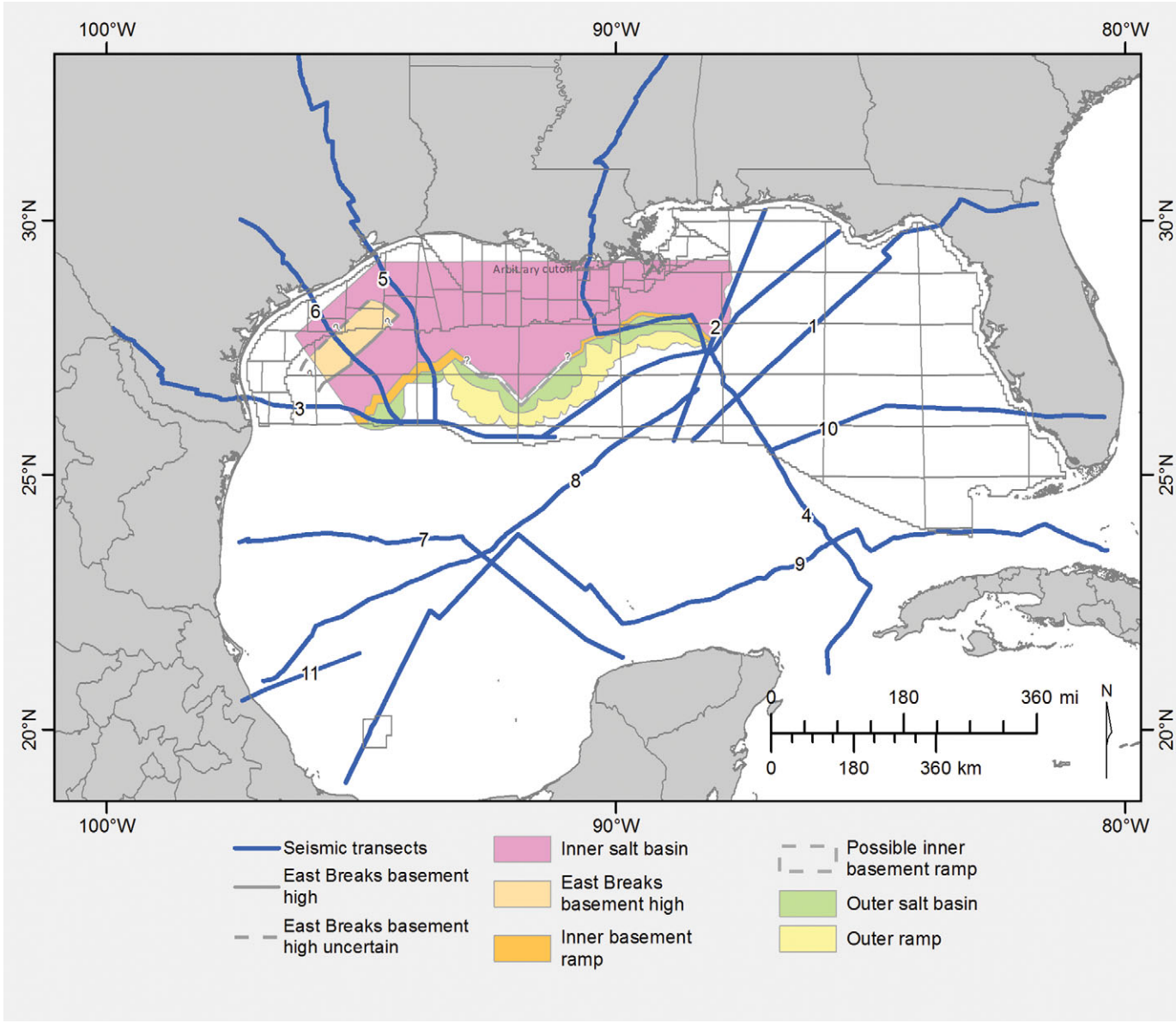

Figure 1.12 Subcanopy structural domain with cross-section locations (Figures 1.13–1.22). Modified from Hudec *et al.* (2013b)

1.4.2.1 Supracanopy Tectonic Domains

With a few exceptions, the northern GoM suprasalt structural domains had a finite time span of primary growth that can be associated with one or more successive episodes of Cenozoic siliciclastic sediment accumulation. Suprasalt domains generally become younger basinward, beginning with the Paleocene–Eocene detachment (at the top of the Cretaceous interval) and culminating in the Plio-Pleistocene minibasin and salt canopy domains of the continental slope (Figure 1.11). These structural domains will be further discussed in the context of the 10 regional cross-sections in Section 1.5.

The Middle Cretaceous Louann detachment, Oligocene–Lower Miocene, and Miocene compressional domains are exceptions to this general pattern. In addition, the full array of gravity tectonic structure domains of the northern Gulf basin includes the salt diapirs and related structures of the East Texas, North Louisiana, Mississippi, and DeSoto Canyon salt basins, which lie around the northern basin periphery, and a series of peripheral grabens, including the Luling–Mexia–Talco, State Line, and Pickins–Gilberton fault zones that delimit the landward extent of autochthonous Louann Salt. As mentioned earlier, growth of structures within these inboard domains occurred largely in Mesozoic time.

1.4.2.2 Subcanopy Tectonic Domains

Subsalt structural domains have only recently been identified due to the thick salt canopy that resisted illumination and imaging (Figure 1.12). Here, Louann Salt rests largely upon

https://doi.org/10.1017/9781108292795.003 Published online by Cambridge University Press

the "acoustic" basement, with limited coherent seismic data below this point. Seismic surveys, first in the Campeche basin of Mexico and then in the deepwater northern GoM, indicated a pronounced landward-dipping step in the acoustic basement, termed the inner ramp (Hudec *et al.* 2013b; Figure 1.12). With an estimated elevation of 1–4 km (depending on area and the local velocity model), this change in the base of salt is thought to represent the limit of the oceanic crust. This implies in turn that inboard transitional crust must be thinner or denser than the outboard oceanic crust (Hudec *et al.* 2013b). It also marks an important boundary for the original limit of the Louann Salt prior to extrusive sea floor spreading. Post-salt depositional creep onto oceanic crust varied as a function of ramp dip and depth, with greater salt advances in the area of the Walker Ridge salient, bounded to the west by the Brazos transfer fault (Figure 1.12). Original salt thicknesses of 3–4 km (1.7–2.5 miles) are thought to progressively decrease from the broad inner basin to the outer basin to the thinnest interval in the outer ramp perched on the oceanic crust (Hudec *et al.* 2013a). Salt canopy feeders are concentrated in the inner basin, where original source salt thicknesses were largest.

The concentration of contractional fold belts in the outer ramp and outer basin is not coincidental. Parts of the outer ramp were reactivated as thrusts during Miocene shortening of the Atwater fold belt (Hudec *et al.* 2013b). Large compressional anticlines of the Perdido fold belt, dated as Oligo-Miocene, are formed in the outer basin of the Alaminos Canyon area (Rowan *et al.* 2000). The Timbalier fold belt is found in the inboard subsalt or sub-weld region, but is thought genetically unrelated but similar in timing, reflecting uplift and seaward tilting of the onshore northern GoM during the Miocene (Jackson *et al.* 2011).

Another prominent subcanopy feature is the East Breaks basement high, where the acoustic basement is thought to be as shallow as 48 km (29 miles), based on new 3D wide azimuth (WAZ) seismic surveys (M. Hudec, pers. comm.). This structure likely effects local heat flow and depositional patterns of sediments as young as Oligo-Miocene age.

1.5 Basin-Scale Cross-Sections

Basin-scale cross-sections (Figures 1.13–1.22) illustrate the fundamental sedimentary and structural architecture of the greater GoM basin. All cross-sections are based upon newer vintage or recently reprocessed 2D depth-imaged seismic lines across the basin. Seismic horizons are correlated from well penetrations, which constrain the age, lithologic character, and paleo-environment of the Mesozoic and Cenozoic stratigraphic units.

These 10 representative cross-sections have been selected to illuminate several important observations: (1) change in deep crustal types (oceanic, transitional, continental); (2) important structural domains; (3) topographic/bathymetric features; (4) notable gravity tectonic features; (5) prominent basement structures; and (6) the large-scale, progressive shift in age of deposition and paleo-environment of the basin-fill. Shelf platform margins (Mesozoic) and shelf–slope interfaces (Cenozoic) are important paleophysiographic features that usually mark the transition from contemporaneous shelfal processes of waves, currents, and tides to the sedimentary gravity flows and mass transport/failures-dominated slope to abyssal plain. Note the boundary between thick and thin transitional crust, which became a subsidence hinge point, and often marks the position of the Mesozoic shelf platform margins, which in turn influenced Cenozoic expanded intervals due to increased accommodation.

Interpretation of subcrustal structure, such as the top of the mantle, was not attempted due to the use of 2D seismic reflection data that rarely permits unequivocal selection of the Moho boundary. Seismic refraction data, discussed in Section 1.2.2 provides guidance on cross-sections 1, 2, and 6 (see Van Avendonk *et al.* 2013, 2015; Christeson *et al.* 2014; Eddy *et al.* 2014), but recent vintage data was not available along the other sections.

It is important to note that in the last five years we have learned a lot more about the GoM through the effort to link onshore and offshore seismic data by seismic companies like ION. The reprocessing of older onshore data and merging with offshore data has allowed the first truly basinal cross-sections to be developed. For example, the presence of multiple, linked extensional–contractional structural belts of Early Paleogene and Oligo-Miocene age became evident (Radovich *et al.* 2007). From Cretaceous to Pleistocene, there is a repeated basinward migration with expansion as each interval fills the space in front of it created by extension and salt withdrawal. Radovich *et al.* (2011) estimated 100+ miles (161 km) of progradation and over 15,000 ft (4570 m) of aggradation. Without the dedicated efforts of seismic companies like ION, our understanding of this complex basin would not have been possible.

1.5.1 Cross-Section 1: Sigsbee Abyssal Plain to Peninsular Arch

Cross-section 1 is a transect from the northeastern Gulf, passing from the abyssal plain at the USA–Mexico international border to onshore northern Florida (Figure 1.13). Continental crust rises to depths as shallow as <1500 m (4920 ft) on the Peninsular Arch, as crystalline basement has been drilled in a number of onshore wells (Jordan *et al.* 1949). Penetrations include granites dated at 159 ± 3 Ma and basalts and diabases as young as 183 ± 5 Ma in the exotic Suwannee terrane of south Florida (Heatherington and Mueller 2003). While the Cenozoic interval is relatively thin in comparison to the central Gulf (reflecting limited fluvial input), the Mesozoic interval thickens substantially to the southwest, into the area of the Florida Middle Ground Arch and Tampa Embayment. The physicographic slope marks an abrupt termination of many Mesozoic units at the Florida Escarpment. Cretaceous strata have actually been dredged from the sea floor, suggesting that

https://doi.org/10.1017/9781108292795.003 Published online by Cambridge University Press

https://doi.org/10.1017/9781108292795.003 Published online by Cambridge University Press

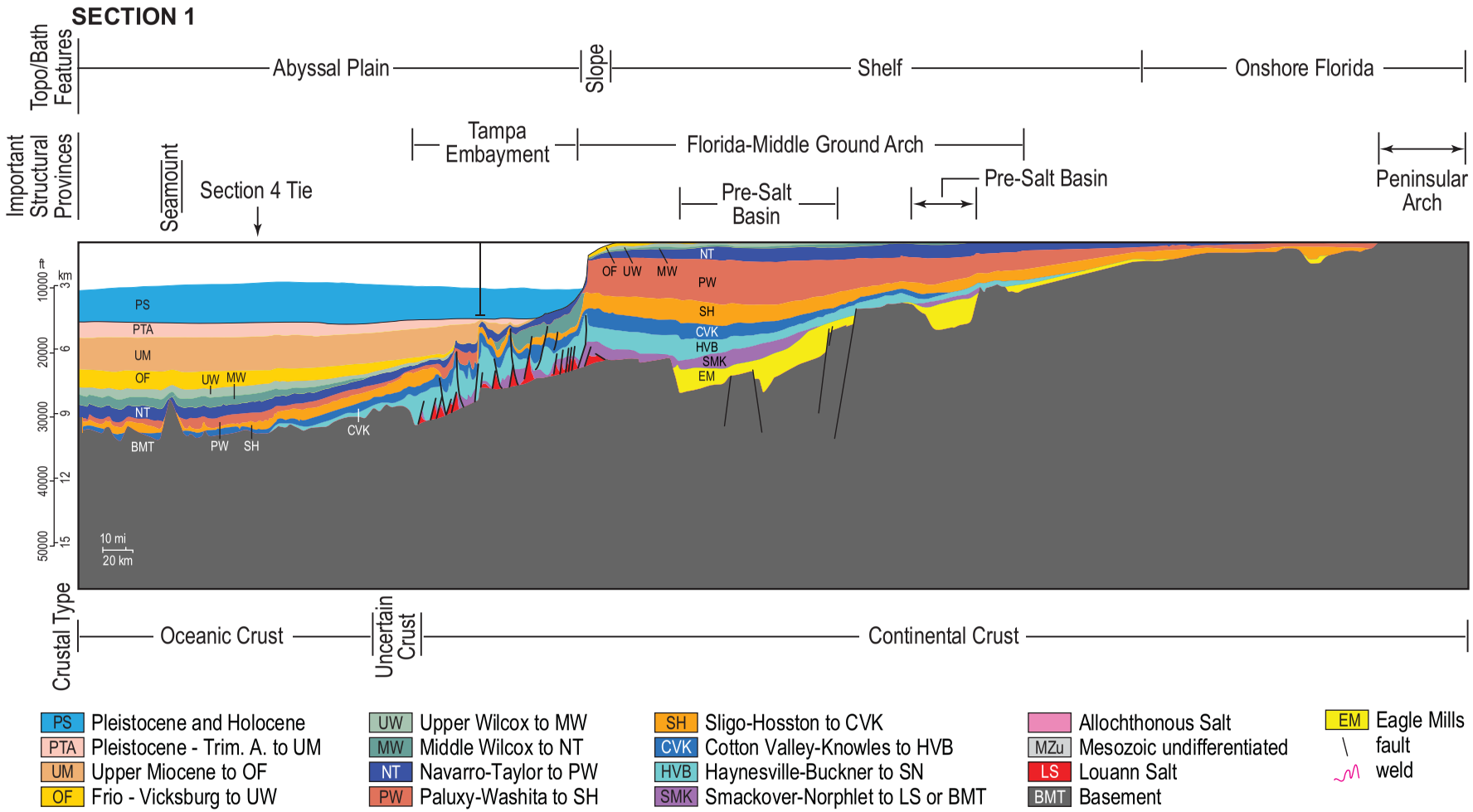

Figure 1.13 GoM cross-section 1: US abyssal plain to Peninsular Arch.

the escarpment is an erosional remnant inherited from the K–Pg impact event and subsequent slope failures and adjustments (Freeman-Lynde 1983).

The shelf portion of the cross-section includes an interpreted pre-salt interval, sedimentary rocks likely of Triassic–Middle Jurassic age, known in onshore areas as the Eagle Mills. The interpreted seismic structure is that of a horst/graben, possibly a continuation of the east coast rift system documented in the coastal plain of South Carolina, Georgia, and other states (Heffner 2013; Goggin and Rine 2014; Rine *et al.* 2014). The nearby well GV-707 penetrated a poorly dated siliciclastic interval between the Cretaceous (Aptian–Valanginian) Sligo–Hosston and Paleozoic carbonates.

Further seaward is the basinal portion of the Tampa Embayment where Louann Salt diapirs and Mesozoic rafts of Smackover and Norphlet are thought to be present, as observed in the DeSoto Canyon area (see discussion of cross-section 2, Figure 1.14). No salt canopy formed here, reflecting the general thinning of original salt toward the southeast.

A pronounced step up in basement, a change in elevation of several kilometers, is coincident with the termination of Louann Salt. This marks the seaward limit of transitional continental crust. A short segment of uncertain crust gives way seaward to oceanic crust, documented by magnetic and gravity data, as discussed in Section 1.2.4).

The downlap of Mesozoic stratigraphic units onto transitional and oceanic crust provides some indication of timing of oceanic crust emplacement (Snedden *et al.* 2013). Oxfordian Norphlet and Smackover rafts appear to have glided onto the oceanic or uncertain crust, suggesting that salt was present during the initial stages of sea floor spreading in order to provide a decollement. In other areas, locally thick minibasins (primary basins) are thought to contain Norphlet- or Smackover-equivalent strata (M. Hudec, pers. comm.).

The Haynesville (Kimmeridgian) and basal Cotton Valley–Bossier (Tithonian) strata continue across the oceanic crust before lapping out onto the oceanic crust near the extinct spreading center. Subsequent depositional units continue across the section, though distal thinning is observed on the seismic sections.

A pronounced structural feature, located at the basement step, fits the established characteristics of a seamount, a basement feature with an elevation greater than 1 km (3280 ft) above the regional basement level (Snedden *et al.* 2014). Such seamounts are relatively common across this area of oceanic crust (Stephens 2009, 2010). As mentioned in Section 1.2.4, the slow spreading rates associated with the GoM opening are thought to be associated with unfocused magmatism and in turn the poorly organized distribution of seamounts like this. Cenozoic strata from Cretaceous upward to Middle Wilcox drape the seamount, and compactional related features extend upward to the Oligocene. A number of these structural features have been leased in recent years, yet no drilling plans have yet been filed with the = Bureau of Ocean Energy Management (BOEM) or Bureau of Safety and Environmental Enforcement (BSEE).

As mentioned, Cenozoic deposition on the Middle Ground Arch and adjacent onshore Florida is thin, with limited accommodation on the Mesozoic platform here. By contrast, Neogene strata, particularly the Pleistocene interval of 5000 ft (1524 m), thicken substantially over the abyssal plain. This marks the Pleistocene Mississippi River input, but also the Miocene contributions by the paleo-Tennessee system. Paleogene deposition thins toward the platform margin, reflecting general western (Laramide) sources and linked drainage networks.

1.5.2 Cross-Section 2: Florida Shoreline to USA–Mexico International Border

Cross-section 2 is located further to the west, extending from the USA international border to just seaward of the Florida shoreline (Figure 1.14). Mesozoic strata, particularly Jurassic and Early Cretaceous intervals, thicken dramatically into the DeSoto salt basin, also known as the Appalachicola Embayment. The Florida Middle Arch is prominent and its extension into the deepwater is the site of significant industry exploration efforts and nearby Norphlet reservoir discoveries such as the Appomattox Prospect (see Section 9.6).

The Norphlet raft province is well illustrated here (Figure 1.14). As described in Section 3.3.4, raft tectonics is a form of thin-skinned extension, with unusually large degrees of extension such that the footwall and hanging wall are often not in contact (Jackson and Hudec 2017). The dismembering of stratigraphic units occurs as blocks glide downslope on a detachment surface, in this case the top of the Louann Salt. Intervening troughs between raft blocks are filled with younger units, providing age control on the timing of rafting. Rafting apart of the Norphlet–Smackover interval must have been contemporaneous with deposition of the Haynesville–Buckner and Cotton Valley–Bossier as these fill in the gaps between rafts. In some areas Cotton Valley–Knowles and even basal Sligo–Hosston also fill raft gaps. The timing of sea floor spreading and rafting is similar enough to consider the possibility that there is a genetic linkage. Rafting is largely toward the oceanic crust, though radial rafting reflecting the Middle Arch structure has been suggested (Pilcher *et al.* 2014). The Smackover–Norphlet Rafts can be separated by diapirs or depositional troughs, making paleogeographic reconstructions very difficult, but essential to exploration well locations, as will be discussed in Section 3.3.4.

Further seaward, the uncertain zone between oceanic and continental crust is also accompanied by a basement step, though with less relief than observed on cross-section 1 (Figure 1.13). Salt appears to have crept onto unequivocal oceanic crust. Though the Louann Salt is now relatively close to its original position, the basinward translation necessitates modification of the term "autochthonous" salt to "**parautochthonous**" salt, following the nomenclature of Hudec *et al.* (2013a). This is also the area where a small segment of the Mississippi Fan–Atwater fold belt is present,

https://doi.org/10.1017/9781108292795.003 Published online by Cambridge University Press

https://doi.org/10.1017/9781108292795.003 Published online by Cambridge University Press

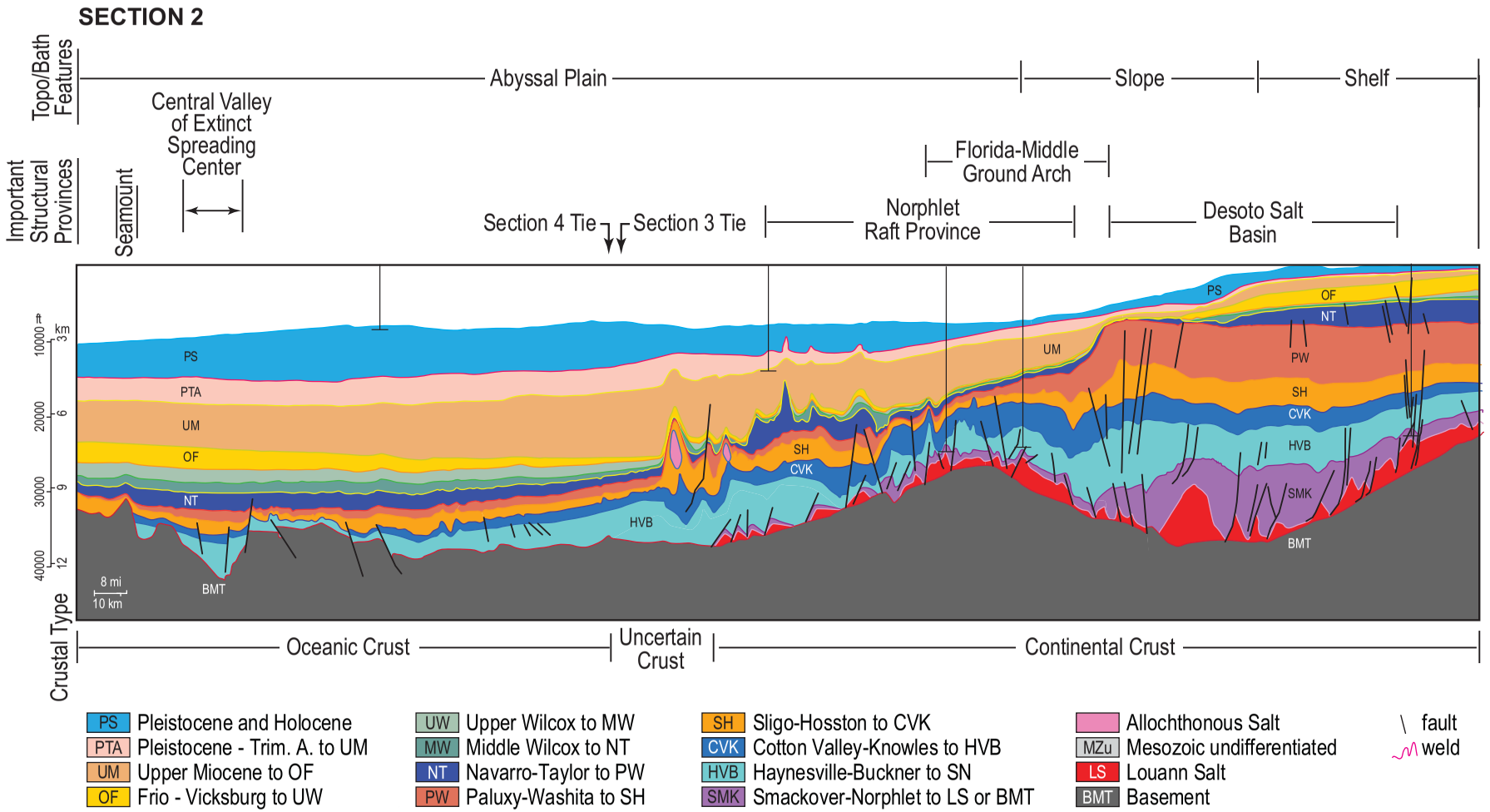

Figure 1.14 Cross-section 2: Florida shoreline to USA–Mexico international border.

with local thrust faults indicating some early crustal shortening.

The extinct spreading center is nicely developed toward the seaward end of the cross-section (Figure 1.14). Here is a large axial valley, about 20 km (12 miles) wide, with bounding basement structures (possible seamounts) and a dim to opaque infill interval below the Haynesville–Buckner seismic horizon. Normal faults dip toward the axial valley, similar to what has been previously described in the area (Snedden *et al.* 2014; Lin *et al.* 2019).

The total basin-fill is relatively thin, depressing the crust only to depths between 26,000 and 36,000 ft (8–11 km). The sedimentary interval is a bit deeper in the DeSoto salt basin at nearly 38,000 ft (12 km). Louann Salt is particularly thick here, exceeding 8000 ft (2.4 km) in the DeSoto salt basin, though this clearly reflects salt inflation.

Mesozoic platforms are well developed, particularly for the Jurassic Haynesville–Buckner (HVB), Cotton Valley–Bossier (CVB), and Cotton Valley–Knowles (CVK) at a position about 30 km (19 miles) seaward of the modern shelf edge. The Cretaceous Sligo–Hosston seems to be located in a similar position, indicating that the crustal boundary between thick and thin transitional crust has pinned the shelf margins due to changes in subsidence rates. Cenozoic shelf margins are all inboard of the Cretaceous and Jurassic platform margins. The Florida Escarpment is less pronounced here, instead a steep margin at Top Cretaceous (Top Navarro–Taylor) is observed, perhaps a byproduct of the Chicxulub impact event.

Growth faults are few in the Cenozoic interval and only Mesozoic growth along salt-detached faults is locally developed. Rafting is the dominant structural style, as discussed earlier.

Cenozoic deepwater reservoirs have been penetrated in portions of the area, but results to date have been disappointing in comparison to the Mississippi Canyon area, where giant discoveries (e.g., Thunderhorse Field) have been made. The lack of Cenozoic traps is one cause, though stratigraphic traps such as termination against the Cretaceous shelf margin have been considered, as will be discussed in Chapter 2.

1.5.3 Cross-Section 3: Onshore Texas to Onshore Florida

Cross-section 3 (Figure 1.15) is a transect from the onshore south Texas to the eastern basin margin and Florida onshore as described in cross-sections 1 and 2. The section in its central portion is located seaward of the Sigsbee Escarpment, where the salt canopy affects the sea floor. The abyssal plain section here illustrates trends in both Neogene and Paleogene strata, and thus is a veritable natural archive of the attendant sedimentary processes.

The variations between the western and eastern margins are notable. The sedimentary load on the west has depressed the crust to over 50,000 ft (15 km) near the present-day shelf margin offshore Texas (Figure 1.15). Gravity tectonics dominates the western margin, with numerous growth faults and multiple levels of fault detachment. The upper decollement is at a salt weld where Oligocene and Miocene age faults detach. The lower detachment surface for older Paleogene strata is founded upon the parautochthonous salt. The updip extension associated with this multi-level extension appears to be balanced, to some degree, by contraction within the Oligo-Miocene and Perdido fold belts, though local squeezing of salt can also occur (Radovich *et al.* 2007). Some faults nucleated at or near the Mesozoic platform margin or at the top of the Cretaceous. Faults also detach on the salt canopy.

The section crosses the Vicksburg Detachment, a well-known listric fault that nearly becomes horizontal as it slips along the Jackson Group Shales (Combes 1993; Feragen *et al.* 2007). The eastern portion of the cross-section shows limited salt stocks, which rise from the largely evacuated autochthonous Louann below, defining the eastern margin of the slope minibasins domain. Again, the Norphlet raft province is located just seaward of the Middle Ground Arch.

The Cenozoic sedimentary architecture is intimately convolved with the structural domains on the western margin. Shelf margins for each of the major Neogene and Paleogene units appear to be located at or just landward of the major growth and expansion of the various intervals. For some units like the Oligocene, much of the expanded interval represents slope deposition. Well penetrations indicate that much of the Oligocene interval is dominated by muddy lithologies and drilling in the Oligocene–Miocene interval has been challenging due to abnormal fluid pressures (P. Flemings, pers. comm.).

The Perdido fold belt is known to be linked to updip Oligo-Miocene extension (Trudgill *et al.* 1999; Gradmann *et al.* 2009; Radovich *et al.* 2011). These contractional folds have high relief and thickness due to the high sedimentation rates in the Cretaceous to Miocene interval that was shortened in the Neogene.

In the central portion of the cross-section (Figure 1.15), the abyssal plain, regional thickness trends provide a window on the source-to-sink processes of the Cenozoic basin-fill. Paleogene units (Middle and Upper Wilcox, Oligocene Frio–Vicksburg, and more condensed Upper Eocene Jackson Yegua Sparta) show clear eastward thinning, suggesting the Laramide source terranes were most important (Galloway 2008). The Lower Miocene shows a transition to eastward thickening in the Neogene stratigraphic interval, reflecting the rejuvenation of the Appalachians and rise of the Tennessee River as a major contributor to sand-prone fans in the Mississippi Canyon area (Galloway *et al.* 2011). The Pleistocene Mississippi Fan, the largest of the submarine fans to be formed, is apparent in the kilometer-scale interval above the Pleistocene Trim A (PTA, see Section 7.2) horizon that is banked against the Florida Escarpment. As will be discussed in Chapter 7, large Plio-Pleistocene channel–levee, mass transport, and lobate fans can be identified on high-resolution seismic data (Weimer 1990).

https://doi.org/10.1017/9781108292795.003 Published online by Cambridge University Press

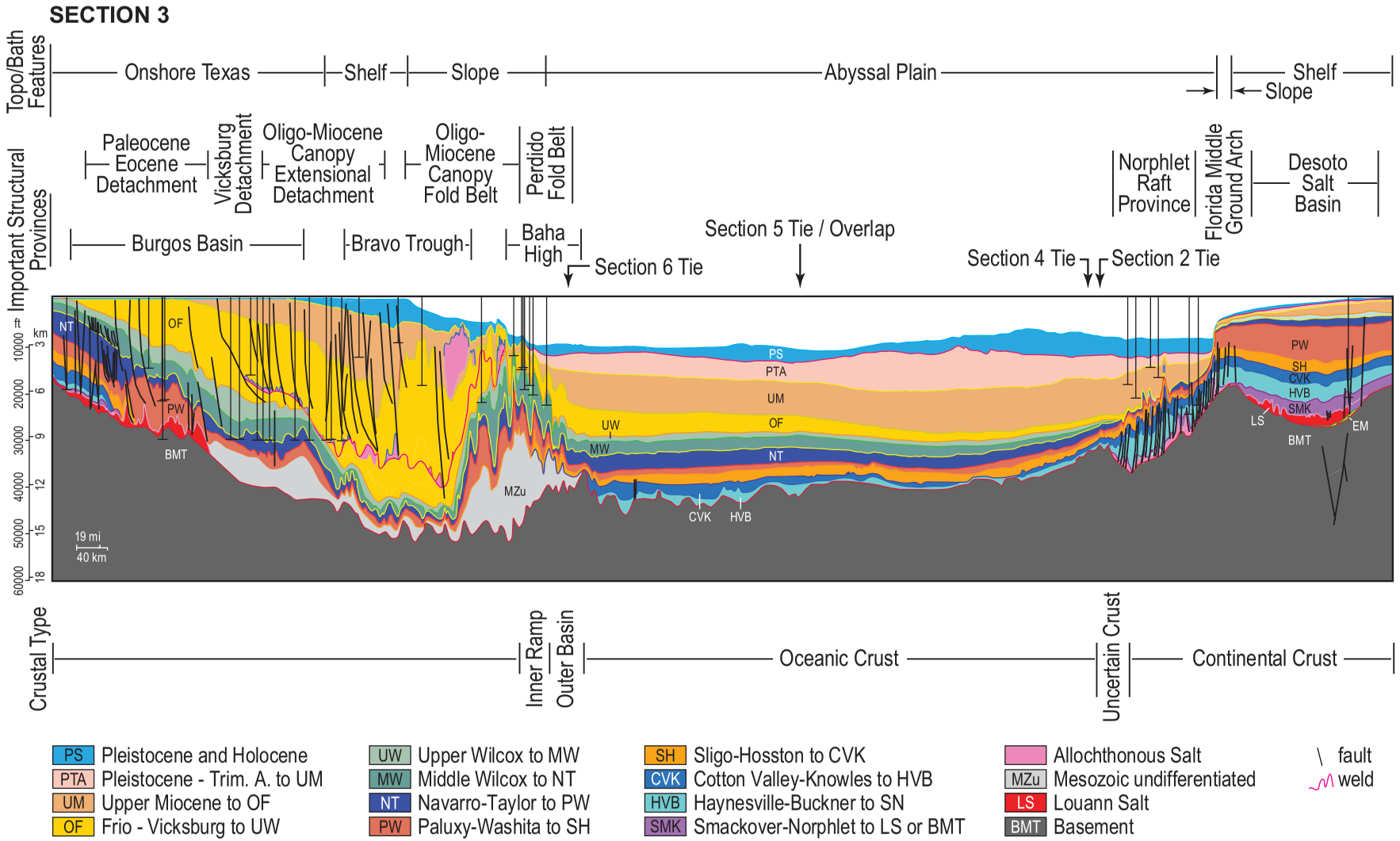

Figure 1.15 Cross-section 3: Onshore Texas to Onshore Florida.

1.5.4 Cross-Section 4: Black Warrior Basin to Yucatán Channel

Cross-section 4 (Figure 1.16) is a transect from the onshore Black Warrior basin to the USA–Mexico abyssal plain to the Cuban Platform, finally extending to the Yucatán Straits gateway to the Caribbean basin. The margin of the GoM basin can be defined at the hinge line between the Black Warrior basin, where Paleozoic sedimentary and basement rock are present near the surface, and the Mississippi salt basin to the south. The substantial thickening of the Jurassic strata in the Mississippi salt basin is clear evidence supporting placement of the GoM basin boundary here. Louann Salt also terminates near this margin and the Louann lapout and associated fault breakway zone are often used to demarcate the salt basin boundary (Ewing and Lopez 1991).

The Wiggins Arch basement structure borders the Mississippi salt basin to the south in Louisiana (Figure 1.16). Besides hosting a number of onshore discoveries, the Wiggins Arch acts as initiation point for successive downdip detachment zones starting with the Middle Cretaceous detachment zone. The crust is loaded to 50,000 ft (15.2 km), but as much as 40,000 ft (12.2 km) of that sedimentary interval is Cenozoic in age, a sign of the long-lived transport through the Mississippi River and its ancestors.

Isolated salt bodies and thick primary basins filled with Miocene to Cretaceous sediments give way to first extensive salt canopy just seaward of the modern shelf slope break. The Terrebone trough roho system, where extensional faults detach on one of the allochthonous salt bodies and/or welds, is denoted as the Oligo-Miocene salt weld (Hudec and Jackson 2011). Reconstructions of the Terrebone trough roho system show Early to Middle Miocene progradation expelled allochthonous salt seaward, toward the toe of the canopy, accompanied by considerable extension. By the Late Miocene, salt was largely expelled along the strike or dissolved, leaving the roho detachment, isolated **salt rollers**, and an extensive weld (McBride *et al.* 1998). Seaward rollover into an expulsion rollover near the Bay Marchand salt diapir (Schuster 1995) is not shown on this cross-section.

Further seaward are numerous supracanopy structures, including young secondary minibasins in Green Canyon and Atwater Canyon protraction blocks, where the section turns east–west (Figure 1.16). Below and at the seaward end of the salt canopy lies the Plio-Miocene Atwater fold belt, where deep salt diapirs (parautochthonous salt) occur along anticlinal axes. At this point, the cross-section turns to become more northwest–southeast trending across the abyssal plain and onward to Cuba.

Below the salt canopy on the modern slope of the USA sector is a relatively thick succession of Louann Salt that is conservatively estimated to be more than 5000 ft (1524 m) thick and to cover 220 km (136 miles) of lateral extent (Hudec *et al.* 2013a). The inner basin is the deepest portion of the Louann salt basin, where the greatest accumulation of evaporite-bearing interval is thought to have been deposited. Like elsewhere, there is substantial step up in acoustic basement, the inner ramp of Hudec *et al.* (2013a). Note that some portion of the relief is generated by the turn in the section at the Atwater fold belt.

The Cenozoic interval thins substantially toward Cuba and the Yucatán Straits to the south. Miocene strata alone thin from 8000 ft (2.4 km) to a few hundreds of feet (>30 m) as the interval lapouts onto the Cuba Platform margin. Mesozoic intervals are also thinner than known in the adjacent South Florida basin. The crystalline basement is as shallow as 12,000–16,000 ft (3.7–4.9 km) in the Yucatán Straits. These trends point to: (1) a distal position relative to major siliciclastic sources and linked river systems; and (2) the relatively recent joining of western and eastern Cuba microplates during the Eocene.

1.5.5 Cross-Section 5: Sabine Uplift to Sigsbee Escarpment

Cross-section 5 (Figure 1.17) extends from onshore Texas to deepwater GoM near the USA–Mexico international boundary. The Mexia–Talco fault zone is an extensional breakaway where salt thins to a zero edge (Hudec and Jackson 2011). The East Texas salt basin contains a series of generally north–south oriented diapirs and salt pillows toward the center of the basin where the original salt was thicker. Turtle structures formed by salt withdrawal into the adjacent diapirs is seen on nearby seismic lines (Jackson and Seni 1984). Note the over-thickened Albian and Aptian interval (Paluxy–Washita to Sligo–Hosston supersequences) located on the flanks of several salt domes. The intervening saddle is a remnant high that in some cases promoted reef development (Seni and Jackson 1983; Pashin *et al.* 2016).

Further seaward is a prominent basement structure called the Toledo Bend Flexure. It is notable as it marks the separation of the updip interior salt basins (East Texas, North Louisiana) and the central Louann basin proper (Hudec *et al.* 2013a). It is also thought to localize Mesozoic platform margins (Anderson 1979).

Strata south of the Toledo Bend Flexure dip rather steeply into the basin to the south, where Mesozoic horizons become difficult to trace basinward under a thick Cenozoic interval and allochthonous salt canopy (Figure 1.17). The Tiber well (KC 102 #1) penetrated the Top Cretaceous at 32,250 ft TVD-ss (true vertical depth subsea) (9830 m), which seismic mapping indicates is the regional level in the Keathley Canyon (KC) protraction block. In other wells, the Top Cretaceous may appear from first glance to be much shallower, but these are usually penetrations of salt-rafted carapace blocks, carried upward by differential salt movement, as described in Section 3.3.4.

Important transitions shown on the section include the rimmed platform margins, built up from the Jurassic to the end of the Albian, which give way seaward to several Cenozoic

https://doi.org/10.1017/9781108292795.003 Published online by Cambridge University Press

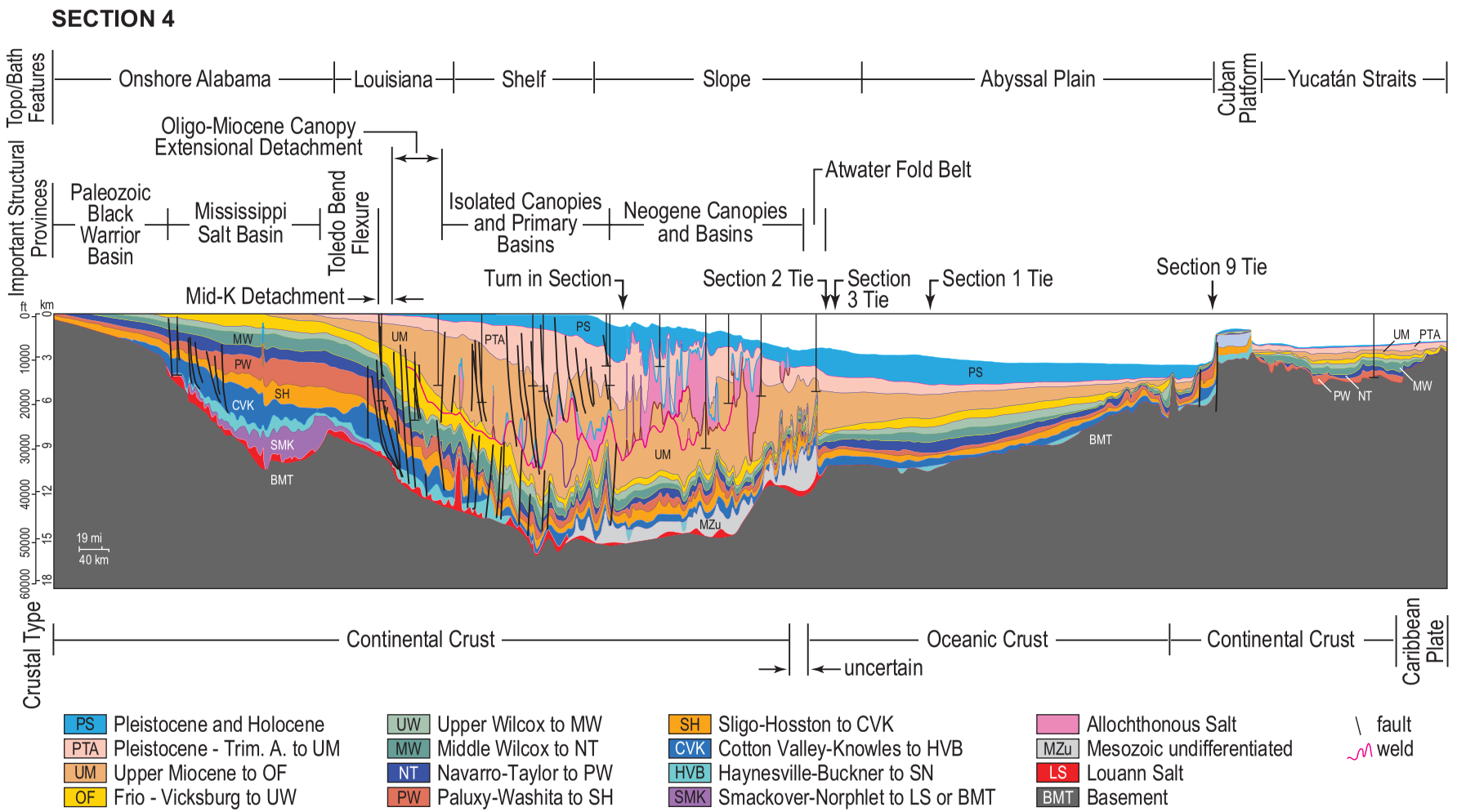

Figure 1.16 Cross-section 4: Black Warrior basin to Yucatán Channel.

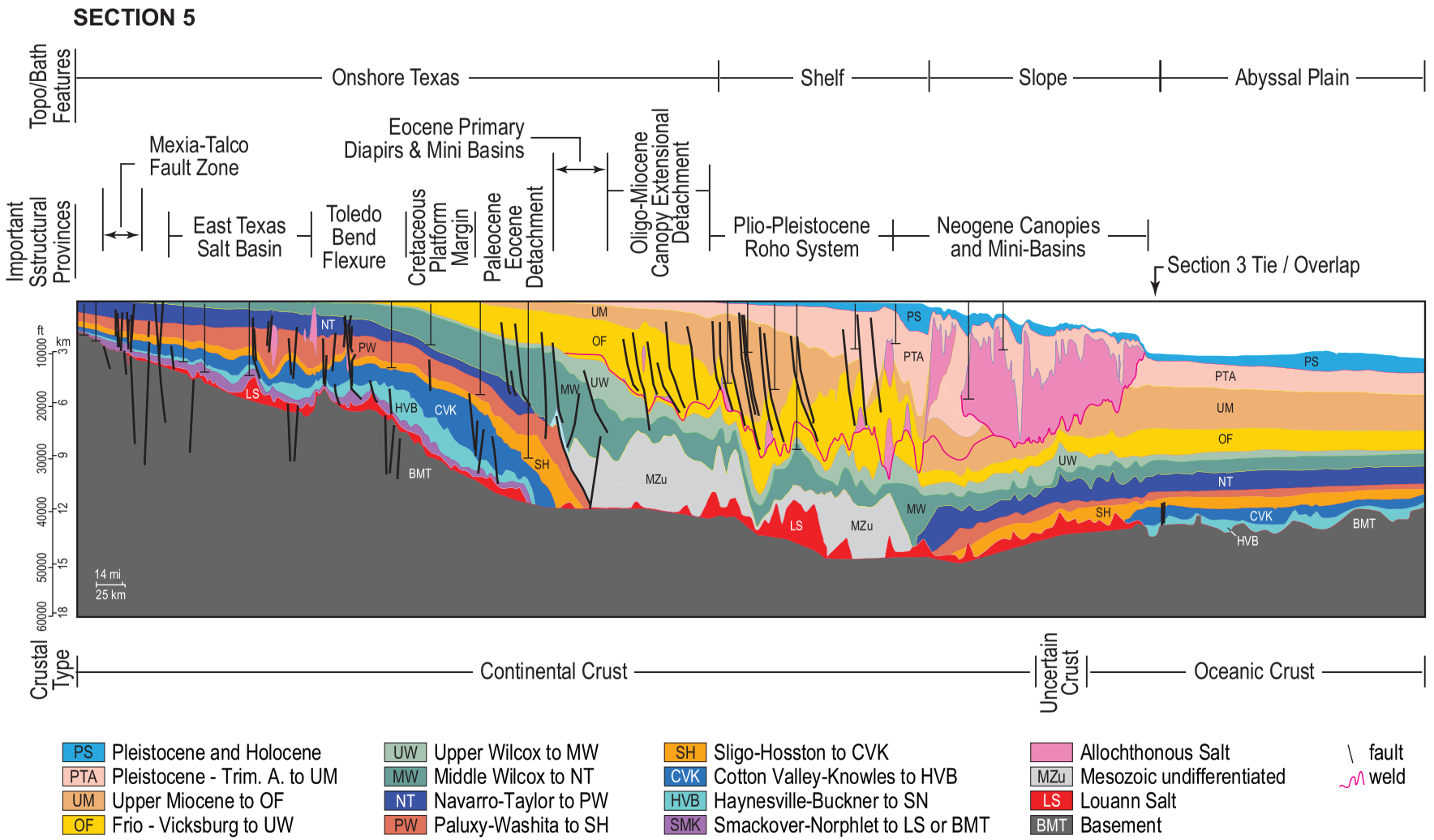

Figure 1.17 Cross-section 5: Sabine Uplift to Sigsbee Escarpment.

structural belts, including the Paleogene–Eocene **expansion zone**, the Oligocene–Miocene detachment zone, and the Pliocene–Pleistocene roho system on the present-day shelf (Peel *et al.* 1995). The present-day slope encompasses numerous Neogene canopies and secondary minibasins. These salt structures terminate at the Sigsbee Escarpment, where the salt canopy clearly impacts the sea floor morphology.

The section nicely illustrates the structure of the northern GoM basin depocenter located beneath the present continental shelf and slope. The Top Cretaceous is as deep as 40,000 ft (12.2 km) in places, loaded by Cenozoic siliciclastic deposition. The Cenozoic prism extends beneath the coastal plain and shelf, reaching its thickest point near the present continental margin. In many areas, the continental slope extends basinward to about the position of the transitional/oceanic crust boundary. Beneath this sediment prism, a large portion of the autochthonous Louann Salt has been expelled, forming a primary salt weld on the basal Jurassic unconformity that is a decollement zone for growth faults. Other detachments occur at salt welds, allochthonous salt canopies, or are rooted in decollements located within deep basinal mudstones of indeterminate age.

As with several previous sections, sedimentary architectures are influenced greatly by accommodation created by gravity tectonics. Shelf margins prograde progressively into the basin from Cretaceous to Neogene, reflecting the robust depositional systems extending from **source terrane** to basinal sink in this central GoM transect.

1.5.6 Cross-Section 6: San Marcos Arch to Sigsbee Escarpment

Cross-section 6 (Figure 1.18) starts at the San Marcos Arch, where Miocene uplift set up a steeply dipping basement surface, to the Perdido fold belt on the abyssal plain on the international border. Several levels of fault detachment are observed: (1) Paleo-Eocene detachment at or seaward of the Cretaceous margin; (2) Oligo-Miocene canopy detachment; and (3) the Corsair–Wanda fault zone.

In contrast to the central and northeastern GoM, this transect across the northwestern Gulf displays broad, complex Middle Cenozoic compressional domains, including the Perdido and Port Isabel (Oligo-Miocene canopy) fold belts. The Port Isabel fold belt is linked by a decollement to the Miocene Clemente-Thomas, Corsair, and Wanda fault zones of the Oligocene–Miocene canopy detachment province (Hall *et al.* 1993).

The Corsair–Wanda fault zone is particularly prominent on this section (Figure 1.18). Over 30,000 ft (9.1 km) of growth along the bounding fault is apparent on seismic sections, with much of it being Miocene in age. The fault detaches on the deep salt allochthon.

Like the Mississippi Fan fold belt, the Perdido fold belt is located near the original depositional limit of the basal (par-autochthonous) Louann Salt (Fiduk *et al.* 1999). The isopachous Cretaceous to Early Cenozoic interval is considered pre-kinematic (deposited before deformation), while the synkinematic (during deformation) phase in the Miocene and younger interval shows lateral variations in thickness (Jackson and Hudec 2017). Additional contraction was accommodated by the compound salt canopy that has been injected up into the Oligocene and Miocene interval.

Interpretation of the remnant thickness of the autochthonous salt is challenging at the depths where it is present. Portions of the salt are deflated and welds likely remain in many unpenetrated structures. Amplitudes of folds in the Perdido trend suggest considerable salt thickness, but few wells penetrate deeply enough to verify this view.

1.5.7 Cross-Section 7: Quetzalcoatl Extensional Detachment, Northern Mexican Ridges to Chicxulub Crater

Cross-section 7 (Figure 1.19) is a west-to-east transect from the slope of eastern Mexico to the Yucatán Platform, the site of the Chicxulub impact event that ended the Mesozoic. The present-day physiography of a narrow shelf and steep slope reflects relatively recent Neogene tectonic activity associated with Pacific plate subduction (Padilla y Sánchez 2007; Witt *et al.* 2012). Associated loading and subsequent gravitational sliding in the Quetzalcoatl extension is linked with compression in the Mexican Ridges fold belt. Uplift in eastern Mexico associated with the Middle Miocene Chiapanecan orogeny resulted in deep incision and canyon formation along a narrow shelf and slope leading to delivery of large volumes of coarse-grained sediments to the basin floor (Ambrose *et al.* 2005).

While the fold and thrust belt shown on the middle of this section is commonly grouped with the Mexican Ridges to the south, newer seismic data suggests that this contractional belt may have also experienced the additional effects of salt being pushed from west to east (M. Hudec, pers. comm.). Though published evidence is currently lacking, there is a notable change in orientation of folds and faults south of this section (Figure 1.19) and a gap in the structure, implying some change in the tectonic forcing mechanism. Another observation is that the southern portion of the Mexican Ridges tends to show more expansion along the Quetzalcoatl faults versus the northern areas. This leads one to suspect pure gravity tectonics in the southern Mexican Ridges versus salt-involved compression in the north. Another difference in between this section and cross-section 8 to the south is the existence of a roho system detached at the Top Upper Miocene level, documented on better seismic data by CNH (2015b). Salt or a weld may be present at the Top Upper Miocene level, but is not shown in the CNH (2015b) compilation. The proximity to salt would be required in any case.

Cross-section 7 (Figure 1.19) continues across the relatively undeformed abyssal plain region of the south-central Gulf before passing across the Yucatán salt subprovince or subbasin

https://doi.org/10.1017/9781108292795.003 Published online by Cambridge University Press

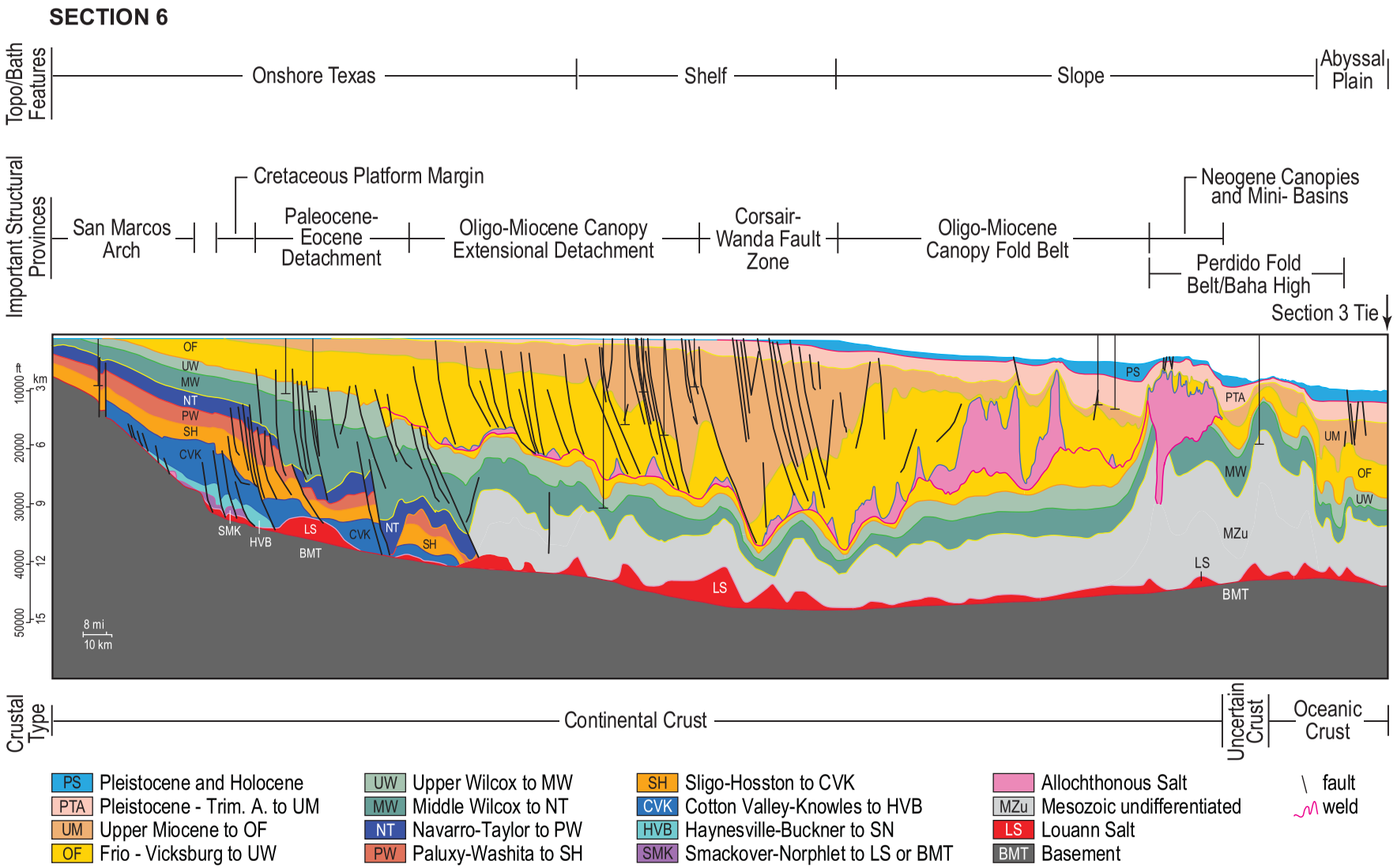

Figure 1.18 Cross-section 6: San Marcos Arch to Sigsbee Escarpment.

https://doi.org/10.1017/9781108292795.003 Published online by Cambridge University Press

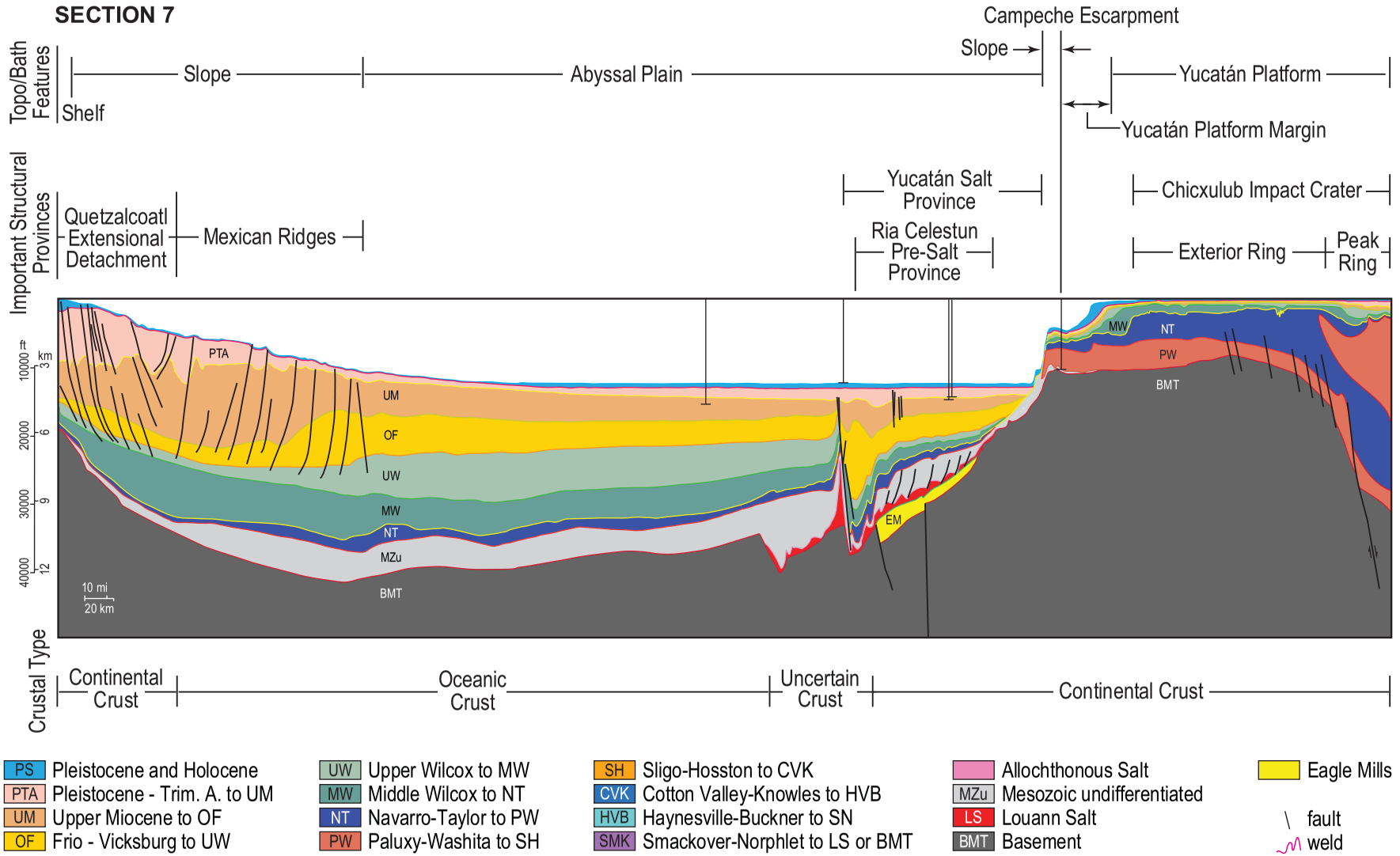

Figure 1.19 Cross-section 7: Quetzalcoatl Extensional Detachment, Northern Mexican Ridges to Chicxulub crater.

(terminology of Hudec and Norton 2018). Two tectonic styles are recognized: (1) a salt diapir complex with high-amplitude salt structures; and (2) lower-amplitude salt rollers. The former occurs near or at the transition from continental crust, thus uncertain crust. There is an interpreted basement step just seaward, where parautochthonous salt is observed to terminate.

The Yucatán salt roller domain has a remarkable similarity to the salt raft structures of the deepwater Norphlet salt raft exploration area of the northeastern GoM (Saunders *et al.* 2016; Hudec and Norton 2018). It has been suggested that this area is a conjugate to that Norphlet exploration arena, separated by sea floor spreading (Miranda Peralta *et al.* 2014; Steier and Mann 2019). However, there are no well penetrations in this area other than the shallow DSDP core sites (see Buffler *et al.* 1984).

The Yucatán salt roller domain also overlies a new, distinctly different structural province with possible pre-salt sedimentary fill. First noted by Williams-Rojas *et al.* (2012), this interval shows a wedge-shaped or rift-graben form, onlapping the Yucatán Platform margin (Hudec and Norton 2018; Rowan 2018). This interval may be analogous to the pre-salt Eagle Mills (Triassic to Middle Jurassic) of the eastern USA (Heffner 2013). High-amplitude, seaward dipping reflections (SDRs) appear at the base of the probable sedimentary interval, evoking global analogs of SDRs associated with initial stages of continental rifting (Norton *et al.* 2015). Alternatively, these may simply be layered volcanics (Hudec and Norton 2018), as commonly observed in the eastern USA pre-salt section (Heffner 2013). We informally refer to this area as the Ria Celestun pre-salt province, named after a local geographic feature. A similar pre-salt interval is noted on seismic sections in the Campeche subbasin to the southwest (Hudec and Norton 2018).

Cenozoic and Mesozoic stratigraphic units all taper and largely lapout against the steep Yucatán Platform margin. Continental crust basement rises from depths greater than 36,000 ft (11 km) to less than 10,000 ft (3048 m) over a short distance. Further inboard on the platform, basement abruptly drops and then rises to depths of less than 6000 ft (1829 m). This unusual basement architecture is a result of the Chicxulub impact, as documented by numerous studies (Denne *et al.* 2013; Sanford *et al.* 2016) and recent IODP coring at site M0077A (Morgan *et al.* 2016). Basement upwarp indicates the location of the peak ring, the deep crustal response to the bolide impact that ended the Cretaceous. Seaward of the peak ring, the Top Cretaceous reflection is relatively flat in the area of the exterior ring but drops 3–4 km on the platform margin. Clinoforming successions representing the post-impact crater fill are evident in this area.

As mentioned, few exploration wells are present in the eastern portion of the area, in spite of prominent salt-cored structural closures and prospective traps. Several factors may preclude any near-term drilling: (1) water depths greater than 12,000 ft (3.7 km); (2) distal thinning of Paleogene reservoirs like the Wilcox and parallel decreases in sand content away from siliciclastic source terranes. Neogene sandy intervals are present in DSDP core sites 87 and 91, but these are likely derived from southern Mexico rather than any local sources. The progressive sorting associated with the distal turbidity flows likely means a reduced grain size of any potential reservoirs.

1.5.8 Cross-Section 8: Mexican Ridges to US Abyssal Plain

Cross-section 8 (Figure 1.20) extends from the Quetzalcoatl extensional detachment to the southern end of the Mexican Ridges, across the Yucatán salt subbasin and continuing northward to the abyssal plain at the USA–Mexico border. As with cross-section 7 (Figure 1.19), both extensional faults and, further seaward, folds and low-angle thrusts of the Mexican Ridges are observed on this transect. However, the expansion along the Quetzalcoatl detachment faults is much greater, for reasons discussed earlier. Drilling of the Pemex Puskon #1 well documented the substantial growth along listric faults of the Quetzalcoatl extensional detachment zone (Alcocer 2012; Porres Luna 2018). The linked extensional–contractional system is thought to detach on overpressured Upper Eocene Shales, with a possible additional detachment surface in the Oligo-Miocene interval, similar to major multi-level detachments documented in the northern GoM (e.g., Radovich *et al.* 2007, 2011). The Upper Miocene interval in the extensional zone is generally thinner here than on cross-section 7, similar to observations made by CNH (2015b).

Large folds of the Mexican Ridges have wavelengths of 10–12 km (6–7 miles) and amplitudes of 300 m to 1 km (984–3280 ft) (Padilla y Sánchez 2007). The Mexican Ridges developed as a consequence of gravitational spreading processes, synchronous with growth faulting of the western onshore and continental shelf areas. Deformation occurred in several stages from Middle Miocene to the present day (Salomon-Mora *et al.* 2009). This deformation correlates with highly active **petroleum systems**, including migration and trapping of hydrocarbons, in turn forming direct hydrocarbon indicators, overpressured traps, gas chimneys, gas hydrates, and sea floor hydrocarbon seeps that are being investigated as part of new regional exploration efforts. Drilling has concentrated largely on the folds of the Mexican Ridges, with a few wells like Puskon #1 testing the updip extensional systems.

The Yucatán salt subbasin (high-amplitude salt diapir domain) in the middle of the section is entirely developed over uncertain or possible oceanic crust. Hudec and Norton (2018) hypothesized significant seaward translation after salt deposition due to the lack of a confining structural boundary, in contrast to the perched Campeche salt subbasin where the BAHA high is present. Shortening is evident in the shallow Cenozoic interval of the Yucatán salt subbasin, with the timing of deformation likely as Miocene or younger.

https://doi.org/10.1017/9781108292795.003 Published online by Cambridge University Press

https://doi.org/10.1017/9781108292795.003 Published online by Cambridge University Press

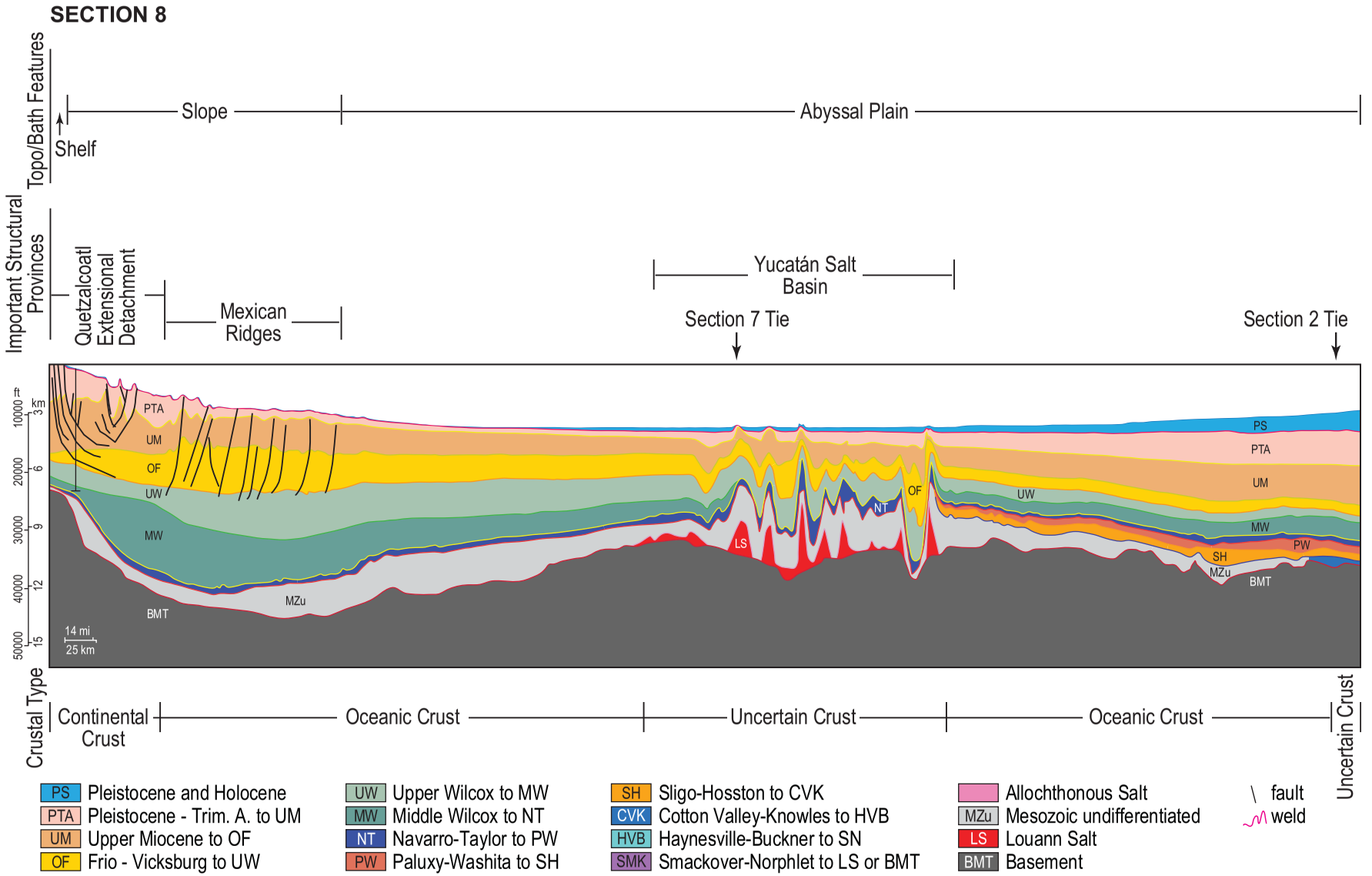

Figure 1.20 Cross-section 8: Mexican Ridges to US abyssal plain.

One interesting observation is the differential thickening and thinning trends of the Mesozoic and Cenozoic. Mesozoic strata thicken toward the salt diapir domain, while Cenozoic strata generally thin toward that area, trends noted both north and south of the subbasin. Local thickening into zones of salt evacuation is noted but does not change the inferred pattern. The Mesozoic thickening may signal development of an inner basin in Mexico, a conjugate to that in the northern GoM, where salt and overlying Mesozoic strata were deposited in greater magnitudes than elsewhere.

1.5.9 Cross-Section 9: Catemaco Fold Belt to Bahamas Platform

Cross-section 9 (Figure 1.21) is a basin-spanning strike transect from the Catemaco fold belt to the Bahamas Platform. The section includes a small segment of the Catemaco fold belt, unfortunately crossing oblique to the westerly verging folds. The Catemaco fold belt has been previously described as a linked extensional–contractional gravity-driven system with tectonic transport to the northwest (Mandujano-Velaquez and Keppie 2009). Northward salt evacuation in the Campeche salt subbasin (terminology of Hudec and Norton 2018) is thought to have occurred during the Middle Miocene Chiapanecan orogeny (Gutiérrez Paredes *et al.* 2017). However, new WAZ seismic data acquired in the Campeche salt basin suggests a longer duration of shortening, initiated in the late Paleogene and continuing today (Snyder and Ysaccis 2018). The nearby Veracruz basin was likely deformed during the Chiapanecan uplift, closely followed by uplift of the Anegada High and Los Tuxtlas volcanic massif (Jacobo Albarabn *et al.* 1992).

The section continues across the fringe of the Campeche salt subbasin, crossing into the Yucatán salt subbasin which is also observed on cross-sections 7 and 8 (Figures 1.19 and 1.20). Not obvious at this scale are the counter-regional fault systems that accommodated a thick Neogene interval, partly aided by salt expulsion rollovers (Gomez-Cabrera and Jackson 2009a, 2009b). CNH (2015a) notes in regional structural intervals that there is a major expansion of the Upper Miocene and Lower Pliocene in the adjacent Comalcalco basin, of up to 200–300 percent.

Like cross-section 7, cross-section 9 (Figure 1.21) carries onward across the Yucatán salt roller domain and underlying Ria Celestun pre-salt province, over the Yucatán Platform and Chicxulub exterior ring. Notable is the elevation of basement near the Chicxulub impact exterior ring <12,000 ft (<3.7 km), dropping several kilometers (to 20,000 ft; 6.1 km) on the rest of the platform. Basement appears to be quite shallow in the Florida Straits, less than 15,000 ft (<4.6 km) regionally and locally near the seabed, such as at Catoche Knoll, where DSDP cores 538 and adjacent cores 536 and 537 were retrieved (Buffler *et al.* 1984).

The cross-section continues to the Bahamas Banks or Platform where basement deepens, depressed under the thick Mesozoic succession (>11,000 ft; 3.4 km) largely Aptian to Albian carbonates (Ladd and Sheridan 1987; Epstein and Clark 2009). Evaporites are interpreted on the far eastern end of the line, making an appearance in the hypothesized seawater entry point for the GoM basin, as will be discussed in Section 4.4.

Exploration has primarily been concentrated in the Catemaco fold belt and adjacent areas (including key discoveries at Kunah #1 and other undeveloped resources), the Mexican Ridges, and adjacent Campeche salt subbasin. Limited drilling has been attempted elsewhere along the cross-section. The eastern end of the cross-section skirts the Cuban fold and thrust belt, where a handful of international companies have drilled wells without success in deepwater and older shallow-water wells near the Bahamas Banks (Epstein and Clark 2009; Melbana Energy 2017).

1.5.10 Cross-Section 10: US Abyssal Plain to South Florida Basin

Cross-section 10 (Figure 1.22) completes the circum-GoM tour, running from the international border to onshore Florida. The Florida Escarpment is particularly steep, coinciding with the interpreted continental to oceanic crustal boundary. The Mesozoic succession is relatively thin on oceanic crust (<7000 ft, 2134 m) compared to the South Florida basin, where it exceeds 12,000 ft (3.7 km) on the continental crust. Over the Sarasota Arch, a major basement-cored structure, the Mesozoic is as thin as 5000 ft (1524 m), documented by the nearby Charlotte Harbor-672 #1 and 622 #1 wells. Unlike cross-section 2, the Jurassic and Early Cretaceous platform margins are not observed, leading to alternative hypotheses of non-reefal development, or more likely K–Pg-related margin collapse (Denne and Blanchard 2013) and continued retrogradational failures of the margin well past the original platform margin position. Inboard well penetrations (e.g., Vernon Basin 654 #1) document only carbonate shelf and platform interior facies. Repeated margin failures and adjustments (Mullins *et al.* 1986) also reflect ocean current bottom erosion during a period of accelerated current flow in the Miocene and Pliocene, linked to progressive closure of the equatorial seaway and development of the Isthmus of Panama (Snedden *et al.* 2012).

As will be discussed in Section 4.5, the Glen Rose supersequence is particularly well developed in the South Florida basin, including extensive evaporites, mainly anhydrite of the Ferry Lake Sequence and stratigraphic equivalents (Punta Gorda Formation of Florida). The center of the basin is known to contain halite as well as anhydrite, indicating restricted conditions and hypersalinity during the Albian. The presence of evaporites in the Albian interval east of the Sarasota Arch is indicated by distinctive high-amplitude continuous seismic reflections.

The Cenozoic interval shows an opposite trend in thickness. On oceanic crust, 14,000 ft (4.3 km) of Cenozoic is present, much of it Neogene siliciclastic sedimentation

https://doi.org/10.1017/9781108292795.003 Published online by Cambridge University Press

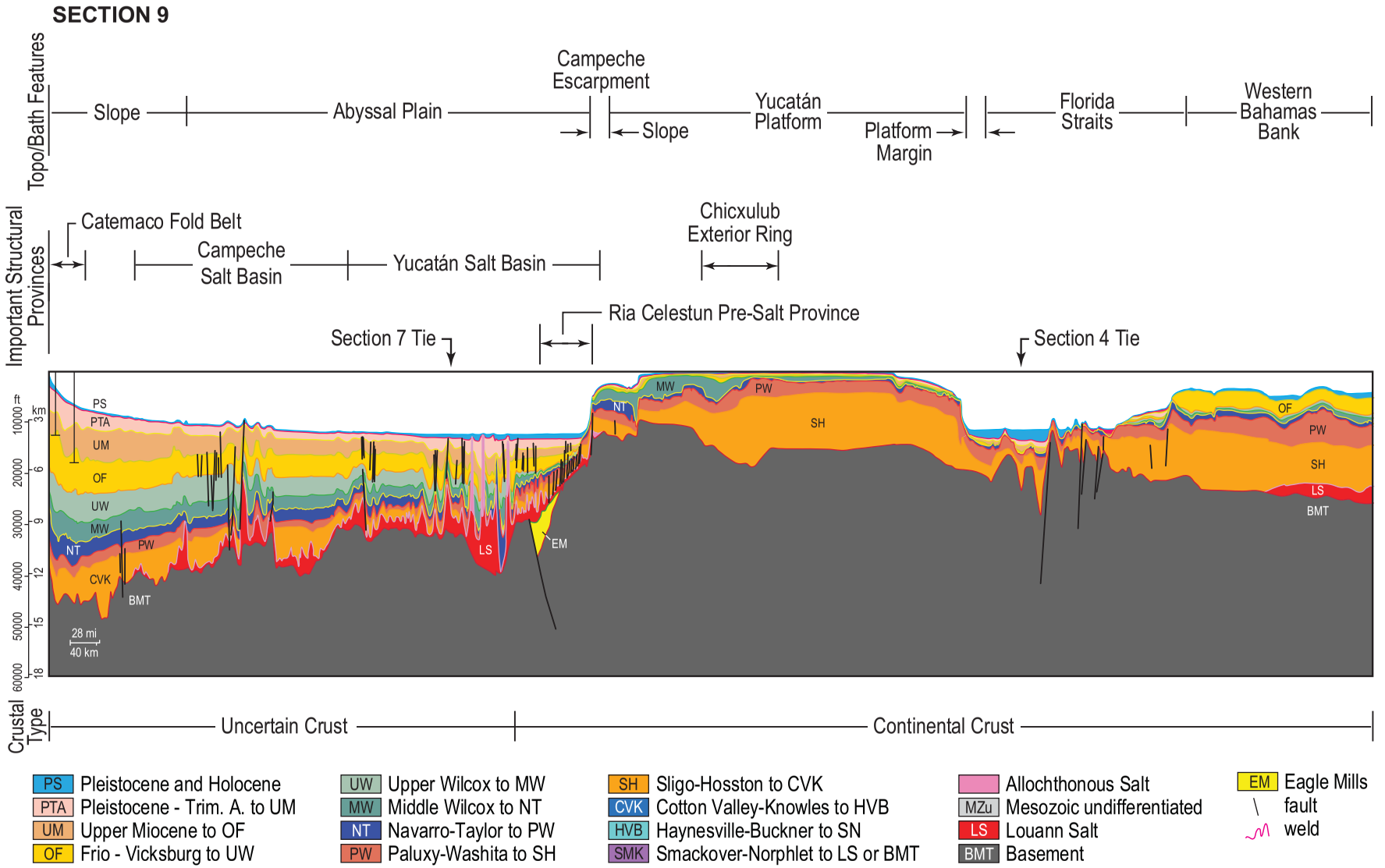

Figure 1.21 Cross-section 9: Catemaco fold belt to Bahamas Platform.

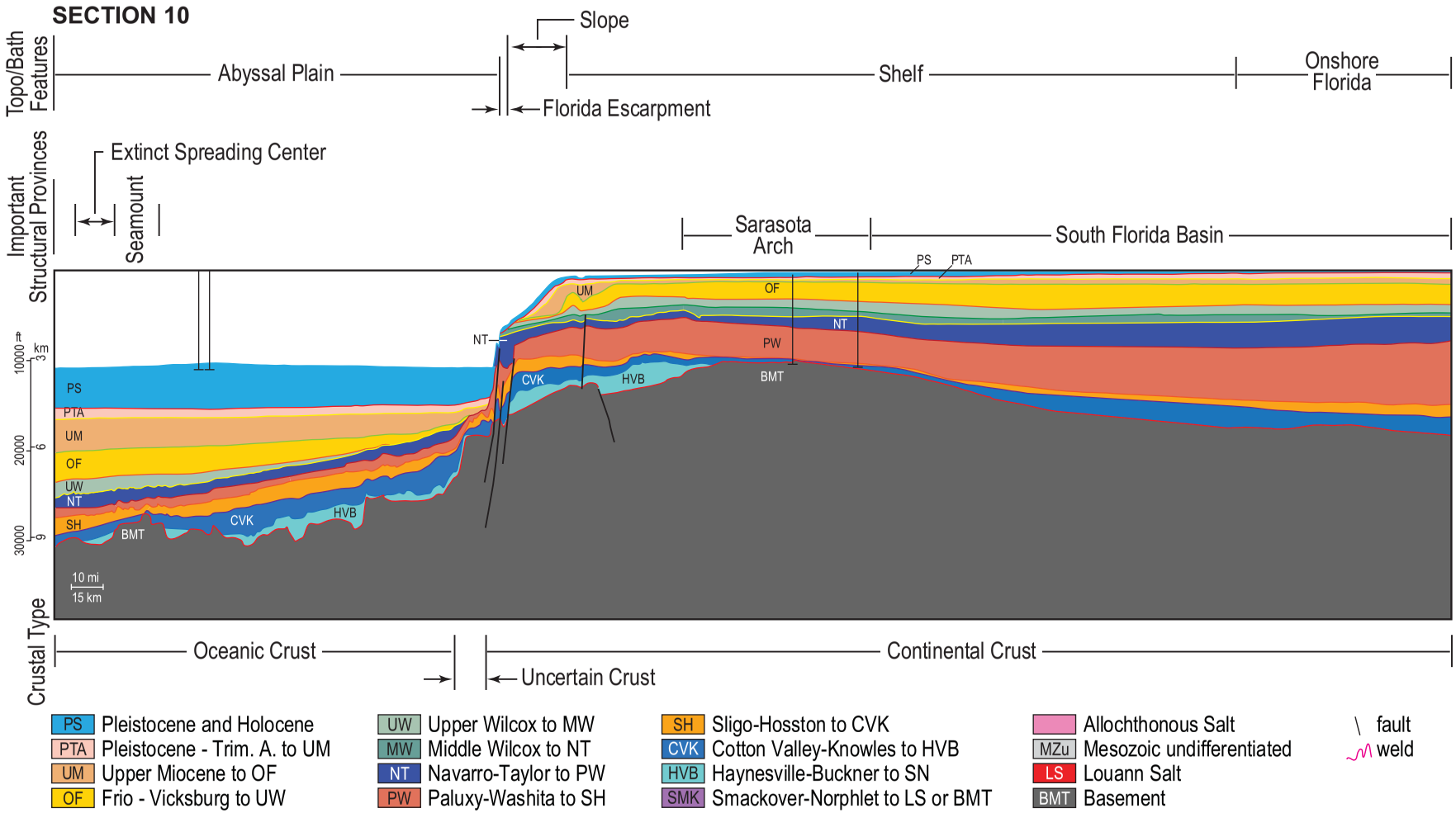

Figure 1.22 Cross-section 10: US abyssal plain to South Florida basin.

(9000 ft; 2744 m) linked to the Mississippi Fan and older systems like the paleo-Mississippi and paleo-Tennessee Rivers, which were sourced by the rejuvenated Appalachians. However, Cenozoic deposition on the platform is much less at 5000 ft (1524 m) and is dominated by carbonate sediments.

Due to the long-standing US drilling moratorium on the Florida shelf, no deepwater wells have been permitted; few wells have been drilled since 1985, all of these dry holes. Sizable onshore discoveries were made as recently as 1964 in the Sunniland trend (e.g., Felda Field) where carbonate reservoirs (grainstone banks and tidal shoals) are well documented (Mitchell-Tapping 1986, 2002). These small fields are largely sealed by extensive evaporites of the coeval Glen Rose interval. However, few wells have been drilled other than field infill wells, related to environmental concerns and other non-geologic factors.

1.5.11 Other Areas: Bravo Trough of Mexico

Between cross-sections 3 and 7 is a zone of major salt evacuation, only recently identified on new WAZ 3D seismic surveys (CNH 2015b; Hudec *et al.,* accepted). Depth to basement is in the range 45,000–52,000 ft (13–16 km), shallowing to 40,000 ft (12.2 km) on the adjacent BAHA high (Figure 1.4). Salt evacuation-related over-thickening of Oligocene sediments into this structural trough in the offshore portion of the Burgos basin is called the Bravo Trough (M. Hudec, pers. comm.). Some thickening of the Oligocene in this extensional zone was shown by Davison *et al.* (2015), but not to the scale of 8000 m (5 km) of expanded Upper Oligocene interval observed on new WAZ data in Mexico. A well drilled by Hess (Port Isabel 526 #1) in Bravo Trough penetrated nearly 17,000 ft (5.2 km) of sandstone-poor Oligocene interval before terminating. The thick Oligocene interval overlies a thin or absent Paleogene and Mesozoic interval, suggesting that a large salt body or diapir was present prior to Latest Eocene/Early Oligocene salt evacuation (Hudec, pers. comm.).

The lack of seismic reflectivity in the trough fill implies a shale-dominated interval. The US GoM interval with a similar seismic character is the basinal Oligocene (Frio–Vicksburg) interval of the Oligo-Miocene canopy detachment and contractional zones including the Port Isabel fold belt, as will be discussed in Section 6.5. Contributing rivers were likely mud-dominated, including volcanics altered to clays.

1.6 Temporal Reconstruction of Central GoM Line

Backstripping of regional cross-sections (Figure 1.23) reveals the dynamic interplay between deposition, wholesale mass transfer of salt, development of growth structures, and outbuilding of the Gulf margin that has characterized the basin's history (Diegel *et al.* 1995; Peel *et al.* 1995; McBride *et al.* 1998). Late Jurassic accumulation of up to 4 km of Louann Salt extended across the subsided, thinned transitional crust (Figure 1.23A). By the end of the Cretaceous, deposition had loaded and expelled much of the landward part of the autochthonous salt basinward, beneath the paleo-continental slope toe and northern basin floor (Figure 1.23B). Extension of the upper slope was accommodated by compressional deformation at the slope toe. A remnant layer of autochthonous salt provided the decollement horizon for basinward gravity spreading.

By the end of the Oligocene (Figure 1.23C), successive pulses of Paleogene deposition had prograded the continental margin over the Cretaceous slope, deflating the thick salt under-layer by intrusion of salt stock canopy complexes under the advancing continental slope and further inflation of the abyssal salt sheet. The Oligocene Frio growth fault zone migrated basinward with the prograding continental margin; here, detachment occurred within Upper Eocene mud as well as in the deeper salt. The resultant continental slope was a mix of sediment and near-surface salt bodies. Miocene–Pliocene deposition loaded the salt canopies, triggering passive diapirism and further gravity spreading, creating roho fault systems and isolated salt stocks separated by welds (Figure 1.23D). Thick secondary minibasin-fills separate the salt stocks. Loading also initiated extrusion of a salt sheet at the toe of the slope. Pleistocene deposition has filled updip minibasins and built the continental slope onto the distal salt sheet, where incompletely filled minibasins dominate present slope topography (Figure 1.23E).

1.7 Tectonostratigraphy, Chronostratigraphy, and Depositional Systems

With the focus of this book on the depositional history within the GoM basin, a brief description of various tectonostratigraphic and chronostratigraphic frameworks, stratigraphic terminology, and depositional classifications are necessary prerequisites. These are foundations for more detailed discussions of the Mesozoic and Cenozoic record in subsequent chapters. We also elaborate upon the evolving database of wells, seismic data, and reference papers in our research on the GoM.

1.8 Tectonostratigraphic Framework

Tectonics has a predominant role in creating the highland terranes that various fluvial systems tap for **terrigenous** source material, modifying routes from continental divides toward shorelines, creating accommodation in the receiving basins, forming bathymetric features that attract photic zone organisms that form carbonates, generating traps to allow hydrocarbon accumulations, and controlling burial that ultimately drives shale-prone source rock though time/temperature windows that generate oil and gas. The long-term structural history of the basin and its surrounding hinterland is the ultimate low-frequency spectrum upon which are superimposed high-frequency **eustatic sea-level changes**, climatic variations, and autocylic depositional processes.

https://doi.org/10.1017/9781108292795.003 Published online by Cambridge University Press

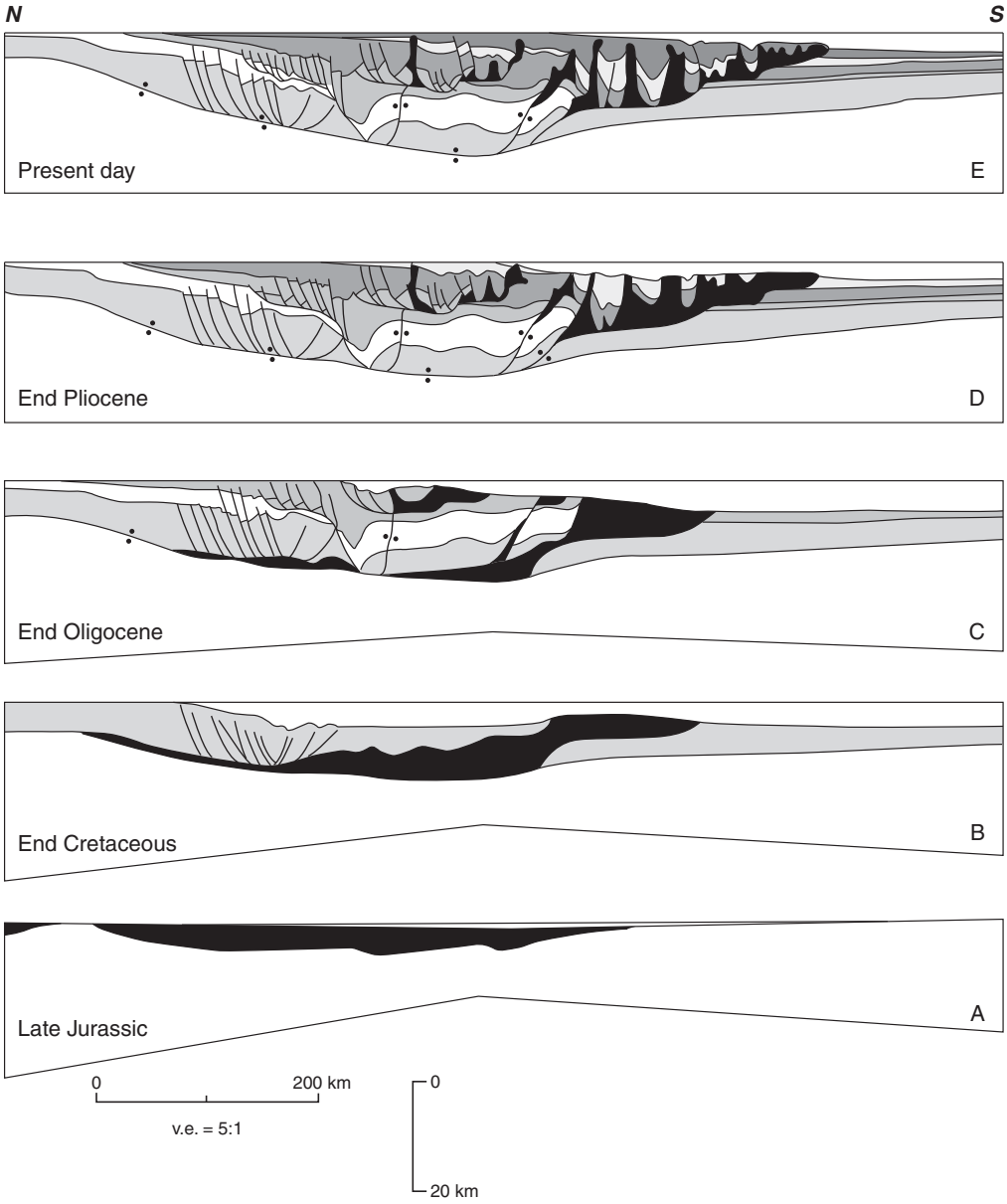

Figure 1.23 Sequential restoration of schematic central GoM section. Modified from Peel *et al.* (1995).

Thus, our over-arching stratigraphic framework, and the pathway we follow in this book from pre-basin history to the end of the Pleistocene, is a tectonostratigraphic scheme. Galloway (2009) first recognized this and subdivided the Cenozoic into four tectonostratigraphic phases:

1. Paleogene Laramide Phase
2. Middle Cenozoic Geothermal Phase
3. Basin and Range Phase (including Appalachian Rejuvenation)
4. Neogene Tectono-climatic Phase.

In spite of an equally long period of oil and gas exploration and scientific investigation, a similar tectonostratigraphic breakdown of the Mesozoic interval has not achieved consensus, in spite of considerable effort. Toward this end, we offer a new Mesozoic tectonostratigraphic classification, based on the same general principles as that of the Cenozoic framework (Figure 1.24):

1. Post-Orogenic Successor Basin-Fill and Rifting Phase
2. Middle Mesozoic Drift and Cooling Phase
3. Late Mesozoic Local Tectonic and Crustal Heating Phase.

These three phases cover the Marathon–Ouachita–Appalachian orogeny to end Cretaceous interval (299 Ma to 66 Ma) and naturally reflect plate tectonic forces that controlled tectonics, source terrane exposure, subsidence, accommodation, and even marine water entry to the nascent basin to form the Louann Salt body, the first basin-wide depositional

https://doi.org/10.1017/9781108292795.003 Published online by Cambridge University Press

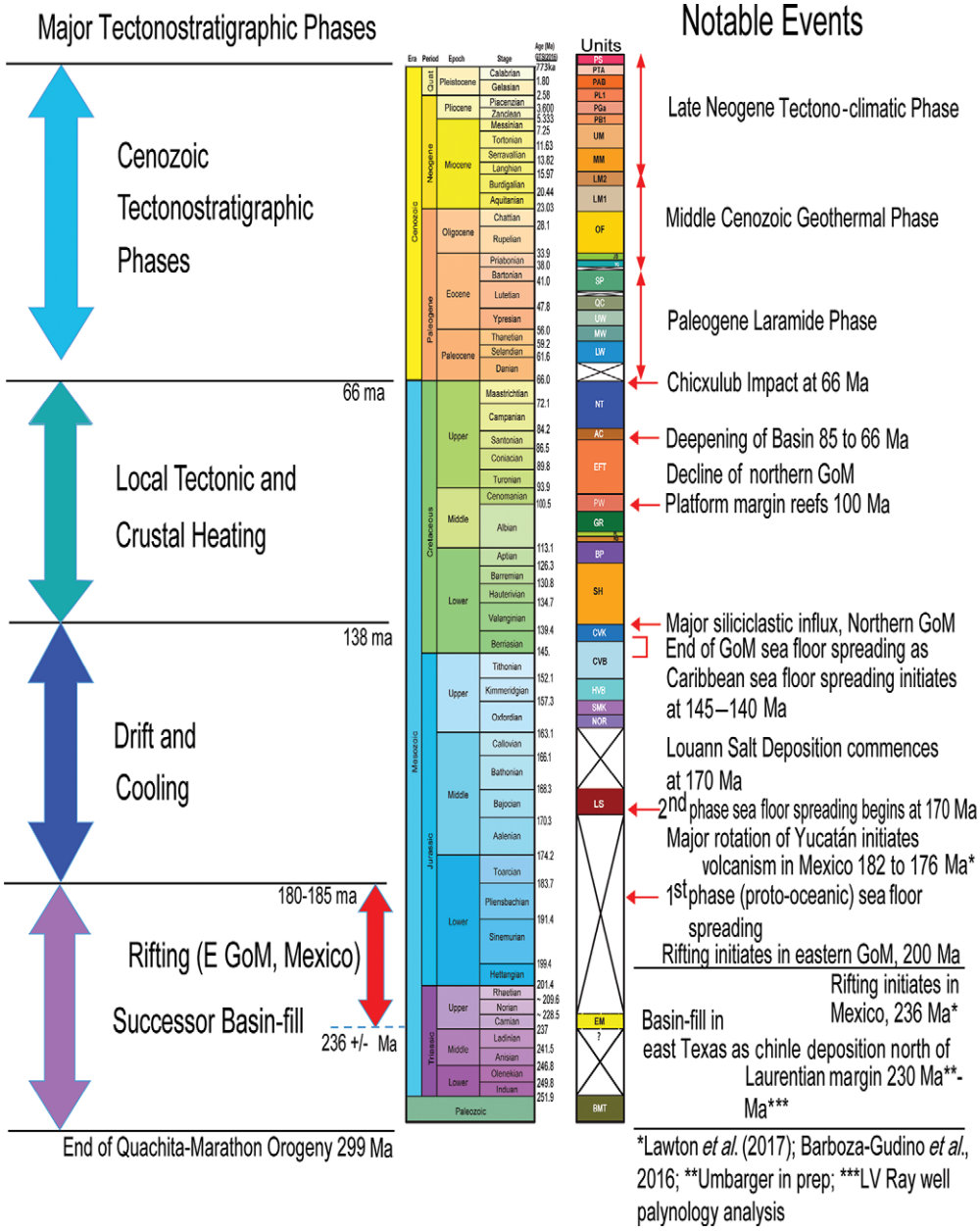

Figure 1.24 Major tectonostratigraphic phases, GoM basin and predecessors.

unit. Our tectonostratigraphic framework is based on new plate tectonic reconstructions, detrital zircon geochronology from deep wells, and analysis of new seismic reflection data in Mexico and the USA. Newly developed concepts depart from conventional GoM thinking both in terms of timing and kinematics, as will be described in detail in Chapter 3.

The stratigraphic terminology and chronostratigraphy that underpins unit-specific identification and correlation over regional to basin-scales is described in Chapters 2–8. Discussion of the Mesozoic and Cenozoic depositional systems classification and assumptions used in creating various depositional maps in this book immediately follows in this chapter.

1.9 Stratigraphic Terminology

Stratigraphic terminology used for naming depositional intervals in the greater GoM range from simple **lithostratigraphy** to **biostratigraphically** age-constrained **chronostratigraphy**. The differences between onshore and offshore nomenclature, reflecting the progressive shift from land to deepwater exploration, can be confusing. Some older formation names are clearly time-transgressive (e.g., Haynesville Shale; Figure 1.25) or facies-dependent (e.g., Ferry Lake Anhydrite, Gilmer Limestone). The southern GoM has similar issues and also suffers from a local lithostratigraphic nomenclature that is specific to each of six or seven geological provinces (e.g., Figure 1.26 for

https://doi.org/10.1017/9781108292795.003 Published online by Cambridge University Press

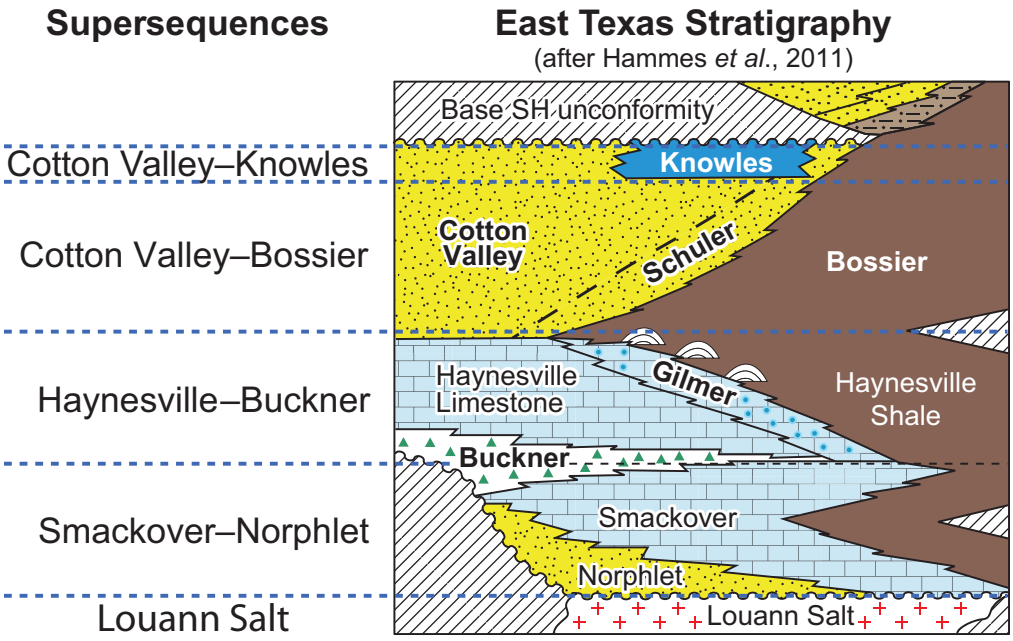

Figure 1.25 Early Mesozoic supersequences. Smackover–Norphlet supersequence. Lithostratigraphic units (e.g., Norphlet Formation, Smackover Formation) are often time-transgressive and essentially amount to paleo-environmental facies. Supersequences incorporate such units into chronostratigraphically significant regional- to basin-scale packages. Modified from Olson *et al.* (2015).

Tampico–Misantla province). Recent reports compiled and provided to the public by Mexico's National Hydrocarbon Commission has followed the same lithostratigraphic approach (CNH 2015a, 2015b, 2017b).

The ultimate goal of the stratigraphic framework in the GoM developed for the GBDS project and used in this book is to enable correlation from the Gulf coastal plain to the deepwater abyssal plain. The GoM exploration effort that began as early as the 1890s has generated a large volume of wells with available ditch (well) cuttings samples that are readily analyzed for **microfossil** and microfloral content. While early charts and zonations focused on benthic foraminifera, which had limitations due to paleo-environmental factors, modern well site biostratigraphy incorporates planktonic forams, calcareous nannofossils, and palynomorphs (Bolli *et al.* 1989; Styzen 1996; Olson *et al.* 2015; www.paleodata.com). Combined with the improved geologic timescales (Ogg *et al.* 2016), the resolution with the Neogene interval, for example, is fast approaching 100 ky or better (Snedden and Liu 2011). The structural complexity of the basin, illustrated by the 10 basin cross-sections (Section 1.5) also necessitates use of biostratigraphically age-constrained correlation surfaces.

Many companies and industry-support vendors have developed detailed chronostratigraphic classifications and biostratigraphic charts for the GoM. Key public domain charts include Styzen (1996), and those online at PDI (www.paleodata.com/chart), as well as the Mesozoic charts linked to Olson *et al.* (2015). Biostratigraphic data from wells drilled in federal waters is released to the public after 10 years or with lease relinquishment or termination. However, many of these BOEM "paleontology reports" are simple summaries of more detailed operator or vendor studies (Weber and Parker 2016). State surveys and universities have a limited number of biostratigraphic reports from wells drilled onshore or in state waters.

1.10 Mesozoic Chronostratigraphy, Northern GoM

Extensive exploration for northern GoM Mesozoic reservoirs actually preceded Cenozoic discoveries. Mesozoic hydrocarbon reserve additions reached a plateau around 1976, and interest shifted to the Cenozoic offshore. As a result, extensive use of microfossil datums was not well established for the Mesozoic prior to that shift in exploration focus, particularly in offshore parts of the basin. However, interest in Mesozoic stratigraphy has been rekindled as a function of two factors: (1) drilling of onshore unconventional plays including the Haynesville Shale gas play (Hammes *et al.* 2011; Wang *et al.* 2013) and Eagle Ford Formation oil and gas shale plays (Hentz and Ruppel 2011; Denne *et al.* 2014); and (2) improved seismic imaging below salt and the thick Cenozoic cover that often puts the Top Cretaceous at depths exceeding 30,000 ft (9.1 km) in slope and deepwater areas of the basin.

The Mesozoic stratigraphy used in this book is founded on microfossil datums that allow correlation from onshore to offshore areas (Figure 1.27; Olson *et al.* 2015). Similar to the Paleogene interval (e.g., Upper Wilcox), we have retained some older lithostratigraphic terms (Glen Rose, Austin Chalk), but each unit boundary is based upon age diagnostic information, including last appearance datums (LADs), first appearance datums (FADs), or, in some cases, faunal acmes (Olson *et al.*

https://doi.org/10.1017/9781108292795.003 Published online by Cambridge University Press

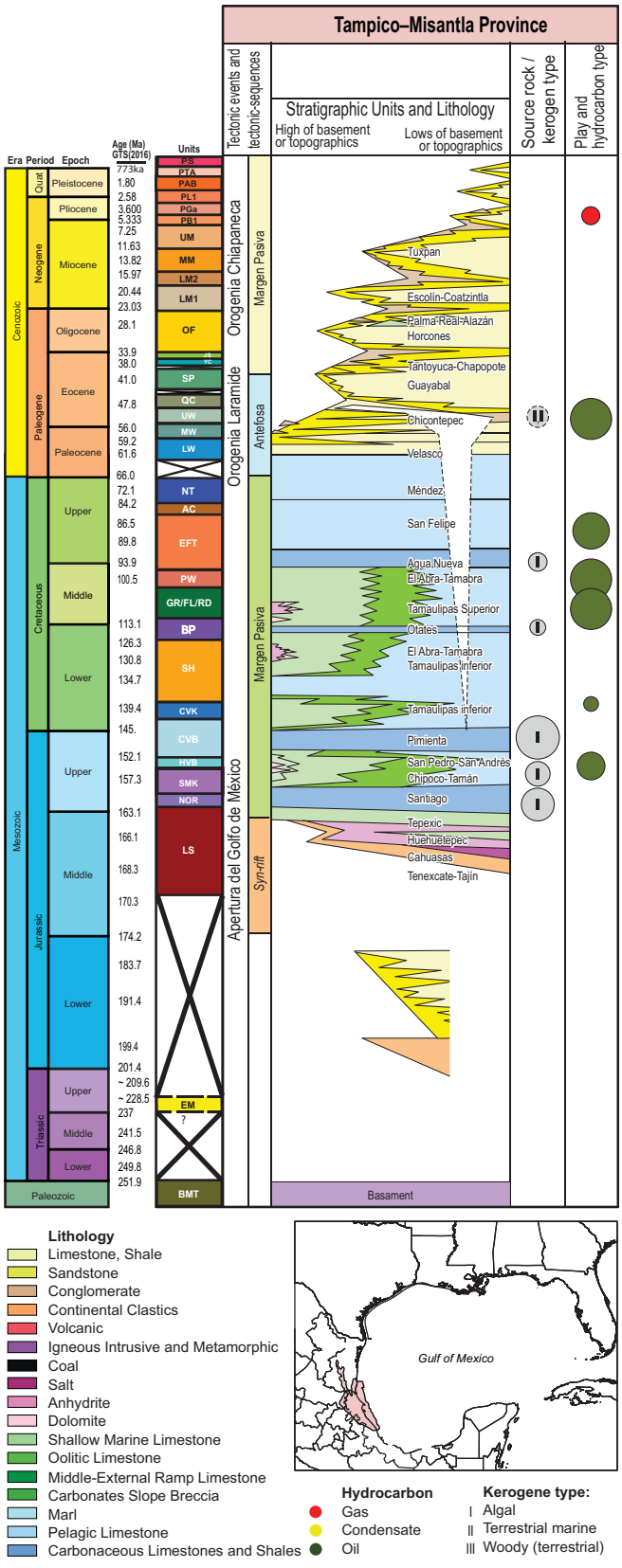

Figure 1.26 Comparison of GBDS chronostratigraphy with Tampico–Misantla oil and province stratigraphic column. Inset map shows Tampico–Misantla province.

2015). Our primary chronostratigraphic information comes from biostratigraphic sources and seismic stratal correlations. Our biostratigraphic data includes published and unpublished information from both onshore (outcrop and subsurface) and offshore sources (Scott 1984; Rogers 1987; Scott *et al.* 2002; Petty 2008; Denne *et al.* 2014). We detail our chronostratigraphic framework through a Mesozoic biostratigraphy table (full table available online at http://dx.doi.org/10.1190/INT-2014-0179.2). In compiling the table, we follow the global chronostratigraphic nomenclature proposed by SEPM Special Publication 60 (Hardenbol *et al.* 1998) and the chronostratigraphic designation system outlined by Snedden and Liu (2011). Additionally, we rely on the Mesozoic depositional architecture for the GoM previously outlined by Galloway (2008).

Practical considerations of basin-scale correlation and database size led us to establish chronostratigraphy at the supersequence level for much of the Mesozoic interval (Figure 1.27). **Supersequences** are longer-duration (5–10 million years) aggregates of sequences, with boundaries usually representing significant regional tectonic events (e.g., Top Paluxy–Washita supersequence). Because the underlying support for stratal correlation is biostratigraphy, we have designated 15 supersequences and a basement unit (BMT) in the GoM with two or three letters referencing lithostratigraphic names familiar to GoM workers (e.g., EFT for Eagle Ford–Tuscaloosa; Figure 1.27) for ease of use. These supersequences divide time-transgressive lithostratigraphic units (e.g., Smackover Formation, Norphlet Formation) into chronostratigraphically significant units (e.g., SN = Smackover–Norphlet; Figure 1.25). For additional details on the construction of the Mesozoic chronostratigraphy and examples of application, the reader is referred to Olson *et al.* (2015).

1.11 Mesozoic Chronostratigraphy, Southern GoM

Establishment of a chronostratigraphic system for the Mesozoic of Mexico has had to overcome several challenges. First, much of the Lower Mesozoic in accessible onshore outcrop sections is non-marine in origin, with fossil plants providing limited age control (Padilla y Sánchez and Jose 2016). Marine deposition is relatively rare in onshore localities until the Middle to Late Jurassic (Oloriz *et al.* 2003). Second, scarce ammonite macrofossils obtained in well cores have provided the primary age diagnostic information for Late Jurassic to Late Cretaceous offshore wells (Angeles-Aquino and Cantú-Chapa 2001; Cantú-Chapa 2009). This is in spite of excellent microfossil biostratigraphic zonations in the Cretaceous interval of northern Mexico (Longoria and Gamper 1977; Ice and McNulty 1980). Third, many of the detailed well reports with these age assignments remain proprietary (note at least four unpublished internal company reports were cited by Angeles-Aquino and Cantú-Chapa [2001]). An exception is the data-rich table included in the biostratigraphy of the Cretaceous–

https://doi.org/10.1017/9781108292795.003 Published online by Cambridge University Press

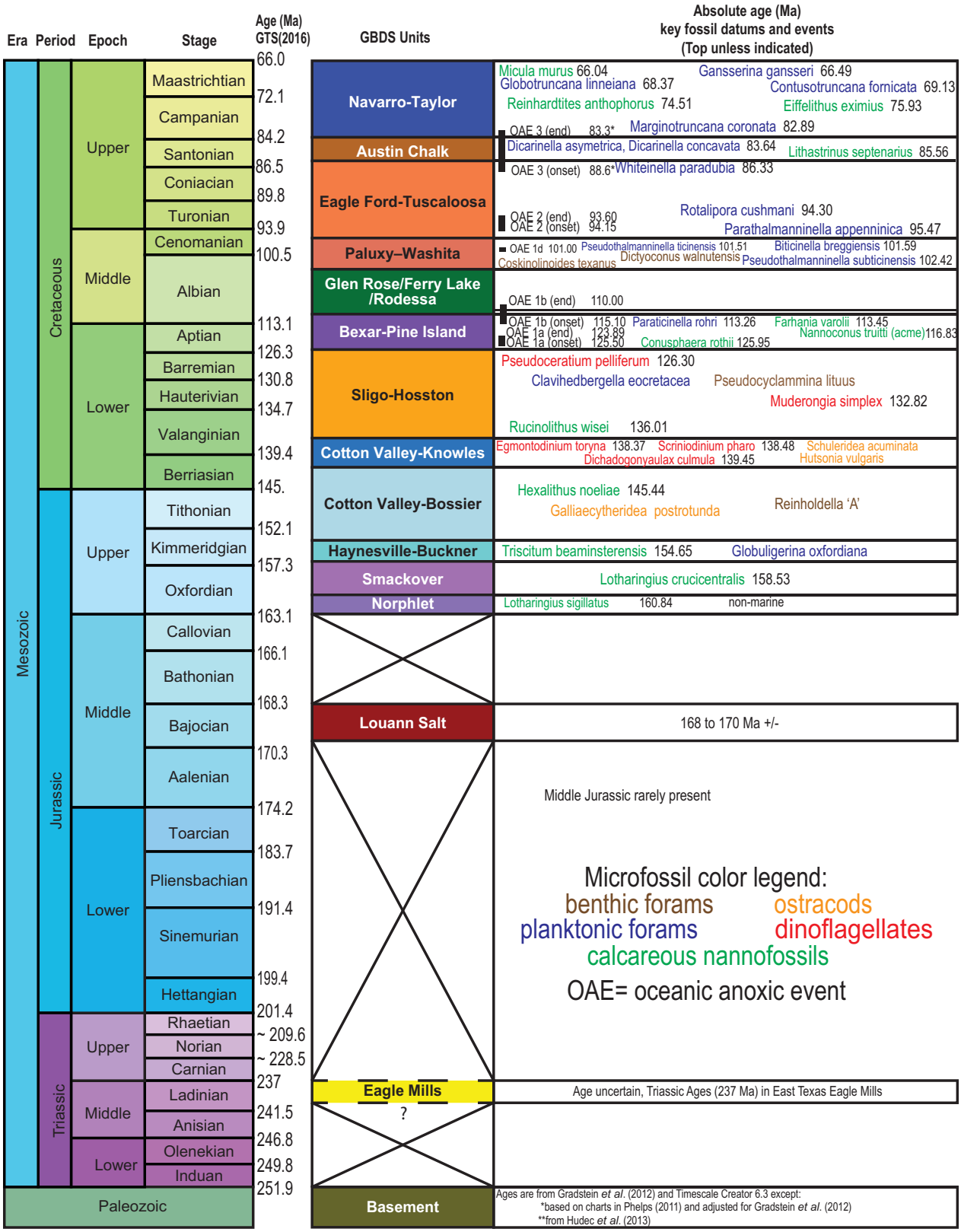

Figure 1.27 Simplified Mesozoic chronostratigraphic chart. Abbreviations for the 15 supersequences used in this book are as follows: EM, Eagle Mills; AC, Austin Chalk; BP, Bexar–Pine Island Shale; CVB, Cotton Valley–Bossier; CVK, Cotton Valley–Knowles; EFT, Eagle Ford–Tuscaloosa; FL, Ferry Lake Anhydrite; GR, Glen Rose; HVB, Haynesville–Buckner; LS, Louann Salt; NT, Navarro–Taylor; PW, Paluxy–Washita; RD, Rodessa; SH, Sligo–Hosston; SN, Smackover–Norphlet. The seismically defined basement unit is noted as BMT. OAEs are oceanic anoxic events and are noted in the GoM by Phelps (2011), with age dates from Gradstein *et al.* (2012), as well as other more recent publications (Elderbak *et al.* 2014; Lowery *et al.* 2014). Additional biostratigraphic datums are available for each supersequence and are detailed in the Mesozoic biostratigraphy table in Olson *et al.* (2015), supplementary material.

https://doi.org/10.1017/9781108292795.003 Published online by Cambridge University Press

Paleocene boundary unit in offshore wells provided by Cantú-Chapa and Landeros-Flores (2001). Here, microfossils (primarily planktonic forams) allowed differentiation of Paleocene and Cretaceous intervals in key wells.

Recently, academic investigators have had some success using advanced absolute age dating techniques to provide sequence stratigraphic correlation points. Lehmann *et al.* (1999, 2000) used isotope chemostratigraphic results in work on the Lower Cretaceous outcrops of northeastern Mexico. U–Pb geochronology (see Box 1.2) based on first-cycle (volcanic) zircons obtained from Mexico outcrop intervals also provided important age constraints in certain Mesozoic intervals (Lawton *et al.* 2009; Lawton and Molina-Garza 2014). The summary stratigraphic chart of Martini and Ortega-Gutiérrez (2016) nicely illustrates the importance of first-cycle zircon U–Pb geochronology for better constraining onshore Jurassic stratigraphy and tectonostratigraphic evolution of the southern GoM. Unfortunately, the same approach is not, at present, being widely used on offshore samples.

Box 1.2 Detrital Zircon Analysis: Advanced Provenance Analysis

In recent years, detrital zircon geochronology has become the tool of choice for provenance analysis that supports detailed paleogeographic reconstructions. It has a number of advantages over previous approaches such as QFL (quartz–feldspar–lithic) ternary plotting from petrographic or compositional analyses that are particularly sensitive to diagenetic removal of framework

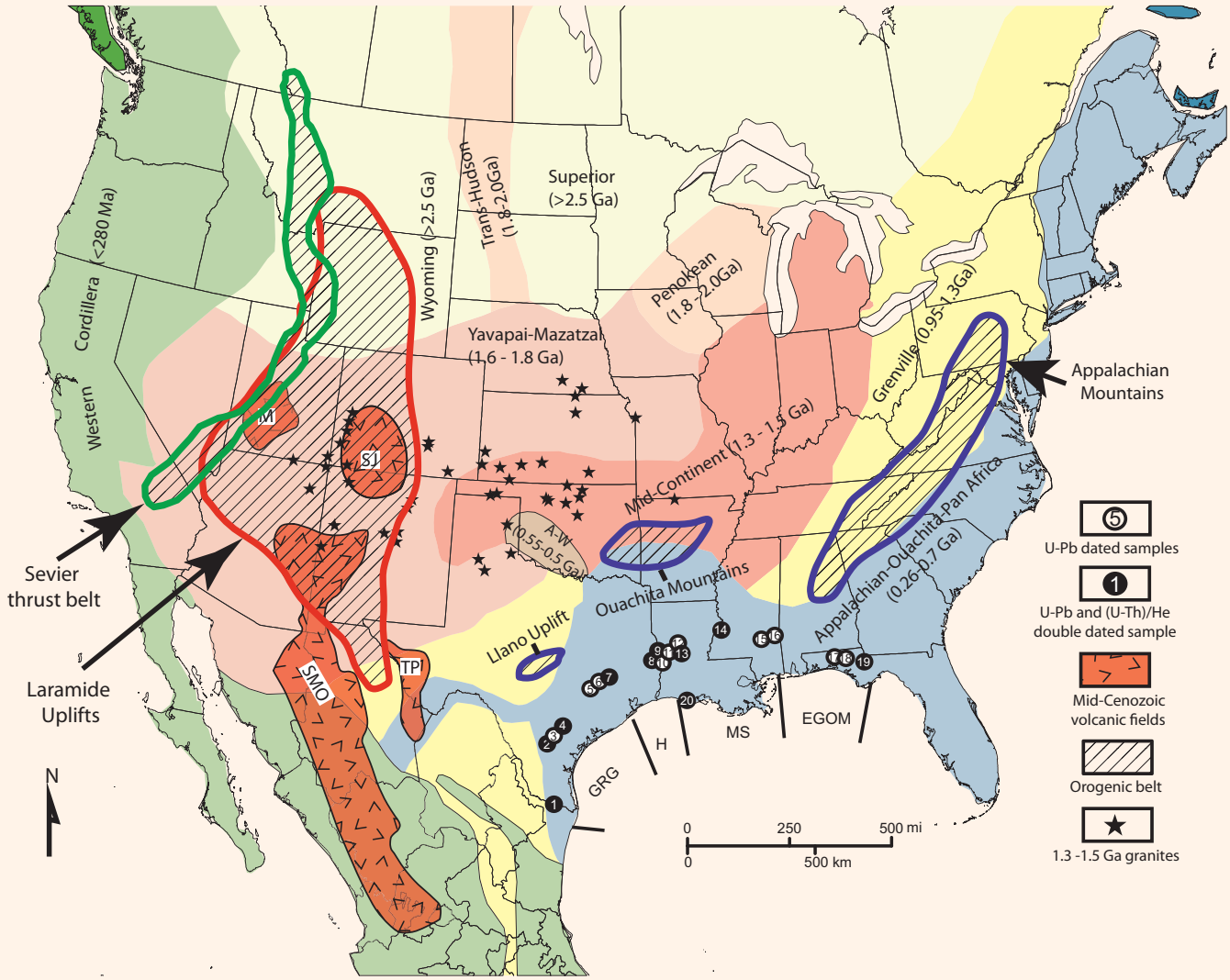

Figure 1.28 North America crustal terranes, orogenic belts, and sample locations in the northern GoM basin. Abbreviations: GRG, Greater Rio Grande Embayment; H, Houston Embayment; MS, Mississippi Embayment; EGoM, Eastern GoM Embayment; M, Marysvale volcanic field; SJ, San Juan volcanic field; TP, Trans-Pecos volcanic field; SMO, Sierra Madre Occidental volcanic field; A–W, Amarillo–Wichita. Modified from Xu *et al.* (2017).

https://doi.org/10.1017/9781108292795.003 Published online by Cambridge University Press

Box 1.2 (*cont.*)

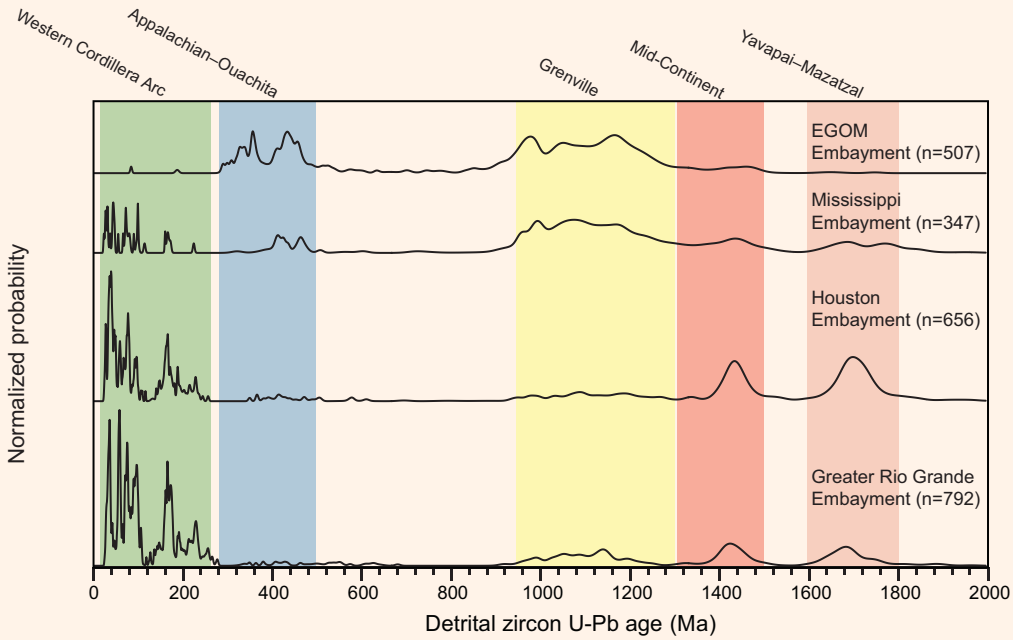

Figure 1.29 Comparison of U–Pb age spectra from detrital zircon grains in the Lower Miocene of Texas. Modified from Xu *et al.* (2017).

grains. Zircon is a heavy mineral, resistant to physical and chemical weathering, and very stable at surface to shallow crustal pressures and temperatures. The zircon uranium–lead (U–Pb) system has a high closure temperature (about 900°C), meaning that U and Pb do not escape the zircon crystal at lower temperatures. As zircon crystals initially have no Pb, the only Pb is from U isotopic decay. Ages derived from zircon U–Pb measurements thus provide the date of the original crystallization of the zircon crystal, assuming that has not been reset by exposures to temperatures over 900°C, rare in deep sedimentary burial without significant pressure–temperature metamorphism or igneous heating.

Because zircon crystallizes at high temperature and pressure, the U–Pb decay provides an age that can be matched to the timing of accretion of different basement terranes to North America (Figure 1.28; Blum and Pecha 2014; Xu *et al.* 2017). From U–Pb detrital zircon age spectra we can identify numerous source terranes such as the Western Cordilleran, Yavapai–Mazatzal, Wyoming, Trans-Hudson, Grenville, Mid-continent, and Appalachian terranes. Once enough zircons (typically 100–300 grains) have been collected and irradiated by laser ablation, a robust and diverse age spectra of the grains is a fingerprint of the contributing source terranes (Figure 1.29).

Zircon geochronology can be useful if there is some uncertainty about the stratigraphic age of a sample. Ages derived from U–Pb analyses of sedimentary rocks are logically considered as a maximum depositional age: young sedimentary intervals can incorporate older zircons but older sedimentary rock obviously cannot include zircons younger than its depositional age. The closest fit between true depositional age and depositional age from zircon geochronology is where first-cycle, volcanic airfall-derived zircons are abundant (Reiners *et al.* 2005). The strict criteria for determining maximum depositional age involves averaging the three youngest zircons that overlap in age at 2σ in a zircon population (Dickinson and Gehrels 2009; Gehrels and Pecha 2014).

One drawback to U–Pb ages derived from detrital zircon is the problem of recycling. Zircon can be liberated by exposure of basement, transported long distances to a new burial site, reburied and exhumed, still retaining the original U–Pb crystallization age. This can be a problem if a sandstone is potentially sourced from two different areas, but retains the signature of only the original source terrane, not the secondary site from which the rivers last drained.

To address this, a more advanced combined U–Pb and (U–Th)/He dating on single zircon grain or "double dating" approach is used to provide the age of cooling or exhumation (Rahl *et al.* 2003; Reiners *et al.* 2005; Xu *et al.* 2017). It makes use of the cooling temperature of zircon, which tells us when the source was uplifted. For example, in the case of the paleo-Greater Rio Grande River, zircons that crystallized 950–1300 Ma in the Grenville basement province were buried and later exhumed at three different sites (Great Plains, west Texas–New Mexico, and Llano area) during four different tectonic events ranging from pre-Cambrian to as recently as 40 Ma (Figure 1.30A). Using double dating one can determine which grains were recycled from the Colorado plateau and which came from the Llano area, for example. The same is true for the younger basement sources coming from the Rockies, in three uplifts ranging from 170 to 25 Ma (Xu *et al.* 2017; Figure 1.30B).

https://doi.org/10.1017/9781108292795.003 Published online by Cambridge University Press

Box 1.2 (*cont.*)

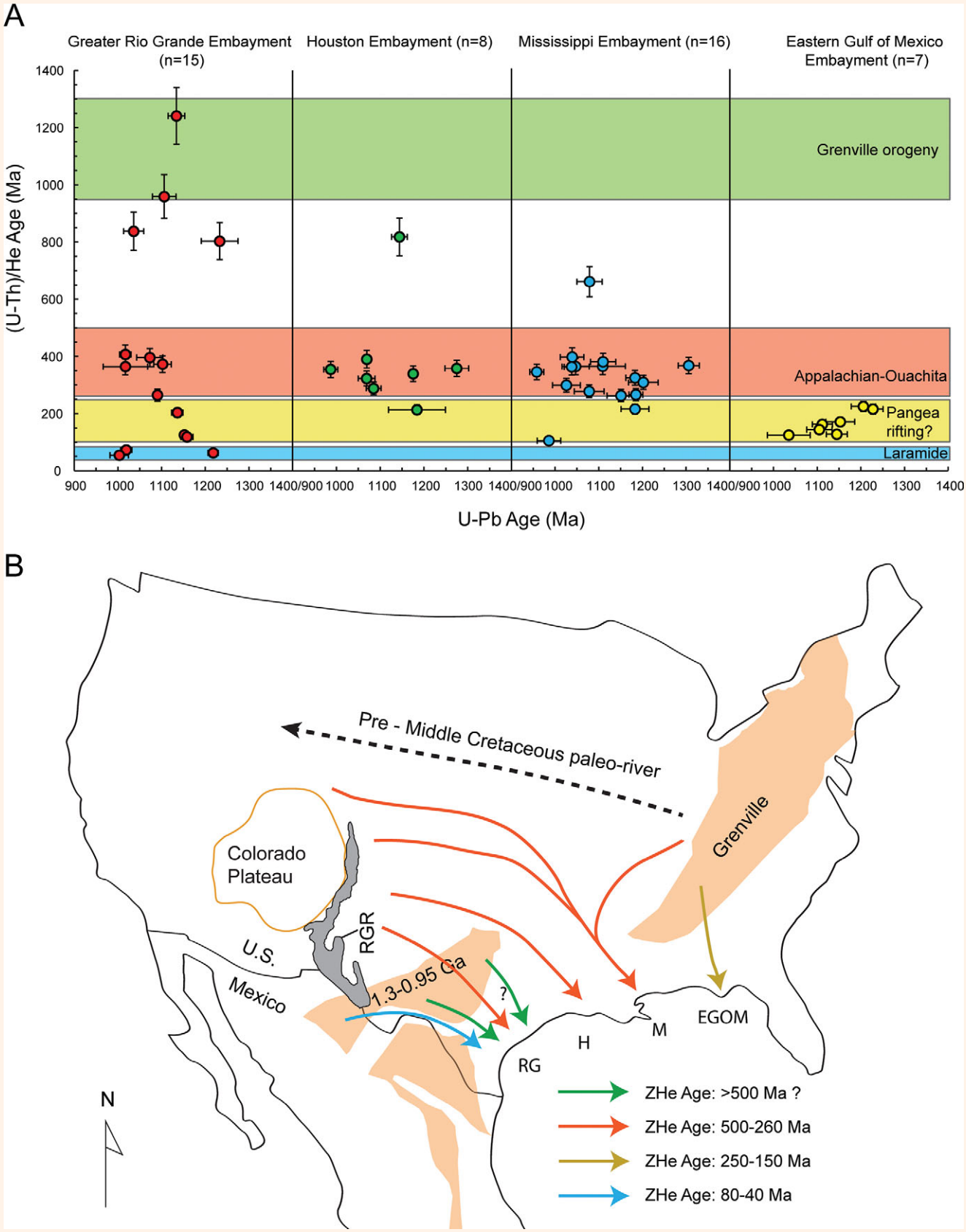

Figure 1.30 Detrital zircon recycling. (A) U–Pb–He ages of Grenville zircons in the Lower Miocene strata of the GoM basin. (B) Sediment routing of Grenville grains. RGR, Rio Grande rift. *n* = number of analyses. Color bars indicate different orogenic events. Modified from Xu *et al.* (2017).

https://doi.org/10.1017/9781108292795.003 Published online by Cambridge University Press

1.12 Cenozoic Chronostratigraphy, Northern GoM

The northern Gulf basin stratigraphic framework, chronology, and nomenclature were established by the mid-twentieth century using conventional stratigraphic concepts. Alternating outcrops of sandy coastal to continental sediments and fossiliferous marine mudrocks provided an initial subdivision for Paleocene and Eocene strata. Early petroleum exploration revealed the subsurface stratigraphy beneath the coastal plain. The thick, repetitious, siliciclastic Cenozoic interval was initially subdivided using the marine shale tongues, and then widespread microfossil-bearing horizons were used to correlate and date the evolving stratigraphic framework. This concept of transgression-bounded genetic units was formalized in a seminal paper by Frazier (1974). Frazier argued that the Gulf Cenozoic fill recorded a succession of "depositional episodes" that deposited by a foundation of progradational marine and coastal facies that were, in turn, overlain and replaced landward by aggradational coastal plain and fluvial facies. This facies succession was capped by a relatively thin succession of transgressive or back-stepping coastal and marine shelf deposits. Importantly, much of the basin margin was sediment-starved at any moment of geologic time. Areas of starvation, bypass, and/or erosion most likely lay in the landward coastal plain and the offshore middle to outer shelf. Thus, the "Frazierian" genetic unit is bounded basinward by submarine starvation surfaces (condensed beds) created during and soon after transgressive retreat of coastal depositional systems. This surface would later come to be known as the *maximum flooding surface*. Such depositional episodes conform to the basic definition of a sequence as a contiguous suite of genetically related strata bounded in part by unconformities. If relative or eustatic sea-level fall punctuates the history of a depositional episode, the genetic unit will contain an internal subaerial unconformity within its landward strata. Fraser's model, in fact, was developed in and for the Quarternary stratigraphy of the Mississippi delta and coastal environs where eustatic sea level was a major factor.

Using the Frazierian depositional model, Galloway (1989a) defined the *genetic stratigraphic sequence* as a fundamental unit of GoM Cenozoic stratigraphy. A genetic sequence consists of all strata deposited during an episode of sediment influx and depositional offlap of the basin margin. It is bounded by a family of surfaces of marine non-deposition and/or erosion created during transgression, generalized as the maximum flooding surface. This pattern is readily recognized in the Paleogene interval, where transgressive marine shelf mudstone and glauconitic sandstone units extend to outcrop (Galloway 1989b). It also applies in Neogene strata, where prominent transgressive markers record **glacioeustatic** sea-level rise events (Galloway *et al.* 2000). Thus, genetic sequences typically correspond closely to widely used northern Gulf stratigraphic nomenclature.

The *depositional sequence* paradigm, which uses subaerial erosion surfaces as sequence boundaries, provides an alternative to the traditional Gulf basin lithostratigraphic framework and has been applied by several authors (Yurewicz *et al.* 1993; Mancini and Puckett 1995; Lawless *et al.* 1997), especially to Late Neogene strata that are strongly influenced by glacioeustasy (Weimer *et al.* 1998; Roesink *et al.* 2004). Depositional sequence models for carbonate and mixed successions, which are appropriate for the Mesozoic Gulf fill, are summarized and illustrated by Handford and Loucks (1993).

The synthesis of Gulf depositional history and physical stratigraphy as presented here largely utilizes the traditional Paleogene lithostratigraphic framework and the regional marine flooding horizons characterized by widely identified faunal markers within Neogene strata. Building upon the syntheses of Winker and Buffler (1988), Galloway (1989b), and Morton and Ayers (1992), Galloway *et al.* (2000) proposed a genetic stratigraphic framework that groups Cenozoic strata into a succession of 18 principal GoM depositional episodes (shortened to deposodes; Figure 1.31). Each episode records a long-term (ca. 2–12 Ma) cycle of sedimentary infilling, typically accompanied by shelf-margin offlap, along the divergent margin of the northern Gulf basin. Deposits of each episode are characterized by lithologic composition (predominantly sandstone and mudstone, with minor carbonate and evaporite), vertical stacking of lithofacies and parasequences, and relative stability of sediment dispersal systems and consequent paleogeography. Almost all of the depositional episodes terminated with a phase of deepening and/or basin margin transgression (Figure 1.31). Deposits of episodes are bounded by prominent, widely recognized, and well-documented stratigraphic surfaces. Bounding surfaces variously include marine starvation and condensed horizons, maximum flooding surfaces, marine erosional unconformities, and faunal gaps that are described and interpreted by multiple authors. They are widely recognized as fundamental stratigraphic building blocks of the basin-fill and are equivalent to the supersequences described for the Mesozoic. They constitute the physical stratigraphic equivalent of the chronostratigraphic deposode.

1.13 Cenozoic Chronostratigraphy, Southern GoM

Like the Cenozoic of the northern GoM, the chronostratigraphic framework of Mexico is based primarily on offshore well biostratigraphy, largely foraminifera of benthic and planktonic forms. Biostratigraphic work by Pemex and IMP has been occasionally incorporated into university theses and dissertations (Sánchez-Hernández 2013) or published papers (Vásquez *et al.* 2014; Gutiérrez Paredes *et al.* 2017). As an example, a data table of Gutiérrez Paredes *et al.* (2017) provides LADs and FADs of planktonic forams and calcareous nannofossils for the Upper Miocene to Lower Oligocene of 12 wells drilled in southern offshore Mexico. The majority of the fossil data conforms to the top unit boundaries of the Upper Miocene, Middle Miocene, and Oligocene Frio used here for the northern GoM. One important exception to the

https://doi.org/10.1017/9781108292795.003 Published online by Cambridge University Press

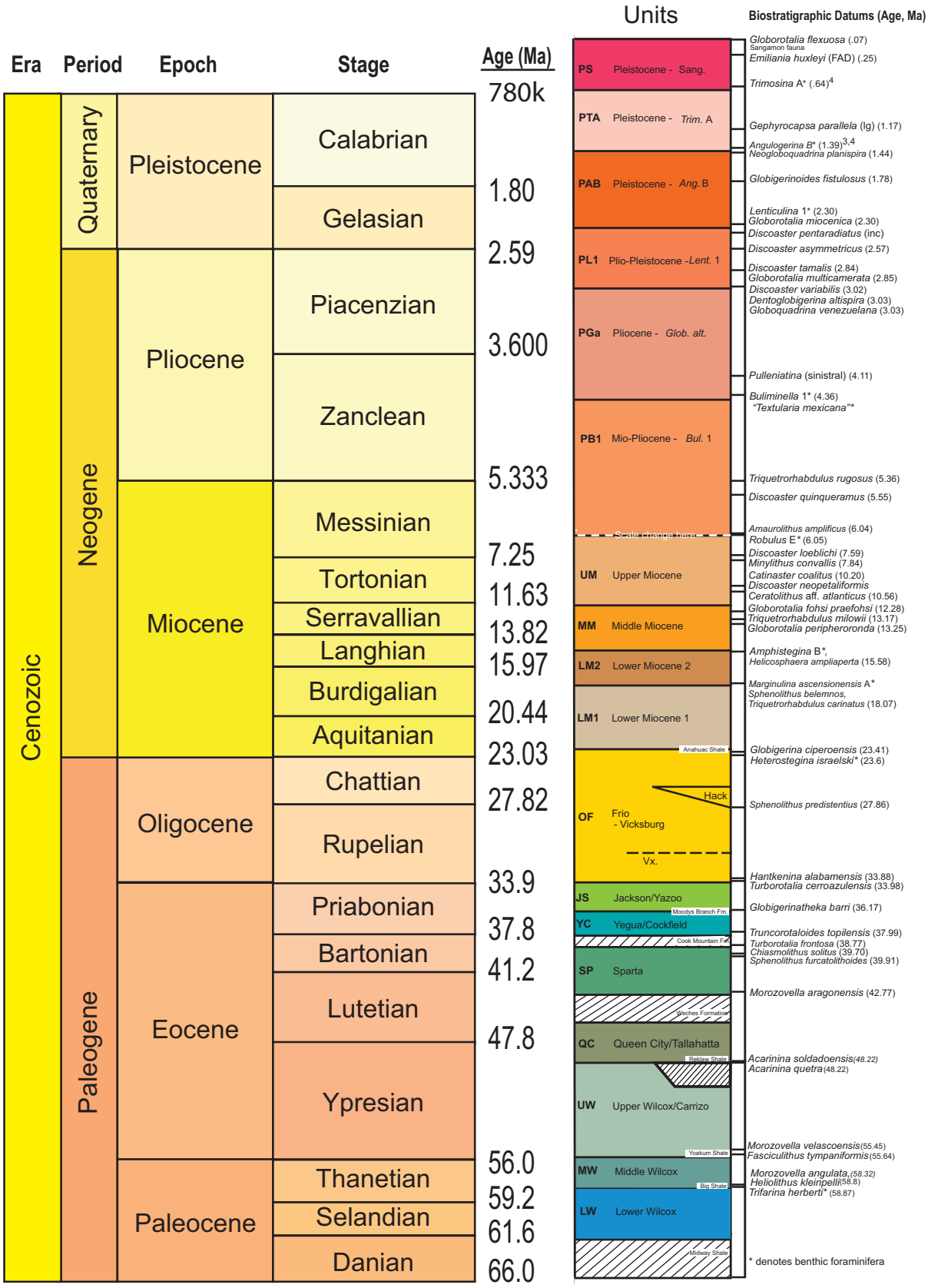

Figure 1.31 Cenozoic chronostratigraphic chart, including key biostratigraphic datums.

https://doi.org/10.1017/9781108292795.003 Published online by Cambridge University Press

Neogene is the boundary of the Lower Miocene and Middle Miocene, which is lower within the GBDS stratigraphy discussed earlier. Gutiérrez Paredes *et al.* (2017) do point out, however, that the bounding Langhian stage is not well represented in the area, with only one well encountering that stage in cuttings. This is relevant to exploration, as Gutiérrez Paredes *et al.* (2017) show a large number of stratigraphic discontinuities in the Middle Miocene Serravallian interval that are accompanied by sandstone reservoir occurrence in the wells. That is consistent with the 9–16 Ma fast exhumation phase of the Chiapanecan orogeny in landward areas (Sanchez-Montes de Oca 1980; Witt *et al.* 2012).

The Paleogene chronostratigraphy is less well documented in public reports or published scientific papers. An exception is the detailed chronostratigraphic chart for the Chicontepec Canyon included in Vásquez *et al.* (2014). The biostratigraphic datums generally conform to global stage boundaries, but there are some notable departures that may reflect local conditions in this large-scale erosional canyon system and the repeated bypass of sands into the basin in the Eocene (Cossey *et al.* 2007).

Biostratigraphic charts provided in relatively rare university studies of Pemex wells provide some direct comparison to the northern GoM chronostratigraphy. For example, analysis of ditch (cuttings) samples by Gutiérrez-Puente (2006) in the Cupelado-10 well is shown as a range chart of various planktonic forams. As analysis was done using the standard micropaleontological scheme of Bolli *et al.* (1989), there is general equivalency of many biodatums in the Pliocene to Paleocene interval here, providing some level of comfort that age-constrained basin-wide correlations between the northern and southern GoM can be made.

1.14 Stratigraphic Framework of Cuba

Most structural and stratigraphic classifications consider Cuba as part of the greater Caribbean (Pardo 1975; Pindell and Kennan 2001). Our treatment of the area is therefore superficial, except where the stratigraphy of the adjacent GoM basin is concerned. Extensions of trends from the USA across the Florida Straits are relevant and the effects of various basin-wide events, such as the Chicxulub impact (K–Pg event) obviously are recorded in the rock record of Cuba. Additional discussion of the petroleum habitat of Cuba is included in Chapter 2. The subsections that follow focus on the Mesozoic and Cenozoic stratigraphic framework that is relevant for an understanding of the greater GoM basin.

1.14.1 Cuban Mesozoic Stratigraphic Framework

The Mesozoic stratigraphic framework of Cuba largely reflects the evolution of the GoM basin, as major differentiation of the GoM and Caribbean basins did not occur until the Late Cretaceous to Paleogene (Escalona and Yang 2013). While the proto Caribbean plate did form during the Late Triassic to Early Jurassic separation of North and South America, the stratigraphic intervals are remarkably similar (Figure 1.32). Initially, interpreted continental to shallow marine siliciclastics filled half-grabens (Escalona and Yang 2013), a pattern also observed in the northern and south GoM at this time. It is important to note that Sequence 1 of Escalona and Yang (2013) has not been penetrated in the offshore area to date, but its seismic character and geometry are suggestive of a syn-rift interval analogous to the Eagle Mills drilled in the northeastern GoM (Marton and Buffler 1999).

Late Jurassic rotation of the Mayan (Yucatán) block during GoM sea floor spreading also generated important tectonic elements in Cuba (Escalona and Yang 2013). Jurassic platform carbonates (Remedios district; Figure 1.32) and coeval distal slope or scarp facies of Oxfordian to Tithonian age show similarities in lithology with the limestones and carbonate mudrocks of the areas to the north (e.g., Smackover, Haynesville, Cotton Valley Formations).

This was followed by a period of relative tectonic quiescence in the Early Cretaceous, with progressive drowning of the proto Caribbean plate and deposition of deep marine carbonates (Sequence 2 of Escalona and Yang 2013). Shallow marine carbonates were restricted to the highest structural features (e.g., Upper Perros Formation of the Remedios district; Morena and Margarita Formations of the Placetas and Camajuani districts, respectively). Palenque Formation carbonates of the Remedios district are correlative to the Aptian to Albian interval of the GoM basin (e.g., Sligo–Hosston, Glen Rose, Paluxy–Washita supersequences; Figure 1.32). Ceno-Turonian equivalents of the Eagle Ford–Tuscaloosa and Austin Chalk supersequences (e.g., Purio Formation of the Remedios district) were deposited just prior to major plate collision in the Late Cretaceous, as described in Section 2.2 on plate tectonic reconstructions. DSDP core site 537, drilled to the north of Cuba, penetrated deep marine to shallow marine carbonates of Early Cretaceous age (Schlager *et al.* 1984).

DSDP cores to the north of Cuba also penetrated limestone breccia units with strong similarity to onshore Cuba deposits related to the Chicxulub impact event on nearby Yucatán. Sanford *et al.* (2016) described over 130 ft (40 m) of carbonate breccia in DSDP Leg 77 Sites 540 and 536 cores, linked to mass transport processes generated by the seismic wave that moved across the entire basin within minutes of the impact. The corresponding Cuba outcrops of the Penalver Formation and Cacarajícara Formations, also related to the impact event, are well documented (Tada *et al.* 2003; Cobiella-Reguera *et al.* 2015).

1.14.2 Cuban Cenozoic Stratigraphic Framework

The Late Cretaceous to Eocene strata collision between the greater Arc of the Caribbean and North American plates set up significant differences in stratigraphy between the two basins. The original Jurassic strata that were laterally continuous to the GoM basin were now subducted beneath the upper Caribbean plate in several stages, forming the Cuban fold and thrust

https://doi.org/10.1017/9781108292795.003 Published online by Cambridge University Press

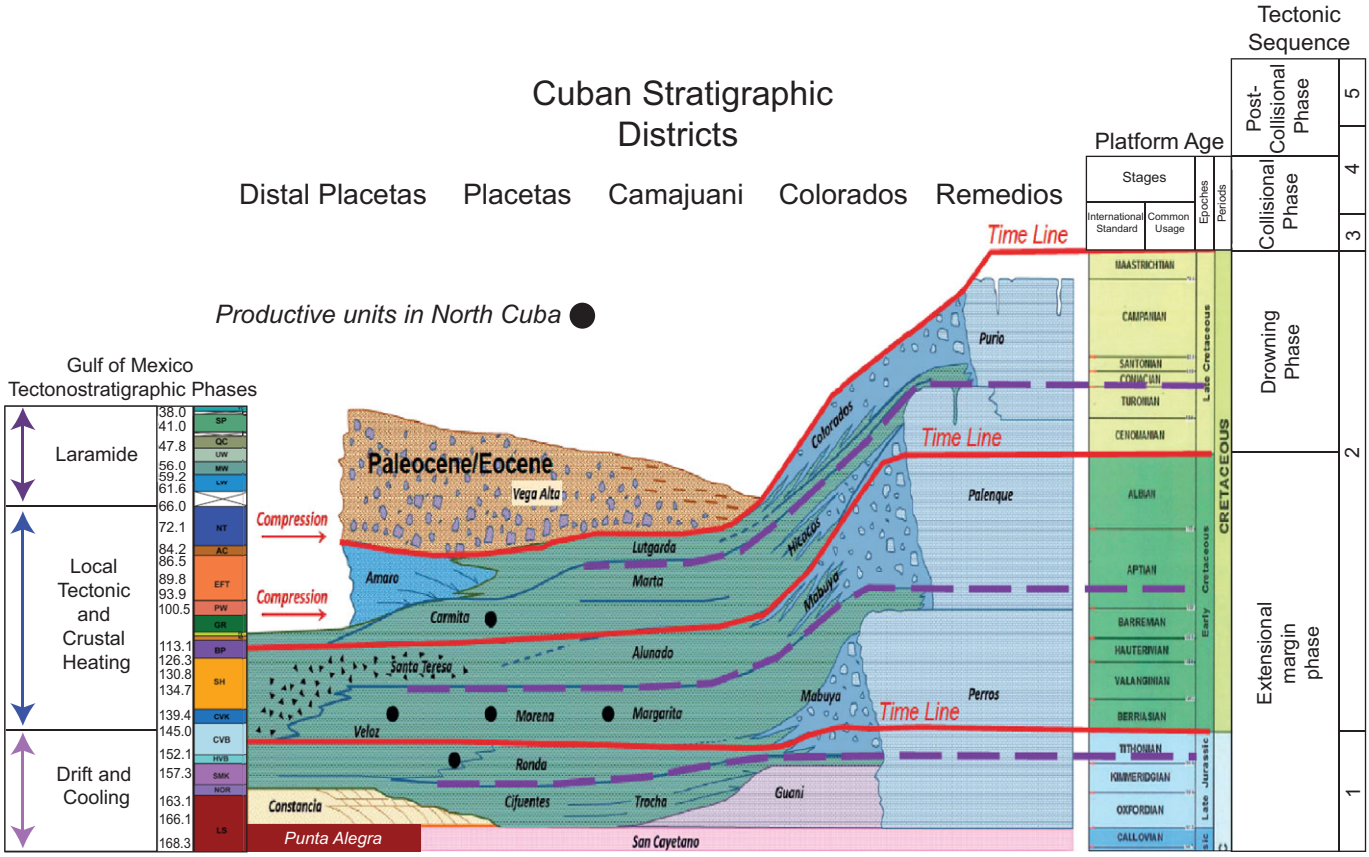

Figure 1.32 Mesozoic and Paleogene stratigraphy of Cuba. Compiled from Escalona and Yang (2013), Gordon *et al.* (1997), and Melbana Energy (2017)

system. Distal shales of Mesozoic age were thrust into the upper plate while more proximal carbonate facies are present in the lower plate, separated by a major mid-level detachment at the Eocene level. Escalona and Yang (2013) confine this collision phase to their Paleocene–Eocene age Sequence 3 and the Oligocene portion of their Sequence 4 (Figure 1.32).

Paleocene to Eocene foredeep sedimentation took place north of the thrust belt, as documented by deposition of the Vega Alta and Vega-Rosas Formations (Gordon *et al.* 1997; Melbana Energy 2017). Later back-thrusting within the upper plate further complicated the present-day structural architecture and has made unraveling the Cenozoic stratigraphy much more difficult (Escalona and Yang 2013). It is also important to note that the western half of Cuba merged with the eastern half during the west-to-east tectonic transport, so the pre-collision strata in western Cuba are linked more closely with the Yucatán (Mexico) stratigraphy (e.g., San Cayetano Formation; Haczewski 1976).

Post-collision Cenozoic strata are influenced by development of the Cayman trough and the Loop Current Gulf stream flowing through the Florida Straits. Large, deep sea erosional features (channels) and constructional sediment drifts of Miocene to Holocene age are present between Cuba and the Florida Escarpment, documenting vigorous bottom currents flowing from the northern Caribbean into the Straits of Florida and to the North Atlantic (Gordon *et al.* 1997). Post-collision strata constitute the Miocene portion of Sequence 4 and the entirety of Sequence 5 (Pliocene to end Pleistocene; Escalona and Yang 2013).

1.15 Depositional Systems Classification

Many classifications of past and present depositional environments exist. This is due to the tremendous amount of scientific effort that has gone into characterizing the various siliciclastic and carbonate settings in which sediments accumulate, to be buried and preserved in the rock record. For siliciclastic depositional systems, this book follows Galloway and Hobday (1996), and for carbonate systems the scheme discussed by Handford and Loucks (1993).

As work on depositional paleo-environments has continued since the original publication of these classifications, it is worthwhile to discuss updates and modifications to these schemes that are relevant for the greater GoM.

1.16 Update to Carbonate Depositional Systems in the GoM Basin

Advances in our understanding of carbonate depositional systems have also occurred as modern environments are newly

https://doi.org/10.1017/9781108292795.003 Published online by Cambridge University Press

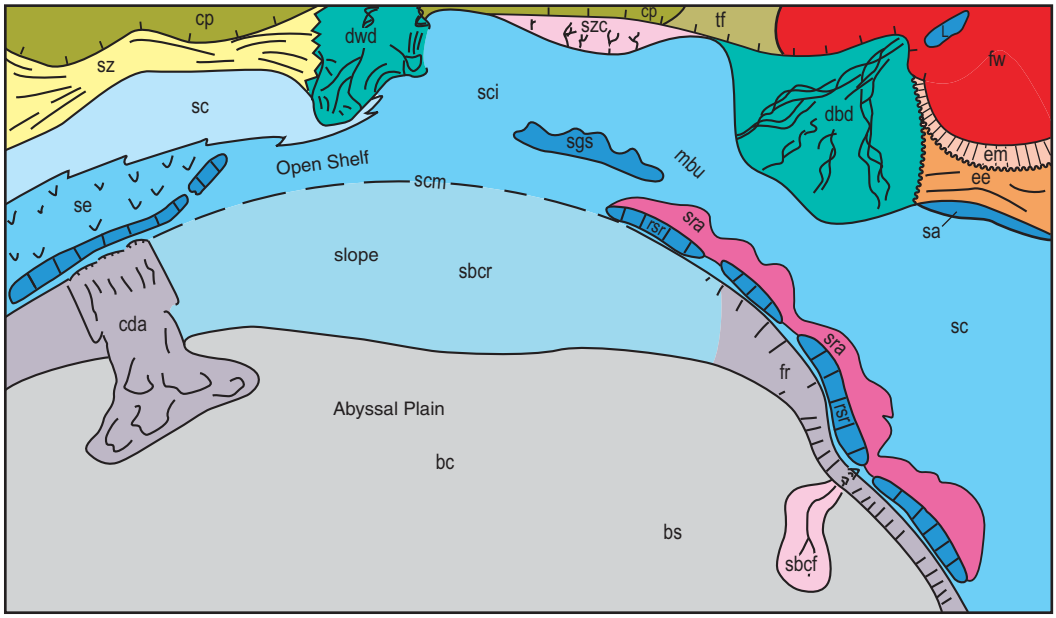

Generic Deposystems Mesozoic

sa	sabhka
tf	tidal flat
sz	siliciclastic shorezone
sci	inner platfor/ramp
scm	outer ramp
se	self evaportie lagoon
cda	carbonate debris apron
dwd	wave-dominated delta
szc	carbonate shorezone
sgs	shelf grain shoal
sbcr	slope to basin carbonate ramp
bc	cabonate-rich basin
bs	starved basin
cp	coastal plain
dbd	braid delta
sc	carbonate shelf, undifferentiated
sra	shelf reef apron
rsr	rimmed shelf reef
sbcf	slope to basin carbonate fan
fr	forereef
ee	eolian erg
em	eolian erg margin
mbu	microbialite buildup
fw	fluvial-wadi

Figure 1.33 Schematic Mesozoic deposystems and classification.

investigated but also as better imaging and characterization of fossilized depositional systems has been carried out by industry and academia. These are particularly relevant to the GoM Mesozoic interval, as documented in well penetrations and numerous publications.

Unlike the siliciclastic-dominated Cenozoic interval of the GoM basin, the Mesozoic succession contains a large portion of carbonate facies, ranging from shallow tidal flat/sabkhas to rimmed shelf reefs to deepwater basin carbonates (Figure 1.33). The long time span of the Mesozoic also saw considerable evolution in different organisms, ranging from Jurassic **microbalites** to Cretaceous framework-building **caprinid rudistids** (Wilson 1975). The Mesozoic also chronicles the rise of massive rimmed shelf reef systems such as in the Aptian–Barremanian (Sligo) and Albian (Washita) and their decline after the Mid-Cretaceous.

Notable recent additions to the classification of Handford and Loucks (1993) include the shelf reef apron (abbreviated as sra), shelf grain shoal (sgs), inner and middle carbonate ramp (sci, scm), and others. For example, reef aprons are exceedingly common in modern systems (Vila-Concejo *et al.* 2013) and recognized in ancient Mesozoic systems as well (Adams 1985). These consist of grainy carbonates and debris transported locally from the rimmed shelf reef systems.

Detailed discussion of the characteristics of these carbonate deposystems and their characteristics in log and core is contained in the online poster titled "Gulf of Mexico Mesozoic Log Facies Interpretation" (www.cambridge.org/gomsb). Well log motifs, placed in a proper paleophysiographic context (e.g., coastal plain, shelf, slope, abyssal plain) define depositional environments for mapping purposes. Iteration with interval thickness, nearby well bores, and regional trends help constrain interpretations, as will be discussed in Section 1.17 and shown in the online resource titled "Gulf of Mexico Siliciclastic Log Facies Interpretation" (www.cambridge.org/gomsb).

At the heart of this book are the **paleogeographic** maps of the Mesozoic and Cenozoic stratigraphic units. One obvious way to validate paleogeographic maps of the embedded depositional systems is by comparison to modern analogs. While most biological components of a carbonate system have evolved since the Mesozoic ended 66 Ma, the physical processes of waves, currents, tides, winds, and sunlight that drive the areal distributions of carbonate systems have not changed.

The Great Barrier Reef (GBR) of Australia (southern sector; Figure 1.34) may be an appropriate analog for the Mesozoic carbonate systems of the Gulf for several reasons. First, the relative paleo-latitude of the Mesozoic (±20 degrees north of the equator) is comparable with the GBR southern sector (GBR-ss) at 22–24 degrees south of the present equator. Second, the GBR-ss is a mixed carbonate–siliciclastic system, with terrigenous input from multiple rivers (see Figure 1.34). In general, siliciclastics dominate landward areas, carbonates dominate seaward (outer shelf, slope, and deepwater) areas and mixing occurs between the two (Maxwell and Swinchatt 1970). A similar pattern is observed in at least four units of the Mesozoic that will be discussed (Paluxy–Washita, Sligo–Hosston, Cotton Valley–Knowles, and Cotton Valley–Bossier). Reciprocal sedimentation, where carbonates give way to sandstone moving paleo-landward, is well documented in the Mesozoic of the GoM, as it is in the GBR. Reefs can flourish in such a setting, as long as the mud content (and thus turbidity) of the input fluvial systems is low enough to permit photosynthesis. Third, the dimensions of key depositional elements are comparable. For example, the GBR extends over 2250 km of the

https://doi.org/10.1017/9781108292795.003 Published online by Cambridge University Press

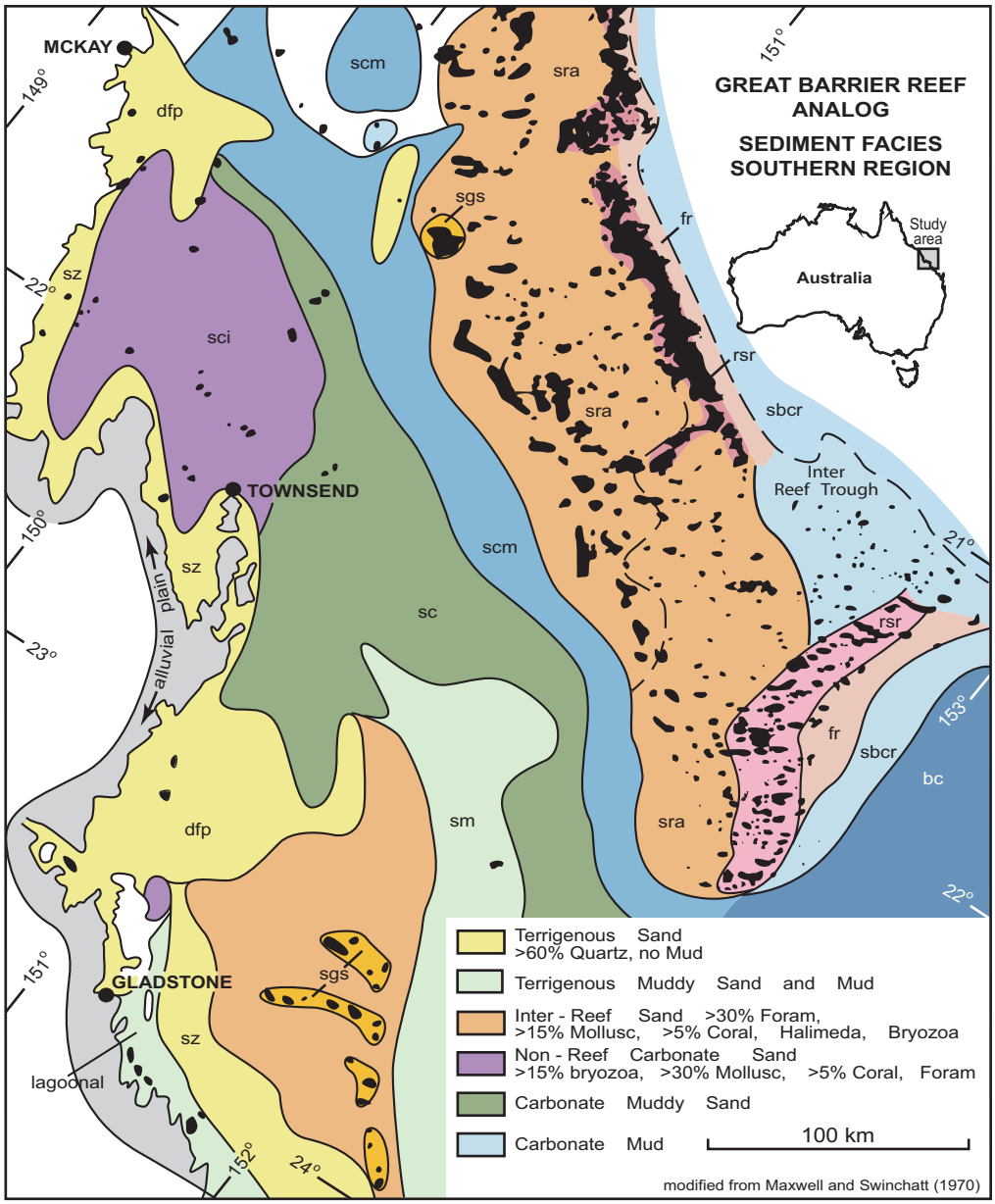

Figure 1.34 Great Barrier Reef analog for Mesozoic mixed carbonate and siliciclastic systems of the GoM. Modified from Maxwell and Swinchatt (1970). Depofacies classification from Galloway (2008). Abbreviations for depofacies used: scm, open shelf outer platform/ramp; sra, reef apron (landward); rsr, rimmed shelf margin (reef or grain shoal); sgs, shelf grain shoal; fr, forereef; sbcr, shelf-to-basin carbonate ramp or distal forereef; bc, carbonate-rich basin floor; sc, carbonate-dominated shelf; sci, open shelf, inner platform/ramp; sz, wave-dominated shore zone; dfp, fluvial-dominated platform delta; sm, mud-dominated shelf. Modified from Snedden *et al.* (2016b).

northeastern Australia margin (Harris and Kowalik 2005) versus the mapped extent of the Sligo rimmed shelf reef systems in the USA, which is at least 2500 km, with another 1000 km in Mexico if one considers the Yucatán margin.

One key difference between the GBR-ss and Mesozoic of the GoM may be the continuity of the rimmed shelf reef system itself. The GBR-ss is segmented at several scales, from small tidal passes that allow open exchange of oceanic and shelfal waters to larger interreef troughs (Figure 1.34) where the rimmed shelf reef is not developed. Most maps of the Sligo (Aptian–Barremanian) and Washita (Albian) systems show only a few tidal passes or interreef troughs (Goldhammer and Johnson 2001) breaking up the long extent of these systems. It may be that well control and 2D seismic line density is insufficient to resolve the tidal passes and other reentrants and thus greater continuity is incorrectly inferred. Even in the GBR, reefs extend along only 70 percent of the shelf edge (Harris and Kowalik 2005). Goldhammer and Johnson (2001) identified at least two interreef troughs or large tidal passes in the Mesozoic of onshore Texas.

The GBR-ss map also shows that the distinct seaward zonation of deposystems from landward to deepwater is

https://doi.org/10.1017/9781108292795.003 Published online by Cambridge University Press

mirrored in the paleogeographic maps from the Mesozoic. Shelf-to-basin carbonate ramp (sbcr) occurs in both the inter-reef trough and a distal equivalent of the forereef (fr). The ramp term is a bit of a misnomer, as rimmed shelf reef is not ramp-like but somewhere in the basin the bathymetry flattens out, but the log facies appear to be quite similar in both locations. Forereef is located seaward of the reef, and shelf reef apron (sra) is landward of the main reef. The shelf carbonate middle (scm), a generally carbonate mud-prone interval, is often positioned landward. Yet further landward is the shelf carbonate undifferentiated (sc). Shelf grain shoals (sgs) occur within this physiographic tract but are generally less continuous than the rimmed shelf reef. In the GBR-ss, these are highly variable in size and shape, and this is mirrored in the Mesozoic carbonate intervals. In the GBR, reefs are oriented relative to wind direction or prevailing currents (Harris and Kowalik 2005) and might be a control on grain shoal and patch reef development in the Mesozoic.

1.17 Update to Siliciclastic Systems in the GoM Basin

Classification of the Cenozoic siliciclastic depositional systems (Figure 1.35) follows Galloway and Hobday (1996). This approach emphasizes the process framework and nomenclature of physical geography and thus is specifically designed for creating paleogeographic maps delineating the landscapes and seascapes created during a depositional episode. The paleogeographic reconstructions that follow expand on and update previous syntheses of Galloway *et al.* (2000) and Galloway (2008).

This synthesis further benefits from a number of recent papers that have provided critical insights into global documentation of the processes, facies architecture, and geography of sediment transport systems and their constituent depositional and erosional elements. The interpretations and maps that follow are conditioned by their conclusions:

1. It has been long recognized that delta systems of large rivers are the major suppliers of sediment to the Gulf basin. The apex positions of large deltas are commonly localized by bedrock or long-lived alluvial valleys (Hartley *et al.* 2015). Thus the delta systems tend to geological longevity and reflect structurally defined basin margin topography. Along the Paleogene GoM margin, a number of specific uplifts bounded likely entry points for large rivers. Paleogene examples include the Tamaulipas Arch, Picachos Arch, Chittum Anticline, and Sabine Uplift. Beginning in the Oligocene, tilting uplift along the northern GoM

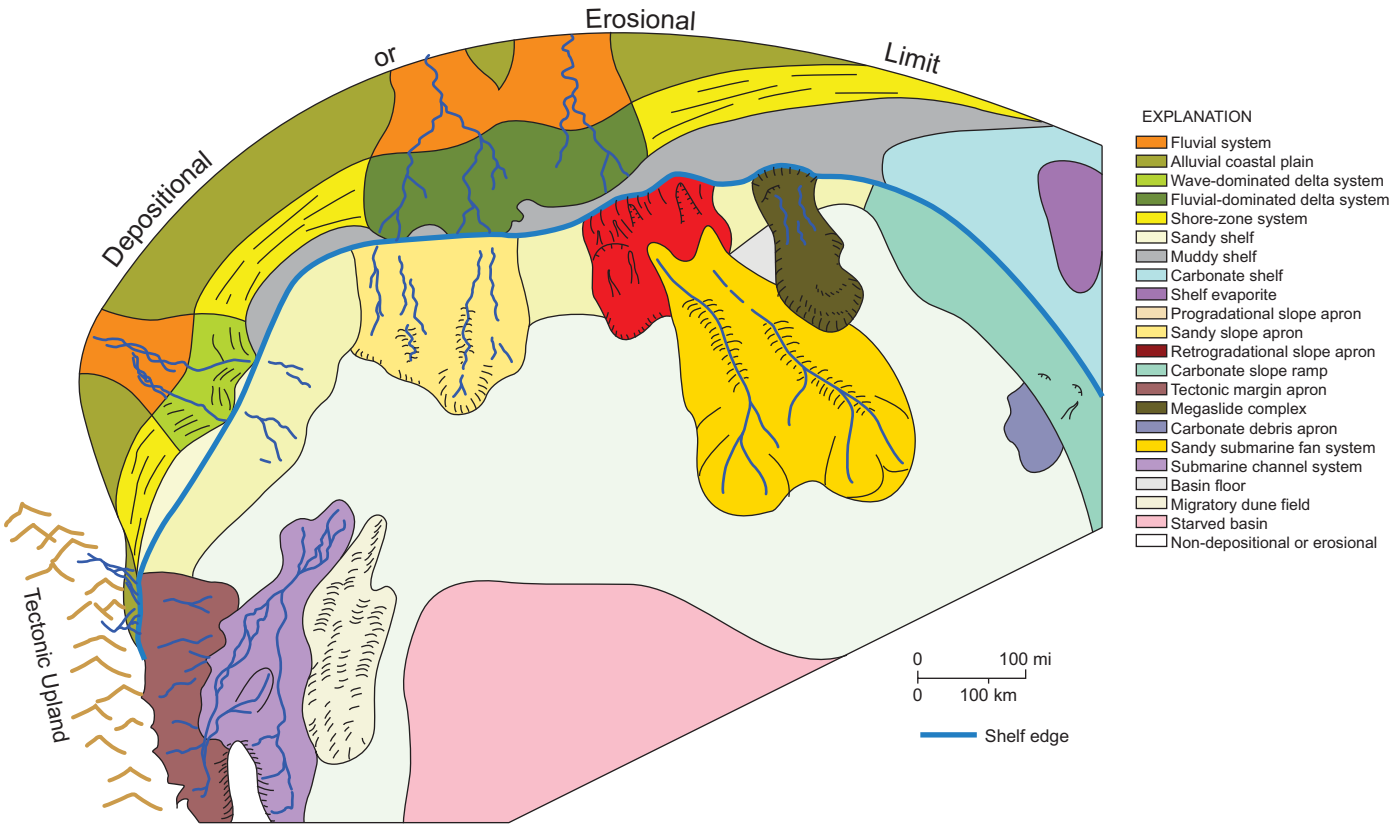

Figure 1.35 Depositional systems paleogeography typical of the Cenozoic deposodes of the Gulf basin. This figure provides a graphical explanation of the color scheme used in the paleogeographic maps.

https://doi.org/10.1017/9781108292795.003 Published online by Cambridge University Press

Box 1.3 Submarine Fans, Ramps, and Aprons

Most sedimentologic literature has described, and continues to describe, sandy, deep marine facies using submarine fan models. Sequence stratigraphic systems tract models reinforced the application of fans as the primary sandy depositional elements of slope and basin settings, associating their origin with sea-level fall and lowstand. However, where regional datasets allow three-dimensional mapping of slope and basin facies, deepwater depositional systems display diverse geographies. Fan morphologies are only one of many areal patterns displayed. Reading and Richards (1994), using datasets from both Quaternary continental margins and ancient analogs, synthesized a suite of conceptual models that emphasized two major variables: (1) grain size of sediment supply, and (2) the geometry of the feeder system. They recognized that the pattern of sediment supply to the slope ranges from highly focused to widely dispersed along the length of the shelf edge. Based on the second variable, they differentiated point-sourced fans, arcuate-sourced ramps, and line-sourced aprons (Figure 1.36A–D). Ramps and aprons produce prisms of slope sediment whose along-strike breadth is subequal to or exceeds the run-out length of the depositing gravity flow dispersal system. Along-strike facies architecture is complex but repetitive. Differentiation of ramps and aprons is based on the degree to which slope feeders are dispersed along the strike.

Recognizing that the ramp model was associated with shelf-margin delta systems, Galloway (1998) suggested differentiation of slope/basin depositional systems into relatively focused, point-sourced fans and broadly sourced slope aprons (incorporating both aprons and ramps). Slope type was further differentiated based on the upslope depositional systems tract. Typical configurations for prograding slopes include arcuate delta-fed aprons and linear shelf-fed aprons. *Delta-fed aprons* are constructed where multilateral and/or sequential shelf-margin delta lobes cumulatively supply sand to the slope along a broad front that, over geologic time, can extend many tens of miles along the shelf margin. *Shelf-fed aprons* are typically linear, extending up to hundreds of miles along the strike. Retrograding slopes

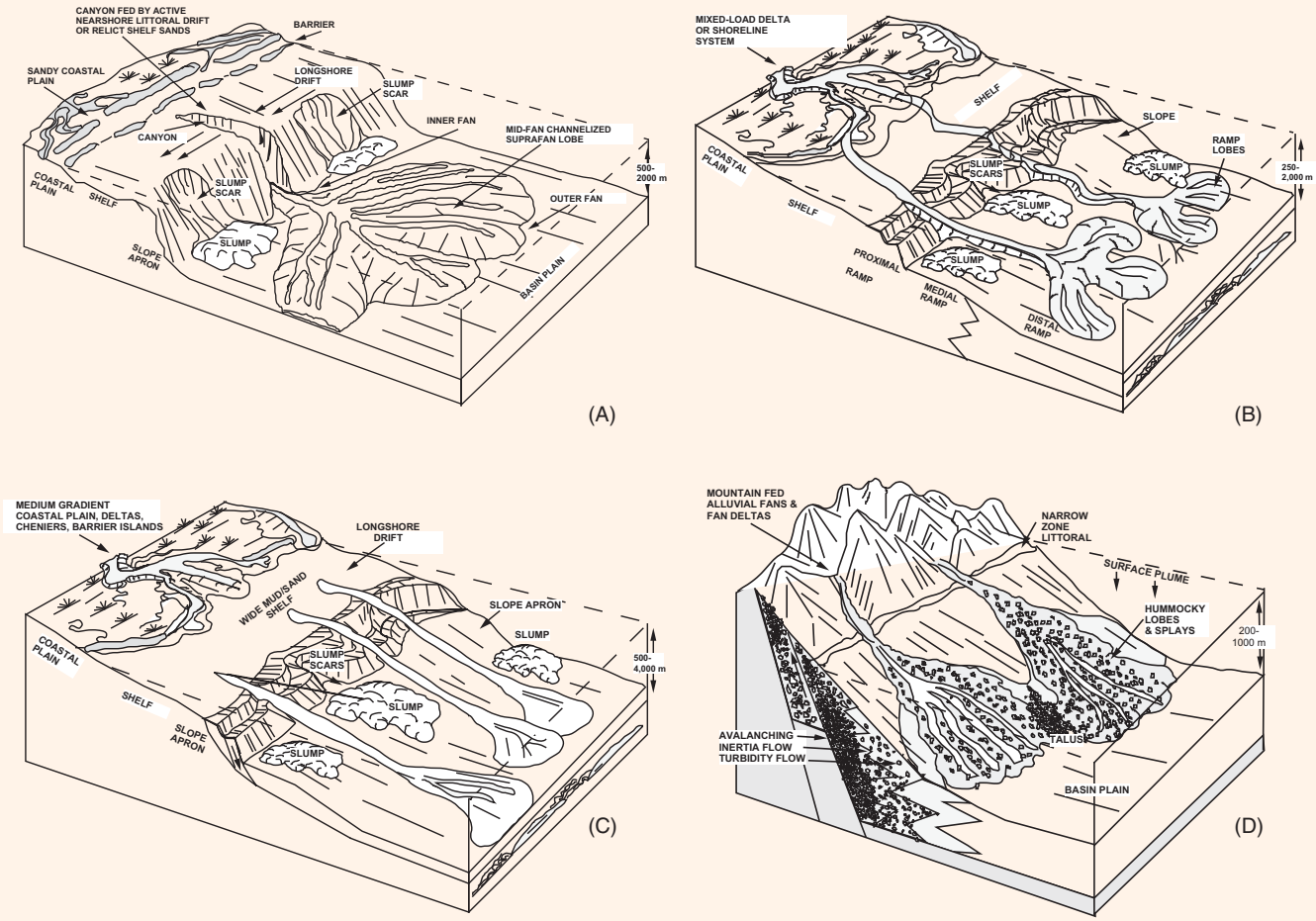

Figure 1.36 (A) Depositional model for a canyon-fed, point-sourced submarine fan. From Reading and Richards (1994). (B) Depositional model for a sandy delta-fed progradational apron. Note the direct connection between delta front and slope channels, which diverts sand directly from the sandy mouth bars and shoreface onto the upper slope. From Reading and Richards (1994) (C) Depositional model for a mud-rich progradational slope apron supplied by muddy deltaic or shelf systems. From Reading and Richards (1994). (D) Depositional model for a tectonic margin slope apron. A very narrow or absent shelf platform allows transfer of sediment load directly from uplands to the submarine slope. From Reading and Richards (1994).

https://doi.org/10.1017/9781108292795.003 Published online by Cambridge University Press

Box 1.3 (*cont.*)

retreat by mass wasting and submarine erosion of the outer shelf and upper slope. Basinward, recycled upper slope and shelf-margin sediments deposit a *retrogradational slope apron*. Along tectonically active margins, adjacent upland sources shed sediment across an erosional terrane directly onto the subaqueous slope or across a narrow coastal zone of coalesced fans and fan deltas, depositing a typically coarse-grained *tectonic margin apron*.

Galloway (1998) models have been customized for mapping of common GoM slope/basin depositional systems. The paleogeographic maps relate all slopes to their updip depositional systems. Slope systems and their continental rise and abyssal plain extensions are differentiated into sandy submarine fans (Figure 1.36A), progradational delta and/or shelf-sourced aprons (Figure 1.36B,C), tectonic margin aprons (Figure 1.36D), and retrogradational aprons (Figure 1.37). Progradational slope aprons that front large shelf-margin delta systems and their adjacent progradational shore zones are commonly sandy. Progradational aprons are typically mud-dominated and front broad shelves or platform deltas that did not prograde onto the shelf margin. Retrogradational slope aprons formed where mass wasting and regrading recycled sediment from the upper slope and deposited an apron along the slope toe.

margin stabilized fluvial axes that cut across the uplifted basin rim (Galloway and Hobday 1996; Dooley *et al.* 2013).

2. A survey of modern world coastlines, which can be considered a snapshot of an instant of geologic time, shows that wave-dominated shores are more abundant than tide-dominated shores, and that both greatly exceed the fluvial-dominated shorelines (Nyberg and Howell 2016). Only the immediate distributary or river mouth preserves clear fluvial imprint. This has important implications. Detailed facies analysis of shoreline deposits of all types of deltas will reveal a dominance of marine features. Most of the delta front is being reworked most of the time by marine processes; shoreface successions displaying wave and tidal features will be abundant even within fluvial-dominated deltas. Differentiation of delta systems types, as done here, depends on interpretation and mapping of the entire suite of prodelta, delta front, and delta plain facies that comprise the deltaic depocenter. Our maps are drawn to emphasize the *maximum* extent of delta systems as defined by lithofacies distribution within the genetic sequence created by the deposode.
3. The transfer of sand from the shoreface to slope channels or canyons is highly constrained by the presence of an intervening shelf. Maximum shelf bypass distance is less than 5 km (Sweet and Blum 2016). For large-scale bypass of sand to the slope, the shoreface must extend essentially to the shelf margin, whether by progradation or by relative sea-level fall. Alternatively, submarine canyons must cut across the shelf to intercept the shoreface.
4. In consequence, high rates of shoreline progradation favor sand bypass to the slope and construction of sandy slope and basin depositional systems (Dixon *et al.* 2012; Gong *et al.* 2016). Our paleogeographic maps are drawn to emphasize the maximum progradational extent of deltas and shore zones, to highlight the regions within a genetic sequence where sand bypass is most favorable.
5. Sand-rich fluvial-dominated deltas and progradational sandy shorefaces also favor sand bypass to the slope (Dixon *et al.* 2012; Gong *et al.* 2016).
6. Particularly in climatic greenhouse times, large deltas are fully capable of prograding across transgressive shelves, bringing their sandy mouth bars and shoreface directly onto the shelf margin (Blum and Hattier-Womack 2009).
7. Local basin margin tectonics and morphology also play a major role in determining the timing and location of sand bypass to the slope and basin (Covault and Graham 2010). As will be shown, this is a dominant element for much of the Gulf margin of Mexico.
8. Geomorphic slope profiles of ocean basins include graded, tectonically over-steepened, stepped above grade, and ponded above grade continental slopes (Prather *et al.* 2017).

Several other generalizations apply to the mapping methodology and reconstruction of paleogeographies of the Cenozoic GoM:

1. The great majority of delta systems are either fluvial- or wave-dominated. Some tidal influence has been recognized in detailed facies analyses.
2. Across the northern Gulf margin, large delta systems have commonly prograded to the shelf margin, where they deposited distinctive assemblages of facies and intraformational structures common to shelf-margin deltas (Galloway and Hobday 1996).
3. Strike-fed shore zone systems are geographically, volumetrically, and economically important elements of the GoM basin-fill. They are well developed in several locations: delta system flanks, broad interdeltaic bights, and along coasts where numerous small streams flow from uplands to the adjacent coastline (Galloway and Hobday 1996; Figure 1.35). Gulf shore zone systems include wave-, mixed wave/tide-, and tide-dominated types.
4. Seascapes of the Cenozoic GoM contained diverse sediment transport pathways and depositional systems tracts, just as does the modern basin. In addition to submarine fans located at slope toes and commonly extending far across the continental rise and onto the abyssal plain, several different kinds of submarine slope

https://doi.org/10.1017/9781108292795.003 Published online by Cambridge University Press

and basin paleogeographic systems are differentiated and mapped (Box 1.3). These include (1) slope aprons, characterized by line-sources along a broad length of the shelf margin; (2) sea floor channel systems; and (3) migratory submarine dune fields (Galloway 1998). Slope aprons can be further distinguished into progradational sediment prisms that construct offlapping continental margins and retrogradational aprons.

5. Using a global database, Prather *et al.* (2017) quantified average sand content deposited in continental margin depositional systems tracts. Shelves, which include coastal plain, delta, shore zone, and shelf depositional systems, average 27 percent sand content. The upper to middle slope decreases to 13 percent sand. In the lower slope and continental rise, which are characterized by decreasing declivity, sand content increases to 18 percent. Different slope profiles and sandiness of the fluvial–deltaic sediment input modify the site-specific percentages, but the pattern remains consistent; sand tends to bypass the upper slope, which is dominantly muddy, creating a bimodal pattern of vertical sand distribution within a prograding continental margin (Galloway and Hobday 1996).

Although volumetrically minor components of individual genetic supersequences, retrogradational slope systems display distinctive stratigraphic and structural architectures. Several create discrete petroleum plays. Structural and depositional elements of retrogradational margin aprons created by large-scale failure of the shelf margin are illustrated in Figure 1.37. Defining

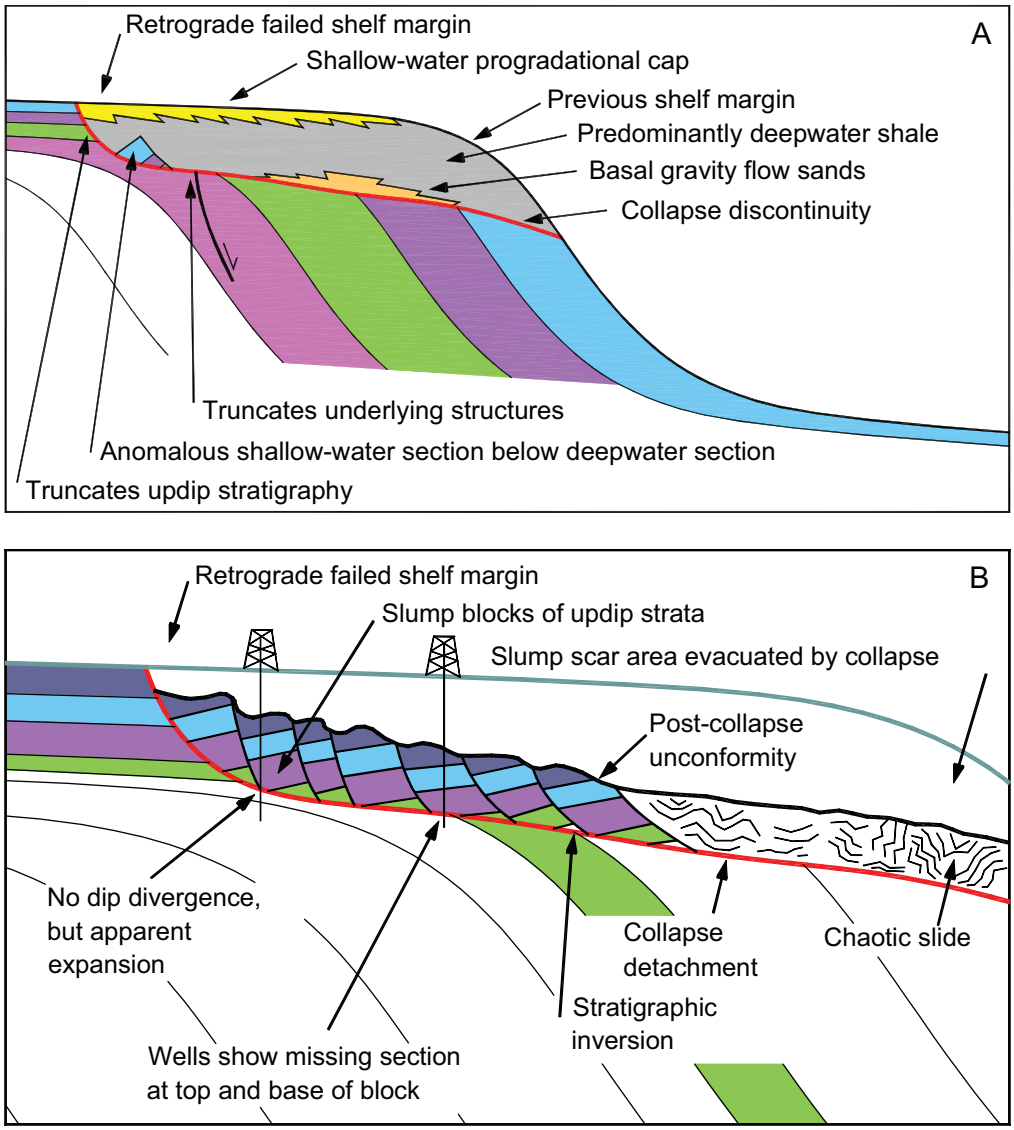

Figure 1.37 Structural and depositional architecture of failed retrogradational shelf margins. (A) Retrogradational wedge largely evacuated by mass wasting, creating a perched terrace upon which gravity flow sands, debris flows, and disconnected slump blocks may be deposited and preserved. (B) Retrogradational wedge within which slump blocks form a large part of the supra-discontinuity fill. In both, the position of the shelf edge was relocated landward from its original position at the top of the slope clinoform to the retrograded headwall position. From Edwards (2000).

https://doi.org/10.1017/9781108292795.003 Published online by Cambridge University Press

elements include a basal erosional discontinuity, perched gravity flow and slump deposits, and a capping wedge of deepwater mudstone (Edwards 2000; Galloway 2005a).

1.18 Explanation of Paleogeographic Maps: Assumptions and Caveats

It is useful to consider the methods, assumptions, and caveats used to reconstruct the depositional history and paleogeography of the Mesozoic and Cenozoic intervals of the greater GoM basin. As mentioned in the discussion of the GBDS database (Section 1.9), wells and seismic data are the primary tools used in our reconstructions (see also Galloway *et al.* 2000). Wells are used for creation of lithofacies suites, and, where possible, are calibrated against published core cuttings information and tied to seismic data. Well log motifs (see "Gulf of Mexico Cenozoic Log Facies Interpretation" poster at www.cambridge.org/gomsb), stratigraphic unit thicknesses, and observed lateral trends in depositional facies guide thickness mapping (unit thickness maps) and structure mapping (unit top maps). Seismically derived thickness maps (isochore maps) and structure maps (structure contours) are also constructed where the density and quality of the 2D seismic grid permit.

These maps underlie and support the paleogeographic reconstructions for each stratigraphic unit. For example, unit thickness maps often help delineate and define depocenters. Depositional "thicks" (areas of prominent stratal thickening) at these depocenters often occur where sediment transported via extrabasinal fluvial systems (major pathways from highland source terranes) accumulate in large-scale deltas, which often act as important point sources for major submarine fans. Salt, where present, often enhances the thickness trends via salt evacuation. It should be noted that local over-thickening of units, for example in salt dome peripheral grabens, is averaged out by use of regional well control. Thinning onto salt highs or carapaces is dealt with in a similar fashion. Growth along extensional normal faults, however, usually can be related to a major sediment input point. By contrast, areas of low sedimentation are associated with development of thin carbonates, defined as condensed intervals *sensu stricto*.

In areas outside of the allochthonous salt canopy, seismic facies mapping adds confidence to the interpreted depositional environments. Seismic mounding, (seismic reflections showing double downlap) is often associated with major submarine fan development (Combellas-Bigott and Galloway 2006).

Identification of other structural and stratigraphic features also aids paleogeographic mapping. Depositional shelf margins often coincide with major fault detachments, as shown in several of the basin cross-sections described in Section 1.5. Submarine canyons are noted in several areas and units (e.g., Lavaca and Yoakum Canyons; Galloway and McGilvery 1995), which in turn are linked to submarine fan development in downdip areas (McDonnell *et al.* 2008).

Distinctive seismic architectures for carbonate systems are also noted and factored into mapping. Rimmed shelf reefs or platform margin reefs are particularly well developed for the Cretaceous stratigraphic units.

Together, the map suite defines location, areal extent, and total sediment volume associated with the major sand dispersal and carbonate development within the Gulf basin during each depositional interval.

There are a few caveats to consider when reviewing these paleogeographic maps. First, maps are reconstructions, back to the original position at the time of deposition, unless present-day position is indicated. Thus, plate reconstructions are used for Triassic, Jurassic, and Early Cretaceous depositional systems. Plate reconstructions of the GoM basin continue to evolve. For example, the timing of sea floor spreading described by Hudec *et al.* (2013a, 2013b) has already been modified (Norton, pers. comm.).

For some specific units, like the Smackover–Norphlet supersequence, post-depositional rafting has also been taken into account. Restoration back to the pre-rafted position has been carried out for the main Norphlet exploration area in the deepwater of the eastern GoM, following the kinematic model of Pilcher *et al.* (2014). If post-depositional rafting is not considered, the Norphlet map, for example, would depict a paleogeography that is far too broad relative to its original depositional geometry.

Finally, it is important to note that the GoM basin is the site of numerous ongoing studies, seismic surveys, and drilling campaigns that provide new information on the Mesozoic and Cenozoic on a yearly, if not monthly, basis. Use of detrital zircon U–Pb geochronology (Box 1.2) for provenance, for example, has had an especially large impact on reconstruction of ancient drainage systems (e.g., Snedden *et al.* 2018a). Our book, therefore, captures the state of the Gulf basin at the moment of publication and it is highly likely some of our interpretations will require future modification as new data becomes available.

1.19 Database

The greater GoM basin has long been known as a superb natural laboratory of sedimentary and structural processes. For example, our understanding of salt tectonics has advanced because of considerable work done in this basin and as featured in the work of Jackson and Hudec (2017), Hudec and Jackson (2011), and Rowan (1995). This is due in large part to quantity and quality of the information gathered in the course of oil industry studies of seismic data, testing of models by drilling wells, and supporting scientific studies of the basin.

Studies of the GoM date back many years. Since the publication of Amos Salvador's seminal DNAG volume J (Salvador 1991a), over 2500 papers have written on the GoM basin. Many of these are from industry workers providing their insights from seismic studies and well results. Another equally important source of information about the basin is the scholarly

https://doi.org/10.1017/9781108292795.003 Published online by Cambridge University Press

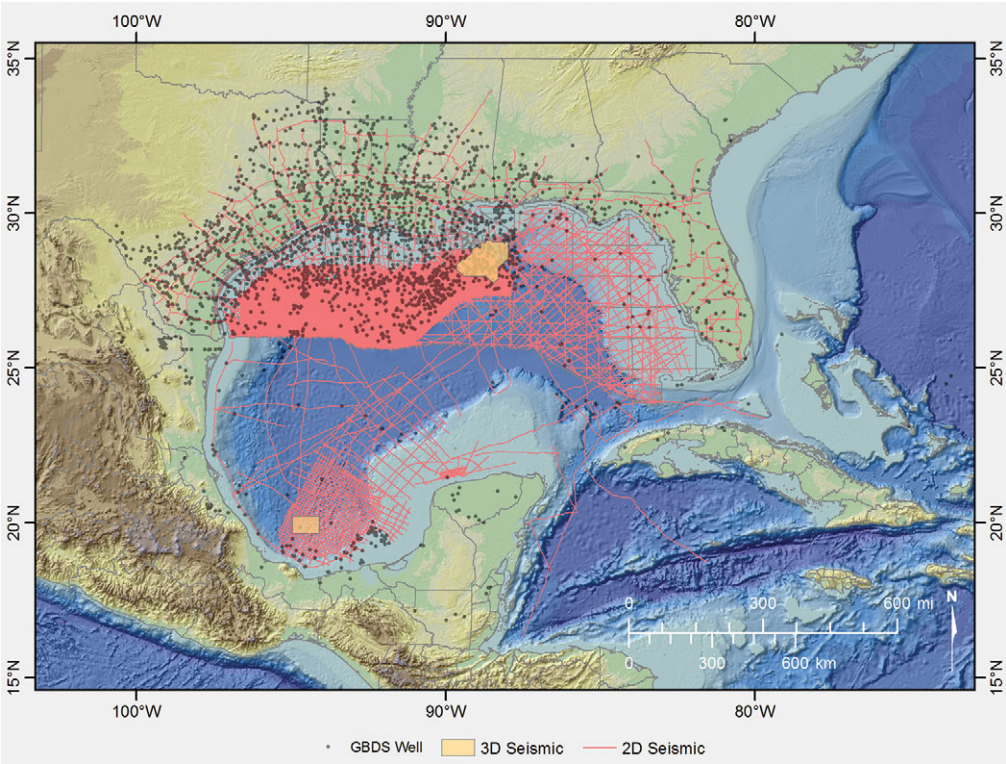

Figure 1.38 Well and seismic database of the Gulf Basin Depositional Synthesis project used in this book.

research at universities. At last count, over 40 students have written theses and dissertations on the GoM, ranging from near-surface sedimentary processes to the deep Louann Salt.

At the University of Texas and other national and international universities, faculty and research scientists have been leaders in the evolving understanding of the basin, often ahead of the industry interest. Dick Buffler, who for many years led the GBDS project, published early papers on DSDP core sites on the Mexico sector that now are being used for calibration of source rock and depositional systems in the Mexico deepwater rounds (e.g., Hessler *et al.* 2018). William Fisher and William Galloway's work on the onshore Wilcox (e.g., Fisher and McGowen 1967; Galloway and McGilvery 1995; Galloway *et al.* 2000) preceded drilling of the BAHA II well and opening of the Wilcox deepwater play. There are too many examples to cite within the limits of this introduction.

This book is founded upon a database built and maintained by the GBDS research project, Institute for Geophysics at the University of Texas at Austin, which enjoyed industry support for more than 20 years. This database includes over 2000 previously published papers, including many spatially referenced maps, but also well log and seismic data (Figure 1.38). The well data from the USA consists of released well data from federal and state waters; onshore US wells are courtesy of state surveys and third-party vendors like DrillingInfo™. Well data from Mexico are entirely public domain, largely university theses from National Autonomous University of Mexico and other Mexico universities.

Seismic data from federal waters was loaned to the GBDS project by seismic data companies, including ION Geoventures, TGS, Spectrum, MCG, and PGS. The data is mainly 2D seismic, with a few 3D surveys available to GBDS researchers and students.

Biostratigraphic data, so important to the stratigraphic age assignments, is mostly from BOEM data releases but also donations to the University of Texas at Austin. Other ancillary data (porosity, permeability, etc.) are provided on an individual basis via request to specific companies.

The ARCGIS database of Cenozoic and Mesozoic maps is the key derivative product from this 20+ years effort and the primary means of investigating the long and complex depositional history of the Gulf basin. The rest of this book sets forth to lay out the depositional framework, form the basin, and fill the basin with Mesozoic and Cenozoic sediments, the primary oil and gas reservoirs of this prolific hydrocarbon habitat.

https://doi.org/10.1017/9781108292795.003 Published online by Cambridge University Press